Titre: Title:	Cold Plasma for Pathogen and Nutrient Control in Hydroponic Systems
Auteur: Author:	Sean Watson
Date:	2026
Type:	Mémoire ou thèse / Dissertation or Thesis
Référence: Citation:	Watson, S. (2026). Cold Plasma for Pathogen and Nutrient Control in Hydroponic Systems [Thèse de doctorat, Polytechnique Montréal]. PolyPublie. https://publications.polymtl.ca/76784/

URL de PolyPublie: PolyPublie URL:	https://publications.polymtl.ca/76784/
Directeurs de recherche: Advisors:	Stephan Reuter, & Jason Robert Tavares
Programme: Program:	Génie biomédical

POLYTECHNIQUE MONTRÉAL

affiliée à l'Université de Montréal

Cold Plasma for Pathogen and Nutrient Control in Hydroponic Systems

SEAN WATSON

Institut de génie biomédical

Thèse présentée en vue de l'obtention du diplôme de *Philosophiæ Doctor*

Génie Biomédical

Mai 2026

POLYTECHNIQUE MONTRÉAL

affiliée à l'Université de Montréal

Cette thèse intitulée :

Cold Plasma for Pathogen and Nutrient Control in Hydroponic Systems

présentée par **Sean WATSON**

en vue de l'obtention du diplôme de *Philosophiæ Doctor*

a été dûment acceptée par le jury d'examen constitué de :

Gregory DE CRESCENZO, président
Stephan REUTER, membre et directeur de recherche
Jason Robert TAVARES, membre et codirecteur de recherche
Frédéric LEBLOND, membre
Valérie ORSAT, membre externe

ACKNOWLEDGEMENTS

To all the people who have helped me and supported me throughout my thesis, thank you. These few words may not be enough to convey my gratitude, nor the magnitude of your help, but it is thanks to you all that I was able to complete this journey.

I would like to start with a special thanks to my supervisor Stephan Reuter for his extensive support, availability and mentorship throughout the entire endeavour. Thank you for believing in me throughout the project.

I would also like to thank my co-supervisor Jason Robert Tavares, for his support, his critical input and offering a paradigm shift from which to observe the project.

I would also like to thank prof. Michael Wertheimer and prof. Frédéric Sirois for their input in the initial phase of the project (supervision and pre-doc committee members).

From génie civil department, I would like to thank prof. Émilie Bédard for her collaboration in the first article, Michèle Prévost, for introducing me to the water filtration and cleaning process in her course, and to Benoit Barbeau for his willingness to collaborate and explain the ozone system in his lab.

I extend also my gratitude to my former colleagues Cédric Pattyn, for his support in the early phase of the project, Pauline Morasse for her work in developing the early versions of the hydroponic growth in the lab and Fady Abdelmalek for his expertise in microbiology.

This work would not have been possible without the help of the support staff; from physics engineering, I would like to extend my thanks to Yves Leblanc for his availability and expertise regarding electrical circuits, to Joël Bouchard, for his help with water cooling and overhaul of the lab and to Mikaël Leduc for his expertise in optics, and Yves Drolet. From chemical engineering I would like to thank Gino Robin and Martine Lamarche, as well as Matthieu Gauthier, Wendell Raphael and David Brassard.

I would follow with my colleagues: Jean-Baptiste Billeau, Julien Bissonette-Dulude, Julien Trahan, Laura Bouret, Juliette Letellier-Bao, Jean-Philippe Comtois, Laura Cacot and Stéphane Simon, with whom I was able to share and develop a passion for plasma science and its related applications.

This work is also possible in thanks due to the participation of the members at IRDA, notably thanks to Mélanie Dominique for starting the project, to Élodie Larouche, for the continuation of the collaboration and for exploring ELISA sampling, to Ariane Duval for helping with lettuce assessment, to Thomas Jeanne for his qPCR and microbiological expertise, and to the supervision of the project by Caroline Côté and Richard Hogue.

The plant expertise brought forth by Julie Monette and Chedzer-Clarc Clément from GenV was also a great asset for the project. I would like to extend my thanks to the on-site visit they extended us as well as for their support and patience during testing in the summer of 2024.

I would also like to thank the interns for their collaboration and their eagerness to learn which was like a contagious spark to push me forward in the lab: Émilien Martel, Mathilde Doyon and Kathleen Lupien.

I also want to take the time to thank Giulia Laghi for her internship and discussion on the matter of measuring energy of different types of plasmas.

I have kept the most important for last: a special thanks to my sister and parents, for promoting my scientific curiosity since youth, and for their continued, unabated support throughout this thesis.

RÉSUMÉ

Dans un contexte de pratiques agricoles durables, visant à améliorer les conditions de culture hydroponiques de la laitue Boston, une approche d'utiliser des plasma froids est proposée conjointement avec la recirculation d'eau hydroponique. Ce travail consiste à valider l'utilisation de traitements plasma de la solution hydroponique comme source alternative pour implémenter des fertilisants à base d'azote et la création de pesticides. Débutant à partir de ressources de bases telles que de l'eau, de l'air et de l'électricité, les plasmas froids peuvent être utilisés pour générer un mélange d'espèces réactives à base d'oxygène et d'azote. Les espèces d'oxygènes peuvent être adaptées pour l'inactivation de pathogènes, alors que les espèces d'azote peuvent être implémentées pour incorporer l'azote dans l'eau sous une forme de nutriment pour les plantes.

La présence d'éléments essentiels à la culture des plantes dans un environnement riche en humidité, combiné avec un système de recirculation hydroponique, donne lieu à la prolifération de pathogènes indésirables. Un des pathogènes en question est celui de la famille des oomycetes, une variété de moisissures d'eau. Lors des mois d'été, au Québec, alors que l'on imaginerait la plus haute saison de récoltes, la productivité est réduite considérablement due à leur présence. De ces oomycetes, une espèce, le *Pythium ultimum*, est l'espèce ciblée et responsable du flétrissement des cultures à partir des racines lors des périodes de fortes chaleurs et de stress pour les plantes.

Une investigation du design de réacteurs chimiques, depuis des jets de plasma en parallèles, jusqu'aux arcs-coulissants et le développement d'une unité mobile employant les micro-ondes, a permis d'augmenter la mise-à l'échelle et l'efficacité des procédés plasma. Parmi ces derniers, le prototype d'arc coulissant a été retenu, après avoir augmenté l'efficacité de générer des espèces par un facteur de 10, dans l'optique d'inactiver des pathogènes. Afin d'accroître encore nos capacités de travail exploratoire et de diagnostiques rapides pour le prototypage, de nouveaux outils ont été ajoutés à notre répertoire : notamment par l'adaptation de tests ELISA d'un usage topique vers une lecture des échantillons liquides et à travers la comparaison de la croissance de masse hyphale du Pythium dans un milieu de culture après avoir assujetti le milieu à un traitement plasma. En combinant l'exploration de l'impact du ratio d'oxygène et d'azote dans l'effluent du plasma pour créer les espèces réactives, un traitement permettant l'inactivation de *Pythium ultimum* d'une solution innoculée dans de l'eau distillée a été trouvé. Le processus de dégradation du Pythium a aussi été observé par microscopie éléctronique à balayage (MEB), démontrant que les structures

contenant les œufs ou les sporanges à la terminaison des hyphes de Pythium ont été endommagés ou réduites suffisamment après le traitement par plasma.

Pour vérifier si la condition d'inactivation fonctionnerait toujours dans un milieu de culture plus complexe, tel qu'utilisé en serres, un prototype de traitement plasma a été mis au point pour son déploiement au site de GenV. Les tests ont eu lieu au cours de l'été 2024, permettant d'investiguer le potentiel d'inactivation du plasma, pour le e-coli et avec une analyse quantitative de réaction de chaîne de polymérase, spécifique aux oomycètes.

Des études de croissance, impliquant des laitues Boston comme outil diagnostique , depuis un état de jeunes plantes jusqu'à une croissance de 2 semaines, ou encore jusqu'à maturité (3 semaines) ont été réalisées à Polytechnique Montréal et dans des chambres de croissances dédiées à l'IRDA respectivement. Les études réalisées à Polytechniques avaient pour but de substituer l'azote en répliquant, à partir d'eau distillée et de nutriments, la solution hydroponique du partenaire industriel. Les nitrates de calcium et de potassium ont donc été substitués par l'incorporation d'azote par un traitement plasma avec un ajout de calcium et de potassium à partir d'autres sources. À l'IRDA, les chambres de croissance ont permis d'investiguer les conditions d'inactivation sur les plantes. Bien que la température de croissance n'ait pas permis de répliquer des conditions de prolifération majeures de *Pythium*, il a cependant été possible de démontrer que le traitement plasma n'avait pas d'effet phytotoxique.

La condition résultante est donc en mesure d'inactiver le *Pythium* sans endommager les plantes, atteignant ainsi l'objectif du projet. Des solutions pour améliorer l'efficacité des procédés et la suite du projet sont par la suite discutées.

ABSTRACT

In a context of sustainable agriculture practices, aimed at improving the conditions of the hydroponic growth of Boston lettuce, a non-thermal plasma approach is proposed jointly with recirculating hydroponic water. This works attempts to validate plasma treatment of hydroponic solution as an alternative source to implement nitrogen fertilisers and pesticides. Starting from basic resources such as water, air and electricity, non-thermal plasma can be used to generate a mixture of reactive oxygen and nitrogen species. Oxygen species can be adapted for pathogen inactivation, while nitrogen species can be tailored to incorporate nitrogen in the form of plant nutrient in the water.

The presence of crop nutrients in tandem with the plants in a humid environment combined with a recirculating hydroponic system, give rise to undesired phytopathogens. One particular pathogen of note is the family of oomycetes — a type of water mold. In the summer months of Quebec, expected to be the most productive, the productivity is hampered due to their presence. From these oomycetes, *Pythium ultimum*, has been chosen as the most likely target underlying crop wilting from the roots in high heat and plant stress periods.

Chemical reactor designs, from parallel plasma jets to a gliding arc and developing a mobile microwave source, were investigated to improve scaling and efficiency of the process. Among these, a gliding arc protype was then retained, after improving the species generation by a factor of 10, for pathogen inactivation. To further expand our capability for exploratory work and prototyping diagnostic, original diagnostic tools were added to our repertoire, namely adapting an ELISA test from solid to liquid analyses and comparing hyphal mass growth in Sabouroud dextrose broth after plasma treatment. Combined with an exploration of the impact of nitrogen-to-oxygen ratio towards the creation of reactive species, a condition leading to *Pythium ultimum* inactivation in inoculated distilled water was found. The pythium degradation process was observed through scanning electron microscopy (SEM) analysis, showing that Sporangium or oogonia containing structures that terminate the pythium's hyphae have been broken and significantly reduced after plasma treatment.

To verify if the inactivation condition was still working with a more complex media, such as the one used in the greenhouse, a prototype was developed for deployment. Tests were conducted

during the summer of 2024, to investigate the pathogen inactivation potential of plasma, for both e-coli and with a quantitative polymerase chain reaction analysis specific to oomycete species.

Growth studies involving Boston lettuce as a diagnostic tool from a sapling stage to a 2-week growth or full maturity (3-week) were conducted both at Polytechnique and in growth chambers at IRDA respectively. In the case of growth at Polytechnique, the substitution of nitrogen was investigated by replicating the industrial partner's hydroponic solution from distilled water. Calcium nitrate and potassium nitrate were then substituted by nitrogen incorporation using plasma, while providing calcium and potassium from other sources. At IRDA the growth chambers enabled to investigate the condition for inactivation on the plants. While the growth temperature was not conducive to a strong *Pythium* proliferation, it was however possible to demonstrate that the plasma treatment is not phytotoxic.

The resulting condition is therefore able to inactivate pythium without harming the plants, thus achieving the objective of the project. Further solutions for improving the efficiency and overall experimental design are then discussed.

TABLE OF CONTENTS

LIST OF TABLES

LIST OF FIGURES

LIST OF SYMBOLS AND ABBREVIATIONS

The list of acronyms and abbreviations presents, in alphabetical order, the acronyms and abbreviations used in the thesis and their meaning.

CMA Corn meal agar

DI Deionized

qPCR Quantitative polymerase chain reaction

IRDA Institut de recherche en agroenvironnement

MW Microwave

PPA Plasma processed air

PTW Plasma treated water

RNS Reactive nitrogen species

RONS Reactive oxygen and nitrogen species

ROS Reactive oxygen species

SDB Sabouraud dextrose broth

SEM Scanning electron microscopy

Spp. Species

WHO World Health Organization

LIST OF APPENDICES

CHAPTER 1 INTRODUCTION

One of the key challenges in the agriculture sector is to sustain the higher productivity required to feed the rising world population [1], without further negative impact on the environment. Enlarging areas of cultivated land does not constitute a long-term solution, as it comes at a high environmental cost, namely in a reduction in biodiversity, deforestation and soil erosion [2]. Productivity per acre can be increased with synthetic fertilizers, but their use affects negatively the environment through soil acidification and eutrophication — oxygen depletion due to excessive plant growth— of water bodies. These fertilizers also carry a significant CO_2 footprint. Their production, via the Haber-Bosch process, requires nearly 2% of the world's energy and produces 300 million tons of CO_2 per year [3]. The hydrogen, required for the Haber Bosch process, is mainly derived from fossil fuels [4]. These in turn contribute to the aggravation of climate change.

Climate change, with unpredictable impact on rainfall distribution and temperature, will have a direct impact on agriculture trends, such as changes in sowing dates, irrigation and geographic areas for suitable production. Variations in climate also bring in other risks such as natural disasters, like droughts and floods, or the geographic redistribution of invasive species, such as pests, diseases or competitive species. In addition to climate change impacts, the recent pandemic highlighted the fragility of supply chains and the demand for autonomous production. The Haber–Bosch process requires large-scale facilities to achieve economic and reliable ammonia synthesis at high temperatures and pressures (350–550 °C, 150–350 atm). However, it is difficult to obtain reliable nitrogen sources in economically developing or remote areas, which further aggravates the uneven distribution of global resources.

A solution to limit the impact of climate change and offer year-long production is the use of greenhouse farming. In Quebec, the number of vegetable farms keeps increasing[5]. The current political and societal interest towards local production stimulates this sector for which water management is a key issue. In a subcategory of greenhouse farming lies hydroponics, a soilless method which makes use of water to deliver the nutrients to plants growing above a water solution. To reduce actual costs and for protecting the environment, water recycling is a common practice in hydroponics. It involves, however, a good monitoring of the water quality to control phytopathogens —plant pathogens—, to ensure the food safety of produce, and control the required

dissolved elements and fertilizers. Water quality issues can lead to reduced yields and production interruption at specific periods of the year.

The dichotomic nature of agriculture and its impact on climate is addressed through sustainable agriculture practices. One of the major steps towards sustainability is to shift towards innovative solutions to reduce the use of synthetic chemicals. To address both issues of controlling water quality and producing on-demand fertilizers, we propose to use non-thermal plasmas jointly with recirculating hydroponic water.

During the last two decades, considerable experimental efforts have been directed at the investigation of the effects of non-thermal plasma application in the emerging research field of plasma agriculture. Plasma is, at least partially, an ionised gas (that emits light) which can produce highly reactive species. It can be generated in any gas, the most common being air, nitrogen, oxygen, water vapor, helium, argon, or gas mixtures at different pressures and temperatures. Plasmas exist in nature, such as stars and auroras, usually sustained by thermal equilibrium or constant bombardment by highly charged particles. Plasmas can also be created artificially, e.g. by using electric fields where electron temperatures can be distinctly higher than the overall gas temperature. Plasmas with high temperature of electrons and lower temperatures of heavy particles are called non-thermal or cold plasmas.

Each plasma is a quasi-neutral mixture of electrons, ions, neutral molecules, atoms, radicals, and excited species. Due to the relaxation of excited or ionised particles, it emits light. Light in the ultraviolet spectral region can contribute to dissociation of molecules and thus to the creation of reactive species. Plasma can be controlled by external parameters, such as the electric field strength and frequency, or the gas composition. The plasma's reactivity can be diagnosed to gain insight into how to tailor the reactive species' composition to form a desired chemistry. In the case of a plasma used in air, it will generate a mixture of reactive oxygen and nitrogen species, the former which can be adapted to inactivate pathogens, and the later can be used to incorporate nitrogen plant nutrients in water [6]. Producing a non-thermal plasma allows to activate biological media without increasing the local temperature, an important feature for plasma agriculture and medicine [7].

Unlike the Haber-Bosch processing facilities, plasma technology does not need to reach high heat and pressure conditions to start. It can be used as a turn-key process, in conjunction with green

electricity, providing in-situ chemistry, even in remote areas. Plasma can be triggered using commonly available resources: air, water and electricity. Chemically active species can thus be produced on demand and locally, in minimally invasive quantities or significant storage requirements. This reduces the risks of combustion involved in transporting and storing nitrates and ammonia byproducts.

The presence of crop nutrients in tandem with the plants in a humid environment combined with a recirculating hydroponic system, however, are prone to the proliferation of undesired phytopathogens. One particular pathogen of note is the family of oomycetes, a new subclassification from fungi, which is a type of water mold. In the summer months of Quebec, expected to be the most productive, the productivity is hampered due to their presence. From these oomycetes, *Pythium ultimum*, has been chosen as the most likely candidate underlying crop wilting in high heat and plant stress periods. Due to its relevance, *Pythium* has been chosen as the target species for the present studies.

The current thesis is presented as a collaboration between the plasma physics and spectroscopy laboratory (PPSL), the Photochemical Surface Engineering Laboratory (PhotoSEL), plasma processing laboratory (PPL), the research and development institute for agri-environment (IRDA) and an industrial partner, Serres-Lefort, which was renamed to GenV within the project time frame.

The following chapter presents a brief literature review, with additional information about plasmas, chemistry, oomycetes and state of the art for pilot scale studies. This section delivers a short introduction to the different topics required to understand the background of the thesis from a multidisciplinary point of view. Further state of the art and literature background is presented within the two manuscript chapters of the thesis, chapter 5 and chapter 6 as described below. The third chapter of the thesis presents the research question and objectives. The 4th chapter covers in detail a chemical scheme original to this work, followed by reactor design exploration and optimization, from parallel jets to a gliding arc, to a mobile microwave source. The 5th chapter presents a first paper of the thesis, which addresses developing diagnostic methods for inactivation of *P. ultimum*, by adapting an ELISA test and looking into the reducing effect of plasma treatment on the growth of *P. ultimum's* hyphal mass. Chapter 6 covers a second paper targeting fertilizer, i.e. nitrogen nutrients incorporation at the best plasma treatment conditions identified in chapter 5, using plant growth indicators as a measure of phytotoxicity. Chapter 7 covers how the

experimentation has been adapted to be deployed for testing on site at GenV for a water analysis test using contaminated water, as well as a presentation of the growth conditions for the plants by the industrial partner. Chapter 8 summarizes the work and presents limitations and recommendations for future work.

CHAPTER 2 LITERATURE REVIEW

2.1 Plasma chemistry

2.1.1 A brief introduction to plasma

Plasma is an ionized gas composed of a quasi-neutral mixture of electrons, ions, neutral molecules, atoms, radicals, and excited species. Ionization is the process by which an atom or molecule assumes a net positive or negative charge through the gain or loss of electrons. The quasi-neutral property of plasma implies that there is an equal number density of oppositely charged particles, to ensure that the number of ions and electrons in the mixture are equal. Another important property of plasma is that its behaviour is determined by the motion of the individual particles subject to electric and magnetic forces from external sources or from the particles' charges [8].

2.1.2 Plasma chemistry in non-equilibrium discharges

Ionization can occur by multiple sources in a plasma: by collision with electrons, ions, neutral particle or excited atom, or by photon absorption (typically ultraviolet or higher energy) and electron attachment, as presented in Table 2.1. The symbol representation is as follows: A is a molecule or atom, A^+ is a positively charged molecule or atom, A^- is a negatively charged molecule or atom; e is an electron; M is a neutral particle, M^+ is an ion, M^* is a metastable or excited atom; $h\nu$ is a photon. The ionization mechanisms are presented with equations 2.1 to 2.6.

Table 2.1 List of ionization mechanisms generating reactive species in a plasma

Ionization Mechanisms	**Simplified representation**	
Electron collision	$A + e \rightarrow A^+ + e + e$	(2.1)
Ion collision	$A + M^+ \rightarrow A^+ + M^+ + e$	(2.2)
Neutral particle collision	$A + M \rightarrow A^+ + M + e$	(2.3)
Excited atom collision (also known as Penning transfer)	$A + M^* \rightarrow A^+ + M + e$	(2.4)
Photon absorption	$A + h\nu \rightarrow A^+ + e$	(2.5)
Electron attachment	$A + e \rightarrow A^-$	(2.6)

Plasma has been classified into 2 different types: a state where the charged particles and ions are in thermal equilibrium (thermal plasma) and a second where the temperature of electron is much higher than that of the heavier particles (non-thermal or cold plasma).

The electron energy distribution function (EEDF) describes the distribution of the electrons with a specific energy within a plasma. When a plasma is in a thermal equilibrium state, the EEDF follows a Maxwell-Boltzmann distribution, and the emission profile follows that of the black body radiation. This is how the temperature of stars is assessed through emission, and the corresponding temperature obtained is the same for the electrons as it is for the other particles in the thermal plasma.

However, when the plasma is generated in a non-thermal plasma, the EEDF is no longer tied to the Maxwell-Boltzmann distribution because certain collisions can augment or deplete specific energy levels, resulting in a non-uniform distribution of the electrons with a specific energy. Electron temperature is therefore separate from that of the ions, neutrals, atoms and molecules, and can reach much higher levels than their heavier counterparts. While temperature can be defined as the degree of agitation of particles, typically from translational movements due to excess energy, when it comes to molecules, the energy can also be dissipated into two other modes: rotational and vibrational thermal dissipation.

Non-thermal plasma can take advantage of its energetic electrons to create ions, dissociate molecules and create excited species that can carry energy for further chemical reactions. An example illustrating this potential is found in the figure 4 of [9], presented in Figure 2.1, where the electrons excite oxygen and nitrogen from air in a plasma which diffuses into the effluent gas to generate the primary species for the plasma chemistry.

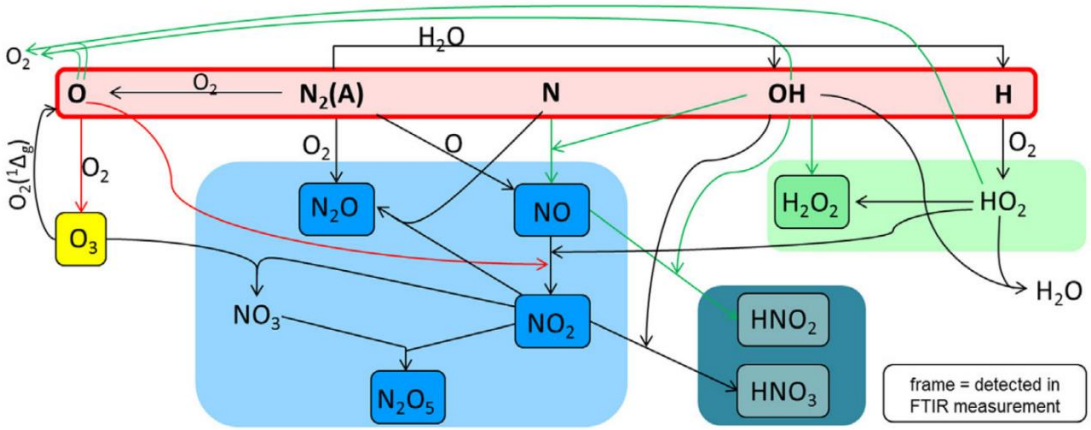

Figure 2.1 Network of reactions assumed to be important for the observed dynamics. The green and red arrows indicate reactions that are assumed to be favorable or unfavorable, respectively, for obtaining an NOx-dominated plasma chemistry. Reproduced with permission from [9].

2.1.3 Plasma sources and technology

Whether it is in the context of wastewater treatment,[10-13] agriculture,[14] plasma medicine or for the reforming of CO_2,[15, 16] most of the relevant plasma reactors for liquid treatment and related work have been developed at a laboratory scale. A good indicator of the progress state of a technology is the Technology Readiness Level (TRL, cf. Figure 2.2)[17]. To date, most of the plasma sources for liquid treatment are at level TRL 3-4 and are waiting for an opportunity to evolve to the pilot scale (TRL 5-6), before eventually reaching TRL 7-8-9, ready for industrial purpose and marketing. Scaling-up allows for a higher volume treatment, increased treatment speed, or possibly even making a plasma reactor portable, all in the interest of lowering costs. The main drawback with current plasma sources resides in the fact that their energy costs are high, which prevents them from gaining a competitive edge [18]. The book by A. Fridman [8] describes the issue in depth, and claims that microwave plasma (MW) is the most efficient method for the example of nitrogen fixation [19]. Most early works in the former Soviet Union with a highly efficient plasma process could, to date, not be replicated. Nevertheless, microwave plasmas (and gliding arc plasmas) are considered to be most efficient at generating nitrogen atom containing species [20].

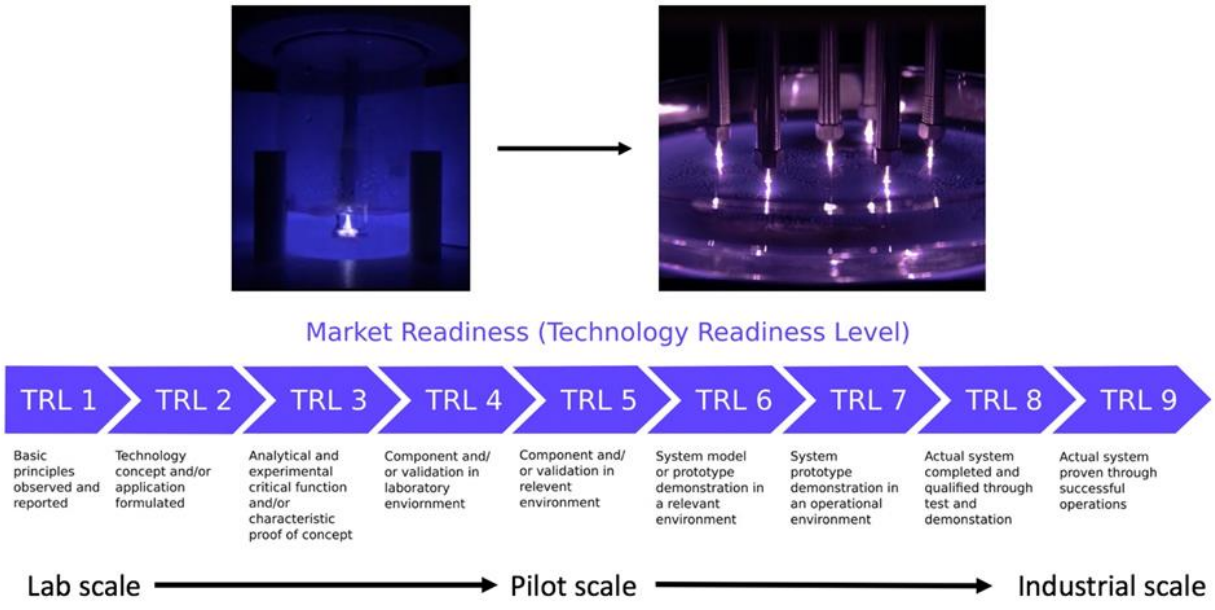

Figure 2.2 Technology readiness level in view of plasma source development. The images illustrated above depict one way of increasing the scale, namely by parallelisation of the plasma sources.

This subsection presents the elements required to design a plasma source, derived from the current laboratory scale parameters. The purpose of this section is to both illustrate the variety of reactors, as well as to allow a reader to understand which plasma sources are being compared and presented in **Erreur ! Source du renvoi introuvable.**.

Geometry

The different geometry types specific to plasma systems in contact with water (i.e. electrohydraulic) will be presented in the same format as in [21]. As such, six general categories can be established where the discharge breakdown occurs:

- In the water (electrohydraulic)
- In the water, using bubbles
- In gas phase over water
- In gas phase with water droplets/mist
- a combination of types 1 to 4
- not in direct contact with the water.

While electrohydraulic discharges have been studied for some time [22], and can lead to interesting results in organic decomposition, they remain the most demanding in terms of energy. Plasma decontamination and reactive species generation was revealed to be more efficient at the interface of a thin water film than in the bulk itself, which is why the discharge categories 2) – 6) present a higher overall performance. For reactors of type 2), it was proven that Ar bubbles are more efficient than He bubbles due to a smaller gas-water interface [23]. In terms of overall efficiency, the reactors of categories 3) and 4) have shown to be the most promising thus far for degradation of phenolic compounds [21]. An increased degradation implies a higher interaction between the plasma and the surface of the liquid.

Applying an electric field

Igniting a plasma requires one to apply a breakdown electric field. Control of the plasma properties by way of this electric field can be achieved by changing frequency, applied voltage and waveform. Malik et al. [18] have proposed to classify electric fields generated by power supplies in terms of their waveform:

a) DC discharge

b) Audio frequency discharge (AF)
c) Radio frequency discharge (RF)
d) Microwave discharge (MW)
e) Monopolar pulsed discharge
f) Bipolar pulsed discharge

It is important to design power supplies for electric fields that are well suited to match the non-linear electrical components of the reactor and the plasma itself. For example, a methodology to design a pulsed power supply can be found in [24]. It is important to maximise the energy transfer to the plasma zone, and to avoid reflection and dissipation of power elsewhere. To accomplish this, an impedance matching unit is often used. These impedance matching devices only offer a fixed compensation; they do not account for dynamic changes in the non-linear element.

Materials

For a plasma source to function correctly, at least one electrode is needed, and these are commonly metallic [25, 26]: Ta, Ti, W are rugged, corrosion- and shock resistant electrodes, typically used in electrohydraulic discharges [21], where there nature will have an impact on the resulting chemistry. Platinum (Pt) electrodes might be suitable on the laboratory scale, because it is inert, corrosion resistant, but due to high cost, Pt is typically excluded from large-scale design. Cu, or alloys such as NiCr, low carbon steel, or stainless steel have also been commonly reported electrode materials. However, they often have shorter lifetimes, depending on plasma conditions [27]. As electrodes corrode, they will release small particles of the same material into the water. This might possibly be beneficial in some cases, acting as a catalyst, but it might also inhibit some reaction pathways, depending on the target chemistry. Examples of such catalytic effects are well documented in Jiang et al.'s review [12].

To protect the electrodes from corrosion, or simply to lower the local electric field (and prevent arc formation) dielectric barrier materials can be added to cover totally or partially one or both electrodes, forming a dielectric barrier discharge (DBD) reactor configuration [28]. While DBDs allow for higher energy efficiency in general, they also reduce the plasma length by reducing the local electric field. Dielectrics commonly used are SiO_2, Al_2O_3, TiO_2 or mixtures of these materials. While polymer dielectrics are not commonly used, they have been researched extensively in

developing roll to roll processes [28, 29]. These can also be tailored to provide a catalytic surface for the desired chemical species [30].

Chemical parameters

The efficiency of a plasma process and source is not only affected by its design, applied electric field and the materials from which it is made, but also by two other criteria: solution parameters and working conditions.

The solution parameters include reactive species and chemical moieties in the solution, temperature, pH [31] and water conductivity. While Jiang et al. [12] made a good summary explanation of these parameters, they are nevertheless often difficult to control. An increase in temperature can indicate that energy is lost as heat to the water instead of sustaining plasma, so it is to be avoided. In a stationary volume, it is normal to expect pH to change over time, accompanying the production of reactive species. A variety of plasma species with a longer lifetime are acidic, while others such as OH- and H_2O_2 are not. Typical acidic species formed in the plasma are nitrites (NO_2^-)/ nitrates(NO_3^-), peroxinitrides ($ONOO^-$) and superoxide ($O_2^{\bullet-}$). Acidity is a large factor in influencing plasma-liquid interaction results [32]. It can be beneficial to have certain precursors appear in more acidic conditions and be used as educt in a process occurring at conditions of lower acidity

With properties of water under treatment changing over time, this implies the overall efficiency of a fixed applied field will also vary over time, because the plasma is no longer in a stationary mode. When comparing batch processing and recirculation of water flow through working conditions, the conductivity of the water will play an important role. It is therefore normal to expect a process that constantly replaces the water being treated to seem more efficient, as was the case in the most efficient reactor design highlighted in the geometry section [21].

On the other hand, it is relatively easier to modify the working conditions. The choice of gas, whether it is a noble gas, air, or mixtures, will affect the required breakdown field, electron density and temperature, plasma homogeneity and density, as well as resulting reactive species [33]. Depending on the desired target chemistry, these parameters allow one to tailor the plasma of a

given reactor to deliver the desired species. If the water is in motion, its flow rate is of importance and will in turn be affected when the plasma is ignited. While this specific topic is not yet fully resolved, the work of Mededovic et al. [34] provides a good introduction.

Pilot scale reactors & different approaches

Table 2.2 Pilot scale reactors, scale and application context

	Group/description	Type - Scale	Application context
(a)	MAPSYN project: Evonik Eco trainer [35, 36]	MW - trailer	Nitrogen fixation
(b)	N2-Applied reactor [37]	MW - trailer	Fertilizer production
(c)	Plasmaleap Pin reactor discharge in open air [38, 39]	Pulsed	Medical
(d)	Clarkson University trailer [40, 41]	Rotary spark gap	Degradation of PFAS
(e)	Greifswald prototype [42, 43]	MW	Lettuce washing
(f)	F. Holzer and B. R. Locke column reactor [44]	Pulsed	Advanced oxidation

Table 2.2 presents a list of several reported pilot scale reactors. From the state of the art of these, it is noted that MW-based systems are being developed at a more rapid pace than, for example, pulsed plasma sources. Another prototype to have reached “trailer” size is the one developed by Clarkson University [20].

Scaling-up plasma sources requires one to address the fundamentals of plasma science and remaining open questions. There is a need to establish standards for comparison: it seems that every group is using their own definitions, and that reference model reactors, such as the COST jet [45] are scarce in the literature. More research is ongoing to understand the fluid dynamics and long-term effects in plasma treated water (PTW) [46]. There is also a need to gain insight on radical transport and production, electric field effects as well as reaction kinetics and intermediates [47]. Finally, one of the most challenging aspects of plasma source development comes from the multidisciplinary aspects which involves chemistry, materials science, physics, electrical engineering, and the end user of the technology, may they be in agriculture, biomedical technology, or any other related fields.

Energy efficiency

As pointed out earlier, the main drawback of current plasma sources lies in their high energy demand. It thus becomes relevant to compare reactors by energy efficiency. The first classification

of plasma energy efficiency was established for deactivating dyes [18] comparing 27 reactors. The comparison parameter, the energy yield (G_{50}), expressed the amount of pollutant converted divided by the energy input required for 50 % conversion of the pollutant. For dye inactivation, a water spray in a pulsed DBD in O_2 was found to be the most efficient. Locke in 2011 established a comparison of H_2O_2 production rates [48]. Here again, a DBD in combination with water spray through an activated gas was reported as the most efficient. Attempts were also made [12] to classify and compare different reactors for the purpose of deactivating phenolic compounds. While the energy efficiency was comparable, the novelty of this review was to include the effect of a catalyst in the water to improve the deactivation efficiency. Miklos et al. [49] established a comparison of plasma reactors against other advanced oxidation techniques. The comparison parameter in his review was E_{E0}, in units of kWh/m^3/order of reduction. While this unit allows a direct comparison between reactors, it does not constitute an absolute performance comparison since the initial concentration of the substance to be degraded is not considered. Studies by Mededovic[50] also indicate that not all substances are readily degraded by plasma. In her plasma configuration, most of the plasma-liquid interactions are occurring at the surface. It has been observed that surfactants molecules, which float on the surface of the liquid, are degraded the quickest. Their work suggest that a surfactant can also be added to bind with the desired chemical for increased degradation rates. The overall message is still clear: none of the advanced oxidation techniques involving plasma have made it to industrial scales. Unsolved issues remain, as there is no consensus in regard to a) the initial concentration of the pollutant to be deactivated; b) the target concentration to achieve, c) the actual capital/operational costs, and d) the resulting secondary reactions with plasma chemistry.

On the side of nitrogen fixation (useful for plasma agriculture, see section 2.2 below), the adopted unit for comparison is in kWh/kg or kWh/m^3 of target species [36, 51, 52], sometimes also indicated with the target concentration (in ppm). In this context again, an exact benchmark is missing, and a lot of work is needed to convert back and forth the units for a proper comparison.

Current discussions in the literature propose many avenues to improve the energy efficiency, depending of course on the discharge type. A first approach would be a parallel array of microplasmas, as for example in reactors (c) or (h) of **Erreur ! Source du renvoi introuvable.**. Their small size inherently enables breakdown at lower voltage, thus easier to configure a power source accordingly.

From studying the electron energy distribution function (EEDF) of plasma simulations, it is possible to predict the relation between the applied energy and the favored reaction kinetics. Such a simulation is presented in Figure 2.3 [49]. Using simulations such as these allow one to visualise how lower energies are needed for vibrational excitation of O_2, and eventually also for N_2. The advantage of using pulsed power, if the pulses are shorter than the vibration-translational transition, in the order of 100 ns, it is possible to transfer the energy into vibrational ladder climbing, instead of the rotational/translational energy which increases the gas temperature, T_g. This allows one to dissociate molecules, e.g. N_2, with much less energy than that of direct dissociation. In their modeling paper, Wang et al.[53] explain how the theoretical limit of such a non-equilibrium process could be lower than that of the Haber-Bosch process for N_2 fixation. However, to date, the implementation of a plasma source that can achieve this non-thermal advantage has not been reached. This is mainly due to the rapid equilibration of the vibrational energy into other sources.

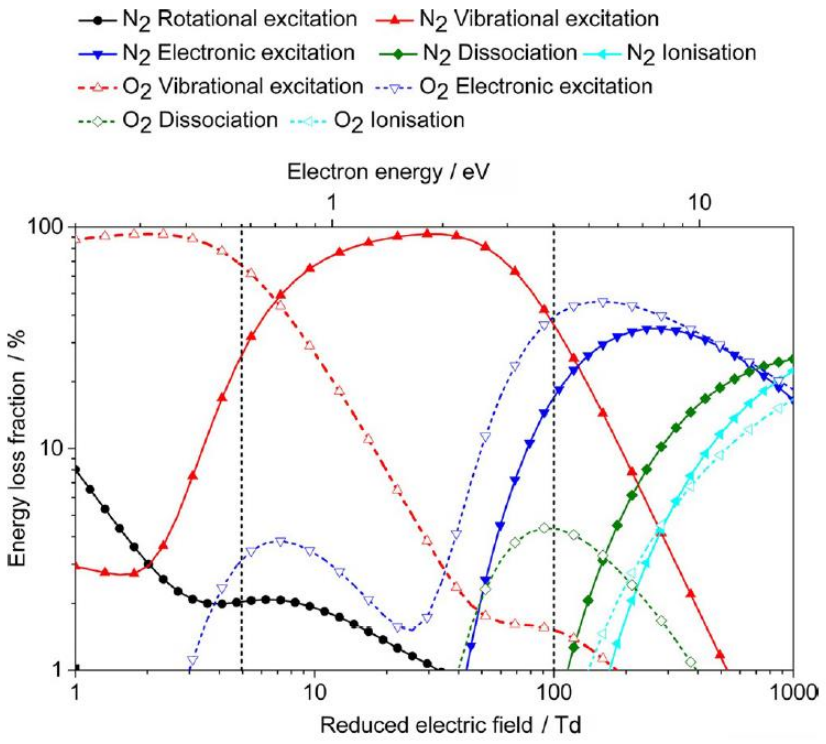

Figure 2.3 Fraction of electron energy transferred to different channels of excitation, as well as ionization and dissociation of N_2 and O_2, in a 50% N_2/50% O_2 mixture; from [53].

The same argumentation also applies for near-thermal processes involving MW power. The use of quenching mechanisms is discussed in the works of Fridman [54] in the context of NO synthesis,

and the group of Bogaerts [20] in the context of CO_2 reforming. Carbone et al. have even proposed to combine the approach and the use of pulsed MW power [55].

Since efficiency is dependent on the chemical species concentration, it is possible to tailor the plasma by controlling the chemical reactions. Controlling the amounts of reactants and products can favor some pathways over others. pH can affect the relation between reactions and be controlled to obtain the desired species [56]. It is also possible to control the chemistry by combining different plasma regimes: Sun et al. [51] demonstrated how it is possible to combine the discharge kinetics of glow, spark and bubble interface plasmas to influence the output chemistry.

2.1.4 Generation of reactive oxygen – nitrogen species (RONS)

Although large scale reactors have been built in the past in the context of ozone water treatment since this technique was developed in the 19th century, modern plasma sources involve more reactive species than just O_3. For more in depth information on these species, the reader is referred to [10]. A quick summary of the main reactive oxygen and nitrogen species (RONS) is found in Table 2.3. They also constitute the main chemical species of plasma treated water (PTW).

Table 2.3 Major reactive oxygen and nitrogen species (RONS) and lifetime τ in water

Reactive Oxygen Species (ROS)			**Reactive Nitrogen Species (RNS)**		
Radicals		τ	**Radicals**		τ
$\mathbf{O_2^{\bullet-}}$	Superoxide	5s [10]	**NO •**	Nitric oxide	0.1 s [32]
• OH	Hydroxyl	0.1-200μs [10] [32]	$\mathbf{NO_2}$ **•**	Nitrogen dioxide	
Nonradicals			**Nonradicals**		
$\mathbf{^1O_2, O_2\ (\Delta_g)}$	Singlet oxygen	100 μs [32]	$\mathbf{ONOO^-}$	Peroxynitrite anion	10–20 ms [32]
$\mathbf{O_3}$	Ozone	30 min [32]	**ONOOH**	Peroxynitrous acid	3 s [57]
$\mathbf{H_2O_2}$	Hydrogen peroxide	$10^6 s$ [32]	$\mathbf{HNO_2}$	Nitrous acid	
			$\mathbf{HNO_3}$	Nitric acid	
			$\boldsymbol{NO_2^-}$	Nitrite	10^7 s [32]
			$\boldsymbol{NO_3^-}$	Nitrate	10^8 s [32]

2.2 Plasma in agriculture

The future of agriculture lies in a continuously rising demand for safe and high-quality produce, in tandem with an environmental awareness and climate change concerns and need for adaptation. New techniques are required to improve efficiency, reduce the carbon footprint, mitigate risks associated with crop failure, while ensuring food quality and nutritive properties.

Plasma technology offers tools for several applications towards a sustainable agriculture practice. A first one is in the synthesis of HNO_3 or ammonia starting from air to create fertilizers. Direct plasma exposure or generating PTW can be used to stimulate plant growth, through the inactivation of pathogens and the presence of fixed nitrogen. Combined with a an on-demand production, it is also possible to limit the quantities produced to be effective yet reduce the footprint of their use on the environment. This also applies to seed decontamination or the deactivation of food pathogens, from a direct approach to a sealed packaging treatment. The potential for such applications has been described in depth in the following references [58, 59]. A brief introduction on their context and current state of the art will be presented here. For each application, the chemical species and example pathways will be identified.

2.2.1 Nitrogen fixation and ammonia synthesis

Since the beginning of the 20th century, nitrogen compounds have been developed industrially to increase agricultural yields. Of the processes developed at that time, two are of particular interest. The first, the Birkeland-Eyde process, was developed by Kristian Birkeland and Samuel Eyde in 1903. It consists of using a thermal plasma arc to produce nitrogen oxide (NO), followed by an oxidation to create nitrogen dioxide (NO_2) and finally absorbing the nitrous oxides into water to form nitric acid (HNO_3). However, this process was later abolished by the more efficient Haber-Bosch process and Ostwald process. This second process produces ammonia (NH_3) and ammonium nitrate (NH_4NO_3). More details on the comparison between both process is provided in [60]. The Haber-Bosch process requires operation at high temperatures and pressures (350–500 °C and 100–300 bar), and is therefore difficult to interrupt, and requires large facilities. Anastopoulou et al. have suggested an eco-efficient analysis of plasma assisted nitrogen fixation [61]. They revisited the Birkeland-Eyde process and proposed improvements to the method of nitrogen fixation, to make it comparable to that of the Haber-Bosch process, while taking advantage of the electrification of chemistry. Nitrogen fixation processes at the plasma-liquid interface has been

studied by Roy et al. [62], Machala and coworkers [63] along with a study of the reactive chemistry of reactive nitrogen species (RNS) and reactive oxygen species (ROS) diffusion in water. The effect of air humidity on nitrogen fixation was investigated by Abdelaziz and Kim [64] using a nanopulsed DBD.

2.2.2 Pathogen inactivation

Pathogen inactivation goes back to early work on plasma sterilization [65, 66]. There have since then been many studies implying that almost all ROS and RNS species can be involved in deactivation of pathogens in a synergistic fashion [67]. The addition of ultrasound or shockwave effects have been suggested [68] to accelerate this inactivation. Among the reported species, ozone was found to be a major contributor [69], but also important in affecting the outer membrane of cells are NO, H_2O_2, and OH [70]. RNS such as peroxynitrites have also proven to be key species, along with superoxide anion radicals [63, 71].

The chemical pathway for Peroxinitride, a key species, is expressed in equations 2.7 to 2.9:

$$H_2O_2 + H_3O^+ \leftrightarrow H_3O_2^+ + H_2 \tag{2.7}$$

$$NO_2^- + H_3O^+ \leftrightarrow HNO_2 + H_2O \tag{2.8}$$

$$H_3O_2^+ + HNO_2 \rightarrow ONOOH + H_3O^+ \tag{2.9}$$

2.2.3 Case study: lettuce

Given the context of the present work, the following discussion will focus on the key problems currently faced when growing lettuce under hydroponic conditions. The key pathogens affecting Boston lettuce will be presented, as well as known studies where plasma was used, directly or indirectly, to control pathogens or promote growth.

Hydroponics and water recycling

To save on costs for artificial fertilizers and to prevent the release of large quantities of concentrated dissolved nutrients, the technique of water recycling has been adapted by the industrial partner. Due to an artificially rich environment for aquatic growth, it is thus important to monitor closely the growth of phytopathogens so that their presence does not harm the growth of the main cultivar. The conditions during which growth becomes problematic are discussed more in depth in CHAPTER 7.

Using a conventional water treatment approach, such as the ones used to treat municipal water, to reduce pathogens would be counterproductive, as it would remove most if not all dissolved nutrients, which is one of the advantages of water recycling. Water pathogens are typically inactivated using chlorine or ozone, but the cultivar, in this case Boston lettuce, is sensitive to both species below their inactivation thresholds in commercial use. As an alternative, UV radiation could be considered but also requires pre-filtration to be used effectively (to avoid turbidity), and is not a cost-effective solution for the water volume intended. As such, PTW presents a compatible solution for pathogen inactivation, provided that it falls under the cost-benefit threshold. More information on conventional methods of treatment and their impact on oomycetes can be found in the Queensland university report [72].

Target oomycetes

Oomycetes are difficult to inactivate, and the target species discussed in this thesis, *Pythium ultimum, Pythium dissotocum* and a *Phytophthora dreschleri* are of particular interest to the industrial partner.

Oomycetes are often associated with fungi, but are rather a subcategory of eukaryotic microorganisms, which are more commonly known as “water molds”. One of the main differences is that their cell walls are composed of cellulose rather than chitin. However, their growth form featuring hyphae, a filamentous structure, and mode of nutrition are the same as fungi. An illustration of P. ultimum can be found in [73] They possess egg like sacks in which the spores are kept for reproduction. Beyond this generic introduction to oomycetes, the Pythium species are then classified using Van der Platernick’s work [74] according to their morphology and size. While some plant diagnostics exist to link oomycetes and their symptoms on plants, these are often unreliable. Without resorting to a qPCR (quantitative Polymerase Chain Reaction) test for genetics, different types of oomycetes can often be confounded for one another.

The mechanism for action is similar for all 3 species and oomycetes overall; they attach to the roots of the plant as parasites and siphon the nutritive elements from the roots directly, causing the plants to lack nutrients and eventually wilt. 3 Species of oomycetes have been researched in this project:

- *P. ultimum* is one of the commonest *Pythium* species in the soil [74] and can cause root rot and wilting as well.

- *P. dissocotum*, was detected in 1986 in Arizona and in 2006 in Connecticut [75], as a source of severe root rot and wilting. From [74], the temperature range of growth is minimum 5°C, optimum 20-25°C, maximum about 35°C, the same conditions as for P. ultimum.
- *Phytophthora drechsleri* has been reported as a root rot disease in hydroponics in Mexico [76] in 2008.

The difficulty in inactivating these pathogens is that they have a thick cellular membrane protecting the approximative 20 μm oogonia (egg-like structure which contains the spores), and that the inactivation has to happen in the water, along with all other floating contaminants and dissolved solids present in the liquid [72]. Moreover, the resulting inactivation should target Pythium more favorably than lettuce, which should be spared for obvious economic reasons. Oomycetes such as *Phytophthora infestans*, have demonstrated how difficult adapting a commercial fungicide to the solution can be [77], due to their adaptation to conventional approaches.

Impact of nitrogen on lettuce

Nitrogen is an essential element in the growth of plants. However, its adsorption mechanism is quite complex [78], and can sometimes be competitive. Essentially, all 3 forms of nitrite, nitrates and ammonium ion can be adsorbed by the root system, with a preference for the latter 2, though this varies from one species to another [79], and there is no consensus yet on which is preferred or why. Essentially, the plants have adapted to intake nitrogen from any source. In hydroponics, the favored source for nitrates is typically calcium nitrate or potassium nitrate. However, the addition of ammonia was also shown to improve nitrogen intake [4].

Another layer of complexity is the impact of that form of nitrogen on the consumer. Nitrate levels in produce have been shown to vary significantly [80], and consuming high amount of nitrate can lead to toxic effects on the human body, as it can transform into nitrite [81]. The introduction of article 2, in Chapter 6 presents more information about nitrite/nitrate norms for food.

Since nitrogen can be incorporated by plasma, which can be controlled in real time with relative ease, it becomes possible to control more effectively the levels for nitrogen intake. Nitrogen availability promotes growth, but excessive intake will stunt the absorption of the other nutritive elements [82].

CHAPTER 3 RESEARCH OBJECTIVES

3.1 Identification of the problem

Plasma technology possesses three main advantages. It is an environmentally friendly method of conducting chemistry, can be started on-demand by applying an electric field and therefore can be used with renewable electricity sources. These three aspects make the use of plasma in contact with liquids ideally suited for research and use in Québec, where abundant hydroelectricity allows for the use of low-cost and green energy. Plasma thus constitutes a potential tool for improving the sustainability of agriculture.

The inactivation of oomycetes plaguing hydroponic systems can be troublesome due to their large outer cellular wall thickness. While commercial antifungals are available, for non-hydroponic growth, it has been proven that oomycetes have a tendency to adapt and develop quickly to their use, and the typical solution is to avoid growing plants in contaminated soil for a few years [72]. There is no known solution to treat oomycete infections in hydroponics.

Both chlorination and ozonation of the water have been previously attempted, unsuccessfully. Moreover, Boston lettuce has been shown to be very sensitive to both ozone and chlorine, in smaller concentrations then the recommended inactivation doses. An efficient plasma treatment of the growth media should therefore also take into account plant phytotoxicity effects such that the lettuce can thrive while the pathogen can be inactivated.

As a side effect of plasma generation in air, both reactive nitrogen and oxygen species are generated. While the oxygen species are more likely to be beneficial for pathogen inactivation, nitrogen species could be used to amend the current fertilizer recipes. Most of the literature only presents tap water and plasma treated water but do not identify the impact of other ingredients in the presence of plasma.

Lastly, from an engineering point of view, there remains challenges to scale plasma technology for implementation in hydroponic cultures and its associated large volume scales.

3.2 Research question

How can plasma-liquid chemistry be tailored for pathogen inactivation while preventing plant phytotoxicity?

In attempting to answer this research question, the following hypotheses will be considered:

3.3 Hypotheses

i. Plasma interaction is most efficient in surface processes because the surface-to-volume ratio dictates the plasma reactor's efficiency
ii. Reactor design plays a significant role in improving process efficiency
iii. A combination of thermal and non-thermal processes may be needed for chemical specificity

Delving into those hypotheses will be achieved with a general objective, and 5 specific objectives:

3.4 General objective:

Develop and evaluate a plasma-liquid processing reactor, for both pathogen inactivation and fertilizer incorporation for hydroponic use.

3.5 Specific objectives:

Aligned with the main objective of this thesis, the present thesis will aim to close the gaps identified previously, such that plasma technology may be implemented to activate water for use in the field of agriculture. Accordingly, this thesis will pursue the following specific objectives:

I. Identify chemical pathways for oomycete inactivation, specifically for *Pythium ultimum*
II. Identify conditions to inactivate pathogens while causing little phytotoxicity
III. Assess the potential of nitrates fertilizer substitution using nitrogen incorporation by plasma
IV. Adapt plasma reactor design for deployment in a hydroponic greenhouse environment
V. Evaluate the up-scaling potential of the selected reactor design

CHAPTER 4 OPTIMIZATION OF PLASMA PARAMETERS

Chapter 4 describes the foundations required to optimize the envisaged plasma process for the application of plasma for nitrogen nutrient generation and anti-pathogen activity in hydroponic systems. The findings described in this chapter will be applied in the following chapters. section 4.1 presents the result of a database and literature search to identify the most relevant chemical reactions in plasma-liquid interaction. The resulting reaction scheme is shown partially in this chapter as well as in publication [83] (see additional details, chapter 5). The reaction scheme highlights the reactions post plasma discharge and their behaviour and provides first insights into optimizing reactors towards chemical pathway specificity. The reaction scheme summarizes the main reactive species' interactions as well as the strengths of the reactions themselves in one single figure. The following sub-sections describe the reactor concepts studied in this work. Section 4.2 explores the applicability and scalability of a high frequency high voltage electrode to water jet configuration. Section 4.3 describes the development and optimization of a gliding arc plasma, the plasma source type used in both publications. Section 4.4 concentrates on a third plasma source type, that may prove useful for scale up of the proposed use of plasma in hydroponics. The present work establishes the first steps in designing a microwave plasma-liquid system based on a commercially available microwave plasma reactor. Design considerations and first implementations are presented.

4.1 Identifying reactive chemistry

The main reactions in plasma-liquid interactions are compiled in one of the key figures of this work (cf. Figure 5.6) to illustrate the chemical reaction network of long- and short-lived species and their propagation from plasma to liquid. This reaction scheme presents a simplified set of the plasma chemistry reactions and is used to describe the dominating pathways relevant for the control of the reactive species composition in plasma treated liquids. The reaction network is compiled from literature (see e.g. [24, 41, 42]) and supplemented with those found on the NIST database. The complete set of equations is presented in appendix A. Figure 4.1 shows the transfer of the reactivity from plasma to liquid phase. The reaction network starts with the plasma-phase reactions, simplified to a few key and major species. As precursor gas, humid air is used. The resulting primary plasma generated reactive species are the atoms of oxygen, nitrogen, and hydrogen. These species interact with the surrounding gas species in collision and diffusion processes. The reactive

species transport into the liquid phase is determined by species-specific Henry's law solubility coefficients, which describes the concentration of a species in the liquid phase in equilibrium with the gas phase concentration. A species with a high Henry's coefficient will result in a high mass transfer from the gas to the liquid phase. Finally, Figure 4.1 shows the chemical pathway of the liquid species, focusing on long-lived species which can be readily measured, such as nitrites, nitrates and H+ ions. In both, the gas phase and the liquid phase, the thickness of the arrows indicates the order of magnitude behind the reaction rate enabling for a visualization of the most dominant processes.

In our studies, presented in CHAPTER 5, the hydrogen peroxide (H_2O_2) was below the detection limit, and the liquid phase oxygen chemistry was simplified in the diagram of Figure 5.6. A more detailed version, including the oxygen chemistry arrows can be found in Figure 4.1.

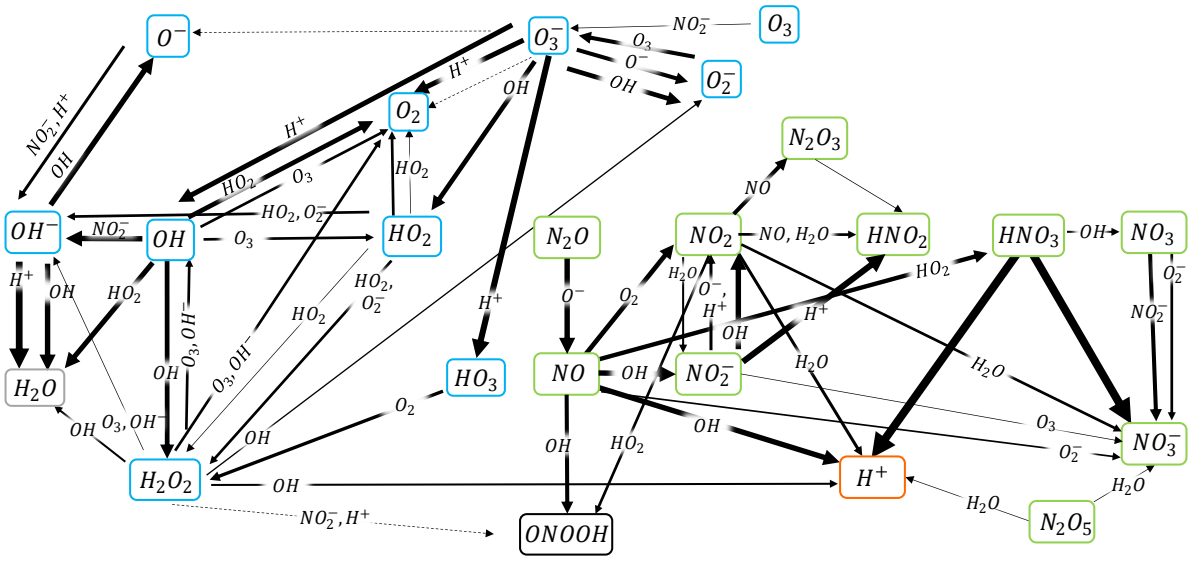

Figure 4.1 Liquid phase chemistry reaction scheme, showing greater detail in the reactive oxygen species propagation. In the same way as for figure 3.1, arrow thickness indicate the orders of magnitude of the reaction rates

Figure 4.1 visually highlights pathways to achieve reaction specificity in the liquid phase. For example, using a gliding arc currently produces both NO_2^- and NO_3^- species, but an ideal solution, for fertilisation purposes, would incorporate only nitrates, since nitrites are toxic to plants.

The reaction networks show the path towards a nitrate rich chemistry originating from the gas phase: Oxidation by adding ozone to the NO_X reactions can transform NO into NO_2 and oxidize it further into N_2O_5, which both result into nitrates after interacting with water.

As a second objective, the scheme was compiled with measurable species in mind. One of the main issues of understanding the reaction process is that there are too few species-specific diagnostic tools for rapid diagnostics. Mostly H_2O_2, NO_2^-, NO_3^- and pH (H^+, OH^-) colorimetric diagnostics are broadly accepted by the plasma community for their specificity. While Ozone diagnostics have been proposed, colorimetric methods to determine ozone concentrations are affected by the presence of the competing species in the liquid phase.

The reactive oxygen species pathway highlights how three key species for pathogen inactivation are created, namely H_2O_2, O_3 and $ONOOH$ (Peroxinitrous acid).

The reaction scheme shows the relevance of H^+ and OH^- ions which are primarily responsible for the changes in pH. The pH value is of great importance for liquid chemistry. As one example, the creation of peroxinitrous acid is favored in the presence of a low pH (<3). However, for the sake of the research topic of the present work – plasma activated liquid for hydroponics growth of lettuce and pathogen inactivation in greenhouse farming – the pH value of the hydroponic solution must stay within a limited range in order to not harm the lettuce growth. To regulate the pH value, buffer medium can be added. For the studies described in Chapter 6, potassium bicarbonate is used to that purpose.

It can be observed at the barrier of the gas and liquid interface, that some species diffuse more readily into water than others as determined by Henry's constant. O_X and NO_X species are slow to absorb into water. To increase the rate at which they cross the interface, interfacial area can be increased (such as by using a Venturi nozzle, or through forced diffusion). Large scale processes, such as municipal water systems typically force ozone to diffuse into liquid media through a several meters high basin. An absorption tower model for NO_X incorporation on a commercial scale, and related equations are proposed by [84]. Section 4.3 shows approaches on how transfer of nitrogen species can be improved by improving the interaction of gas and liquid phases in gliding arc plasmas.

4.2 Pin over liquid design development

The first design concepts of this work for cold plasma interaction with water are based on a plasma jet system (cf. Figure 4.2) developed for earlier studies [85] on algae treatment with plasma activated water [85]. The plasma jet has a pin to liquid geometry. The jet nozzle consists of a stainless-steel 3D-printer head. This allows for a cheap and easy replacement of the plasma jet nozzle from off the shelf components. The plasma jet is operated with a 20 kHz, 14 kV supply voltage. The jet was operated using 100 sccm of air and separately with 100 sccm of an argon oxygen gas mixture with a ratio of 9 to 1. The jet is operated in ambient air or in a protected environment defined by a quartz cuvette covering the active plasma region and reaching into the volume of 15 mL of distilled water (cf. Figure 4.2). The single jet studies demonstrated the potential of the jet to inactivate cyanobacteria: In previous studies, the temperature and pH value was measured, as well as degradation of Rhodamine B and viability of a green algae mixture treated with the plasma jet. The results are published in our previous works [85].

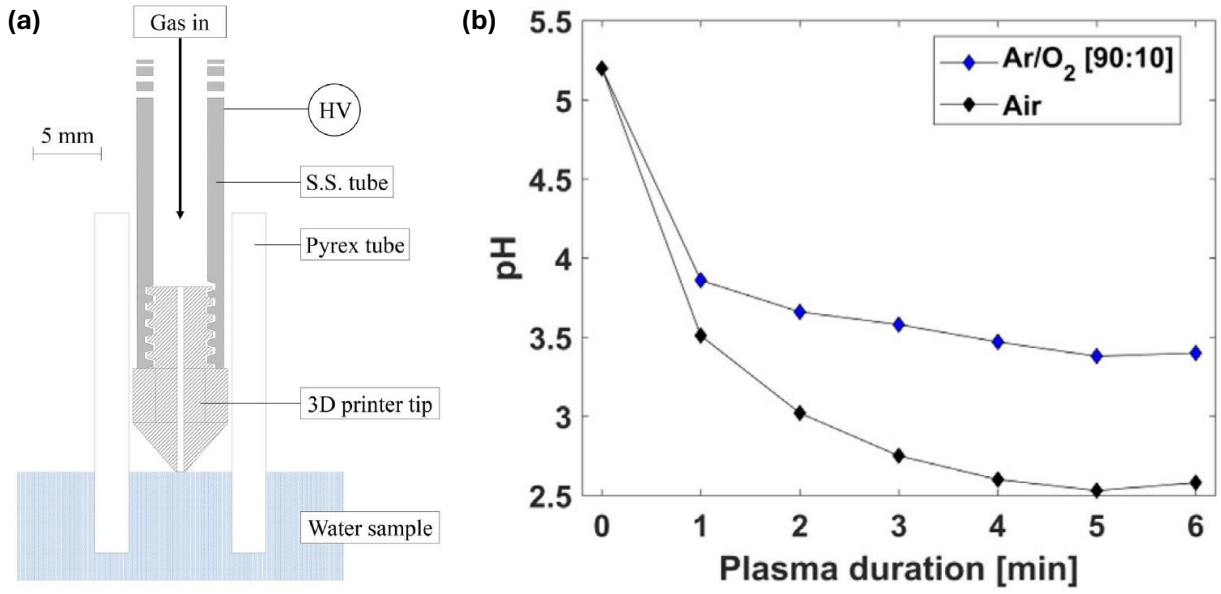

Figure 4.2 a) Single jet configuration consisting of a 3D-printer head nozzle screwed into a hollow tubular high voltage electrode and inserted into a protective pyrex tube to provide a protected gas environment when inserted into the liquid volume; b) pH values of 15 mL distilled water samples after indicated exposure durations to air and Ar/O_2 HV AC discharge effluents.

As a first scaling approach, the same single electrode plasma jet was explored with a larger volume of water at the otherwise same treatment conditions. To treat larger volumes of water, the plasma

jet was placed into a recirculation loop, using two peristaltic pumps (cf. Figure 4.3). Once again pH and temperature measurements were obtained, as well as the concentration of nitrites in water. The power source used was an Enercon power supply at 14-16 kV discharge (nominal power setting ca. 100 W, the lowest available).

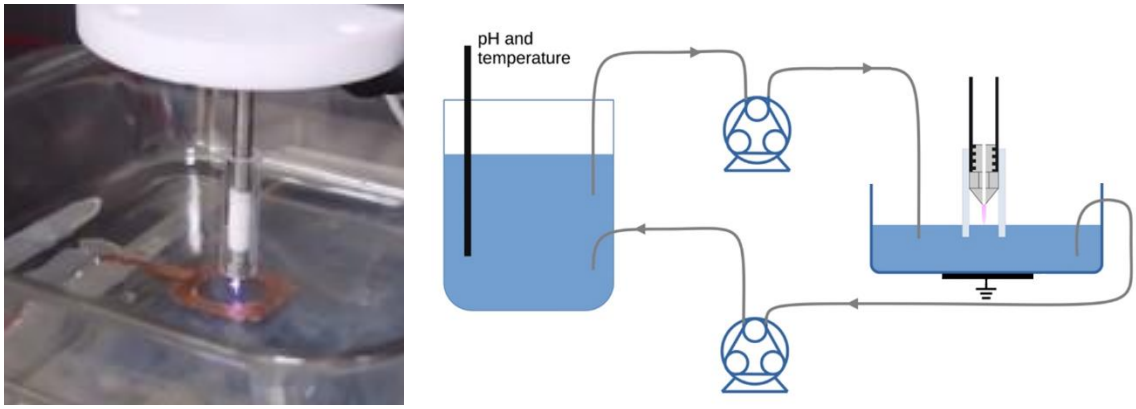

Figure 4.3 Single plasma jet configuration in water recirculation setup for larger volume treatments. Left: implementation; right: schematics showing peristaltic pumps, pH and temperature meter, grounding, and plasma jet.

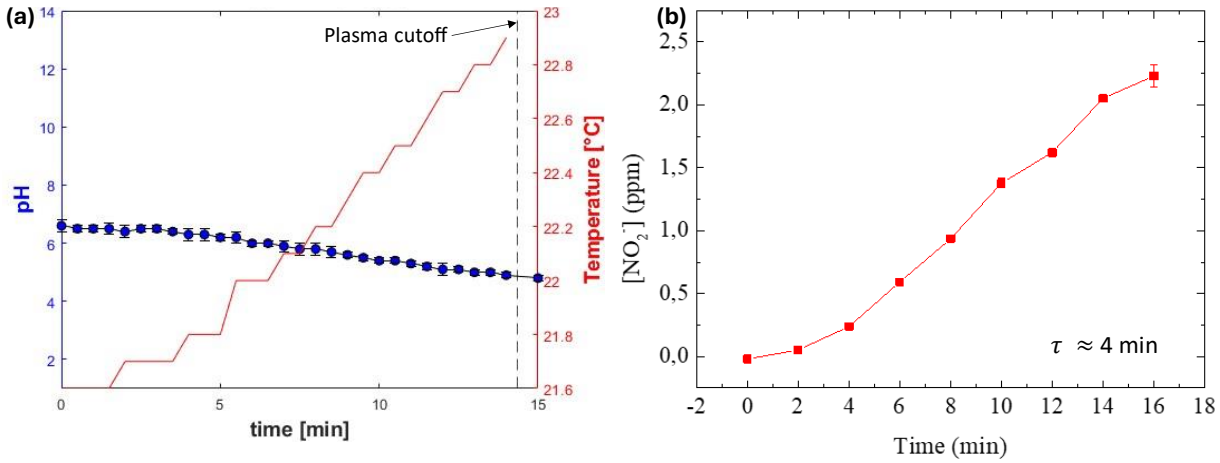

Figure 4.4 pH, temperature, and nitrite concentration development water recirculation system with single pin electrode in air plasma; (a) pH and temperature vs treatment time; (b) nitrite concentration measured using colorimetry. Residence time of the liquid was around 4 minutes.

A second approach to scale up the plasma treatment system is to use multiple electrodes. A prototype of 7 jets arrayed in a hexagonal pattern was created. Pictures of this setup and operation can be found Figure 4.5(b) to (d). The objective of this setup was to determine the effect of using

1 to 7 jets in parallel and to evaluate how the efficiency is impacted, therefore how parallelisation might be optimised.

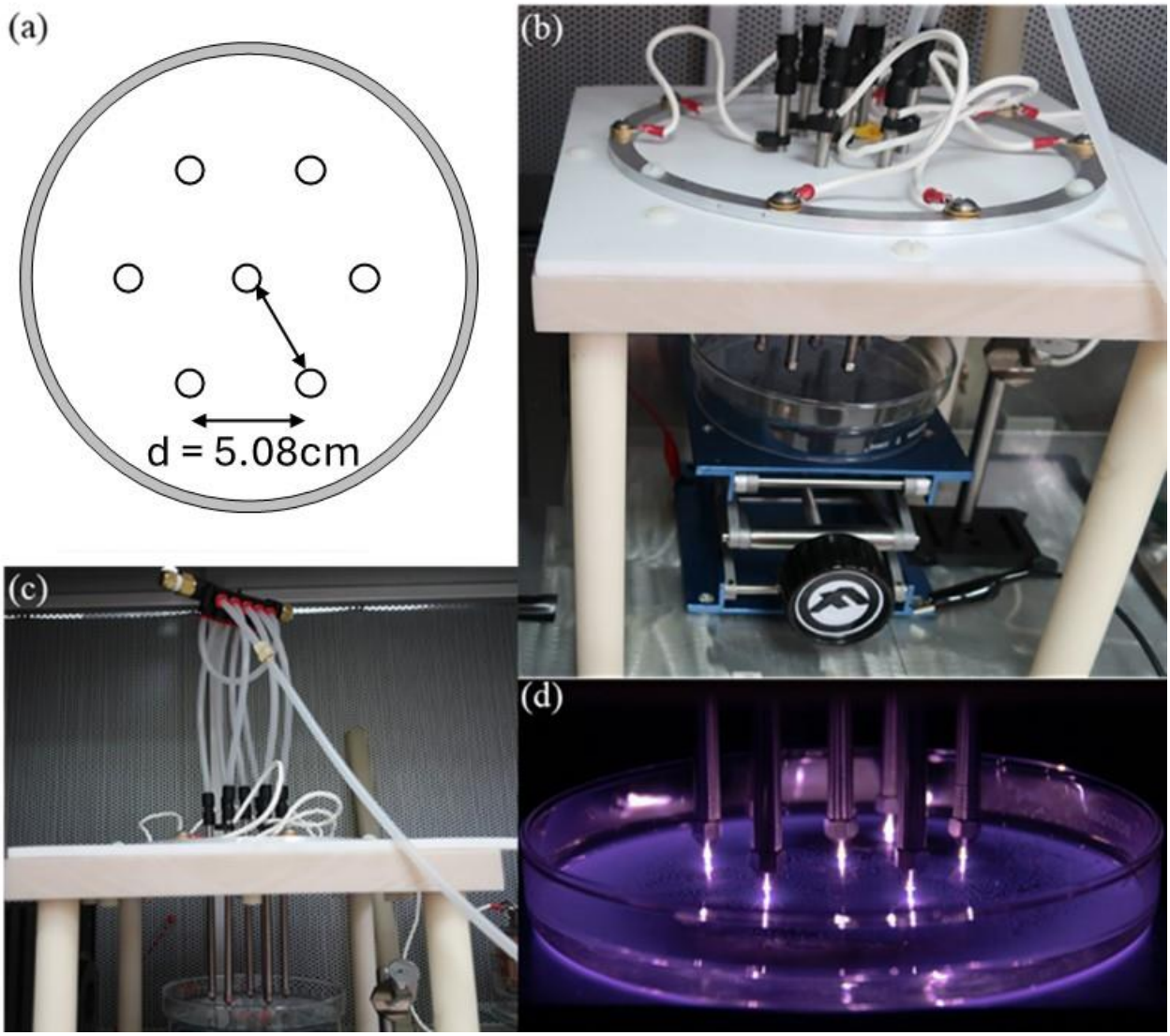

Figure 4.5 (a) Cold plasma oxidation setup single jet; scale-up to 7 jets in a hexagonal layout (Hexjet): (b) and (c) pictures of the setup; (d) picture of the plasma in operation

While initial tests using deionised (DI) water proved to be fruitful and led to impressive pictures, (cf. Figure 4.5(d)), the following problem was encountered in the presence of Rhodamine B: The discharge initially ignites on all seven jets but over time reduces from seven jets in parallel to only a single one in operation. While initially, the first few jets stop igniting within 1-3 minutes, this phenomenon increased in speed after 3 to 4 minutes of treatment, such that eventually only a single electrode ignites. Multiple factors influence this behaviour, and which jet ignites depends on

electrical, geometric, and gas flow conditions. The problem mainly arises from differences in the individual impedances of each nozzle head, originating from its distance to the liquid, as well as its status of plasma breakdown. Breakdown occurs on the nozzle with the lowest impedance, which causes that nozzle's impedance to drop significantly, resulting in a reinforced path towards plasma ignition in that nozzle and an increased current flowing through that nozzle, ultimately leading to a strong plasma ignited on only a single nozzle head.

An improvement to optimize homogenous breakdown across the plasma jets concerned the homogeneous gas flow conditions to achieve equal distance of the individual nozzles to the water surface. The gas flow distribution was improved over a few iterations and simulations by developing a uniform gas flow diffuser (cf. Figures 4.7 and 4.8).

In the first iteration, each nozzle was connected directly to a gas line (cf. Figure 4.5c). This resulted in significantly varying gas flow conditions for each nozzle as could be observed by the different dip depth forming in the liquids under each jet nozzle.

In the second iteration, the gas lines were replaced by a common mixing chamber volume, in which the plasma jet tubes were directly inserted, with the possibility to adjust each jet's individual height above the water (cf. Figure 4.6 – Prototype 01). Simulations using SolidWorks showed that the flow conditions are favouring the gas flow through the central nozzle. Prototype 02 (Figure 4.6 center) introduced two sets of diffusor plates inserted into the gas mixing chamber with an improvement of the flow homogeneity. Only 3 diffusor plates, however, allowed to establish a homogeneous gas flow through each of the seven plasma jets, as shown for the simulations of prototype 03 (cf. Figure 4.6 right). This design was ultimately implemented and is shown (together with the electrical circuitry improvements) in Figure 4.7. Both improvements together finally allowed a homogeneous breakdown across all jet electrodes at the same time.

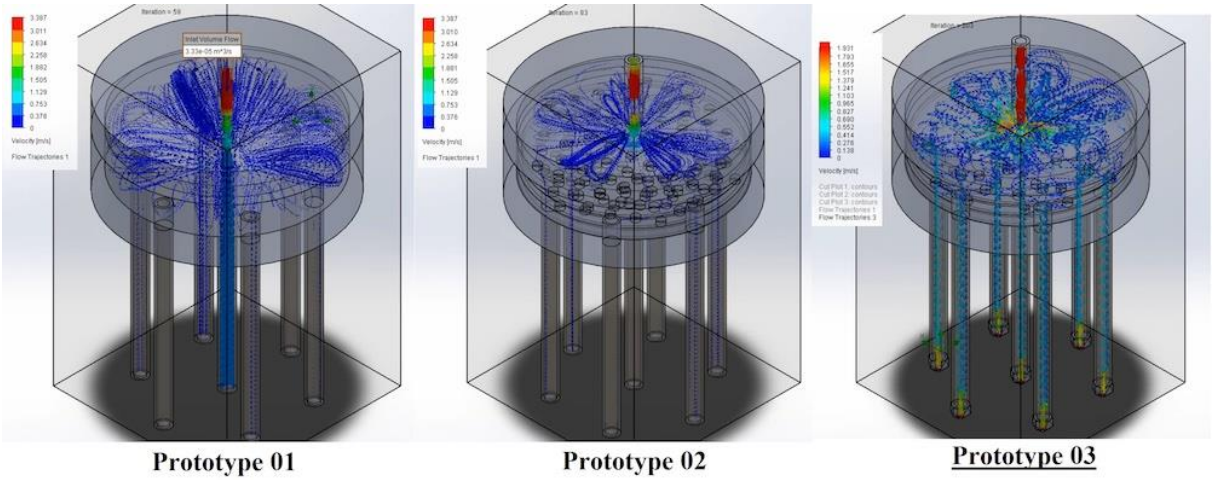

Figure 4.6 Gas flow simulations during different development stages; prototype 3 was the final development stage.

In addition to the improvement of gas flow, the discharge homogeneity was improved also by limiting the current in each nozzle using impedances as ballast. Figure 4.7 shows implementations of ballast resistors on each nozzle. The configuration is chosen in a symmetric configuration with a common ring ground surrounding the jets.

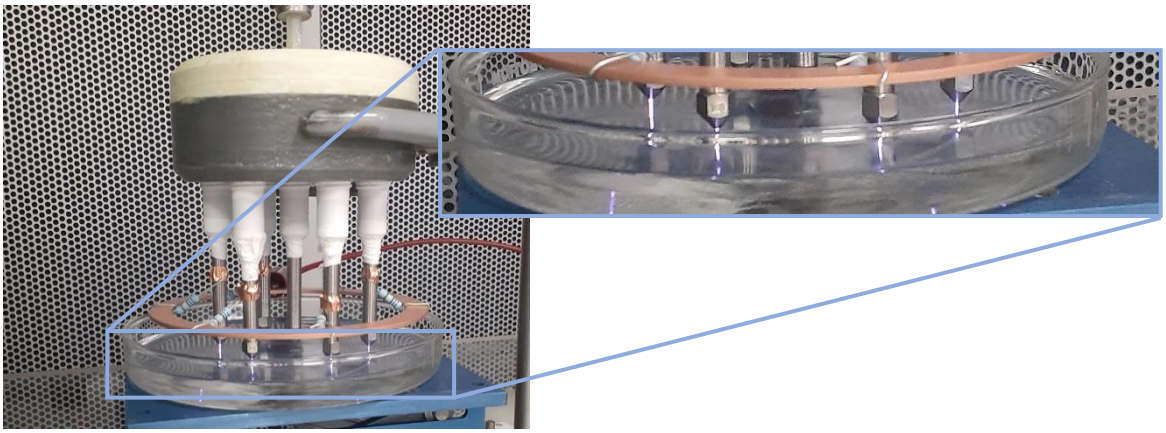

Figure 4.7 Simultaneous plasma operation of six parallel pin electrodes with homogeneous air flow.

While parallelisation of the plasma source using a uniform gas flow and the implementation of ballast resistors was achieved, the reactor design exhibited a flaw for scaling and application purposes. Since the electrode-plasma combination is in direct contact with the liquid, which acts as a grounding electrode, the efficiency of the plasma treatment will be related to the liquid

conductivity, which can change overtime during the treatment, but also from one liquid type to another. For the following studies, it was therefore decided to move the exploration to a plasma reactor which would be independent of the liquid conductivity. In the following studies, a gliding arc with water independent electrodes was developed and used for the application studies.

4.3 Gliding arc discharge design

For the gliding arc design, a 2D-electrode geometry was chosen. The gliding arc is placed in a beaker system over a liquid surface (cf. Figure 4.8). The electrodes are held in a 3D-printed lid that is inserted into the beaker and sealed off with Teflon tape. The lid has one centre opening in which a quartz tube is inserted as gas inlet; additionally, two holes serve as gas outlet. This design ensures a controlled gas atmosphere determined by the feed gas composition, while the gliding arc is operating at atmospheric pressure.

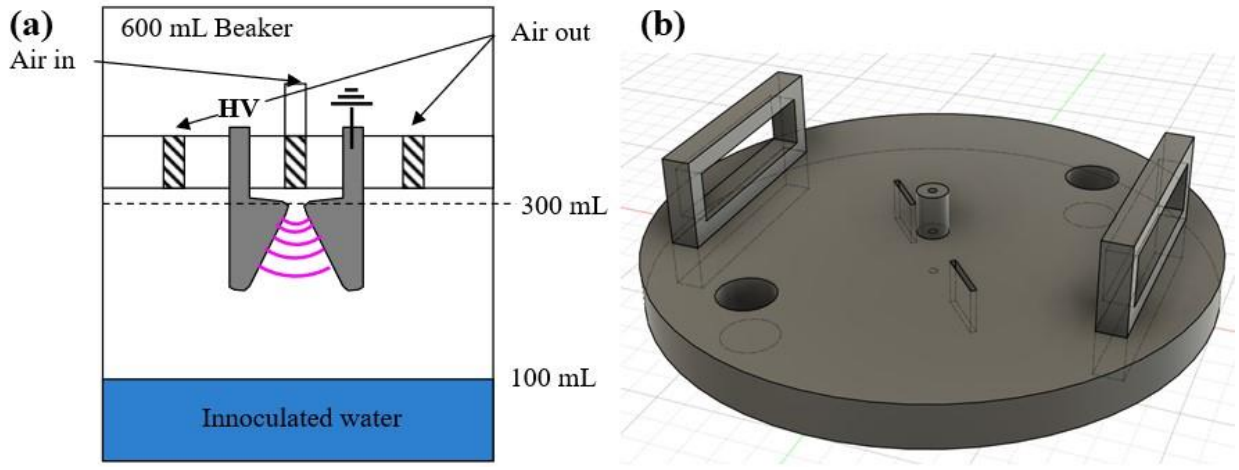

Figure 4.8 (a) schematic representation; (b) CAD design of the 3d printed lid. Two holes in the cover structure (ca. 10 mm Ø) serve as gas outlets. Thus, the reactor is open to ambient pressure, but the gas composition is controlled within the treatment chamber.

The initial prototypes were developed using a copper filament over a 3D printed structure mount (Figure 4.9 (a)). While this setup offers rapid adaptation possibility for electrode shapes, the epoxy used to hold the electrodes is subject to degradation during plasma treatment and interacts with the plasma. Furthermore, copper electrodes oxidise too rapidly for long term use. Therefore, a second prototype, using water jet cut flat stainless-steel electrodes, was developed, as presented in Figure 4.9 (b).

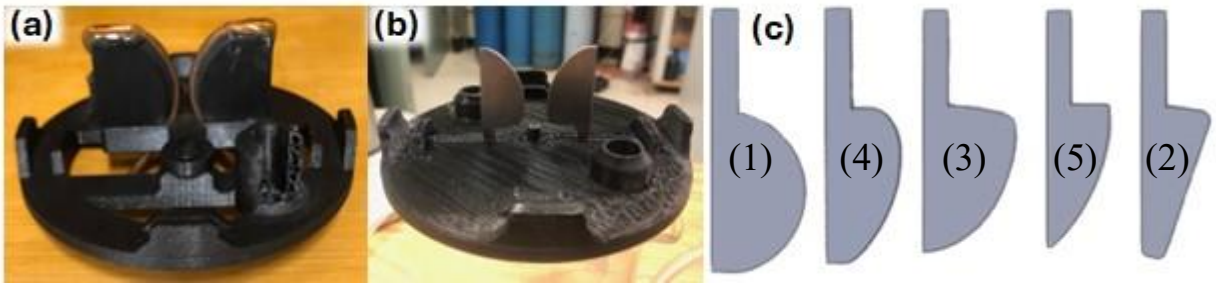

Figure 4.9 Prototype development steps for a gliding arc; a) Initial copper electrodes prototype; b) replacement of electrodes for stainless steel; c) various electrode geometries studied along with reactor b) design. The numbers correspond to the electrode shape as found in figure 4.10.

To increase the nitrogen species generation efficiency of the gliding arc discharge, the plasma properties were modified by changing the electrode geometry and furthermore by varying the inter-electrode distance (cf. Figure 4.10), the feed gas humidity from 0 to 75 RH%, the gas flow 1-10 slm, and the water composition (miliQ, distilled water, and tap), as well as by changing the way the gliding arc interacts with water. With these approaches, it was possible to increase the efficiency of nitrogen species (with nitrite concentration as nitrogen representative species) incorporation into the liquid by a factor of 5-10, compared to the initial prototype.

Changing plasma properties in a gliding arc can be achieved by changing the electrode geometry. Changing the electrode geometry, based on geometries found in literature [86-88], has a direct impact on the spatial distribution of the thermal vs. non-thermal plasma regions of the gliding arc. As a gliding arc is progressing, it can be categorised into the following three phases [86]:

1) the reagent gas break-down,
2) the equilibrium heating phase and
3) the non-equilibrium reaction phase

The reagent break-down phase is directly linked to the inter-electrode distance, applied voltage and gas composition. The geometry of the electrodes will have an impact on the different geometrical lengths of phases 2 and 3, allowing to find the ideal thermal non-thermal equilibrium ratios for the generation of NO_x.

The extended Zeldovich mechanism [89], with of the 3 reactions (4.1 to 4.3):

$$N_2 + O \rightarrow NO + N \tag{4.1}$$

$$N + O_2 \rightarrow NO + O \tag{4.2}$$

and

$$N + OH \rightarrow NO + H \tag{4.3}$$

is responsible for the thermal generation of NO in phase 2 [31, 49]. While under phase 3, with lower temperatures only reaction (3) remains dominant, and less atomic oxygen is produced. Changing the geometry therefore has a direct impact on the chemical species present in the plasma phase.

To study the effect of electrode geometry on nitrite generation efficiency, five electrode shapes were designed (cf. Figure 4.9c). The nitrite concentration was determined for different electrode shapes and different electrode distance between the closest points of the electrode (spark gap).

The results are shown in Figure 4.10.

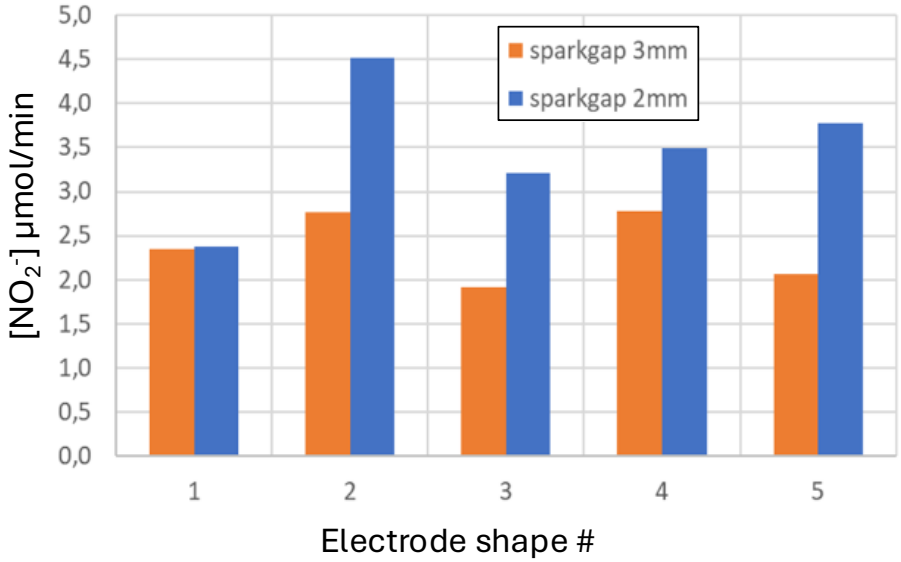

Figure 4.10 Nitrite generation rate comparison between electrode shapes (cf. Figure 4.9 c) The highest nitrite concentration was achieved for electrode shape 2 at a spark gap of 2 mm, which was then chosen for subsequent experiments.

To allow for treatment of larger volumes of water, this electrode configuration was used in a recirculating system described in Chapters 4 and 5. For this recirculating system, 4 holes were made for a water recirculation system with the same constricted flow: 2 holes for water circulation and 2 holes for the gas outlets. The water circulation was brought to the beaker with the use of glass tubes within the beaker space, to not have combustible polymer tubes in the discharge chamber. The results with this discharge systems are presented in Chapters 5 and 6.

A second, successful approach to increase nitrogen species generation in the plasma treated liquid was to change the way the plasma activated gas interacts with the liquid: for this, the electrode support was fitted air-tight within the beaker without any holes other than in the beaker wall so that the gas would be forced to go through holes in a beaker (6 of about 2mm Ø in a hexagonal pattern), as seen in Figure 4.11. This design allowed the same plasma liquid interaction as in the previous gliding arc setup, with a beneficial addition of a bubbling process that enforces a stronger diffusion of plasma generated species into the liquid. This plasma source design has demonstrated increased nitrite generation compared to the one used in Chapter 6 (about 2-3 times more), using a slightly forced diffusion (<5 psi) through bubbling on the side of the beaker.

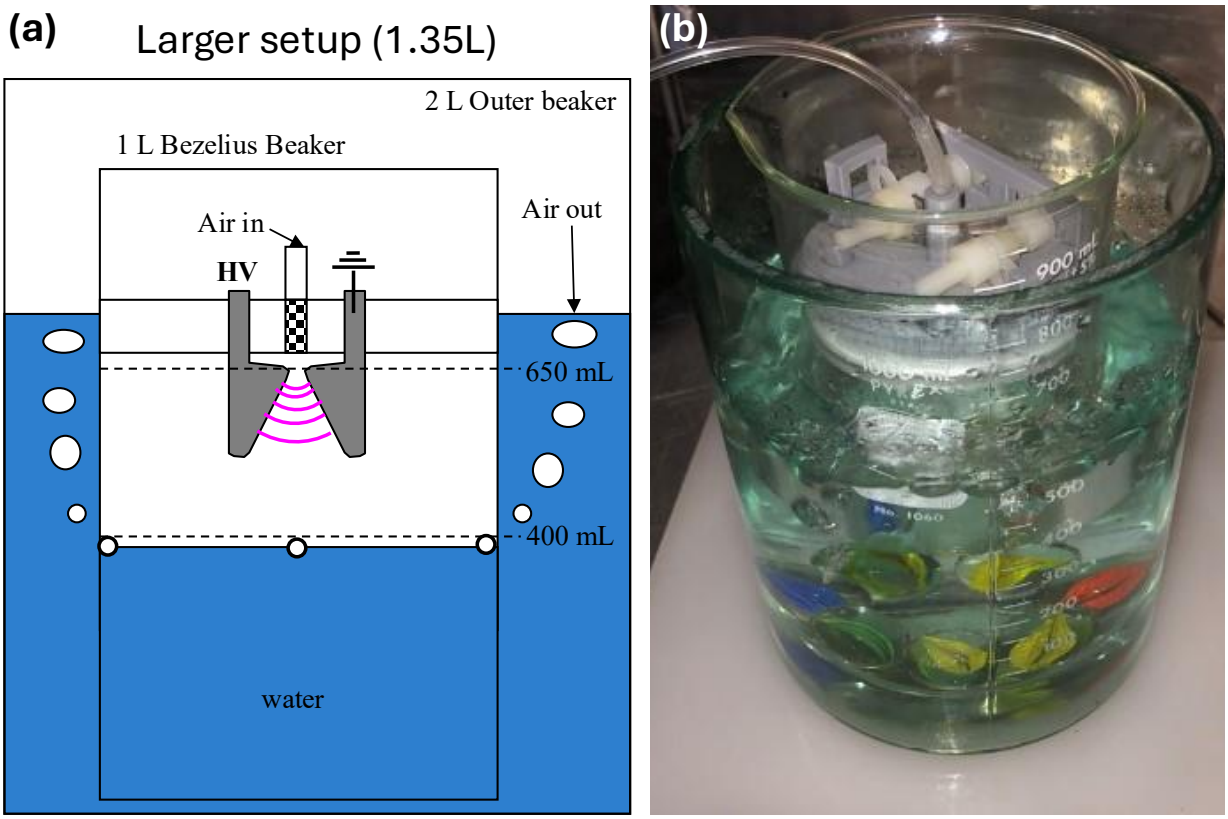

Figure 4.11 Larger water treatment reactor, making use of forced diffusion to increase species generation. (a) schematic representation; (b) photograph of the gliding arc in operation. The glass beads at the bottom act as a counterweight to counter buoyancy.

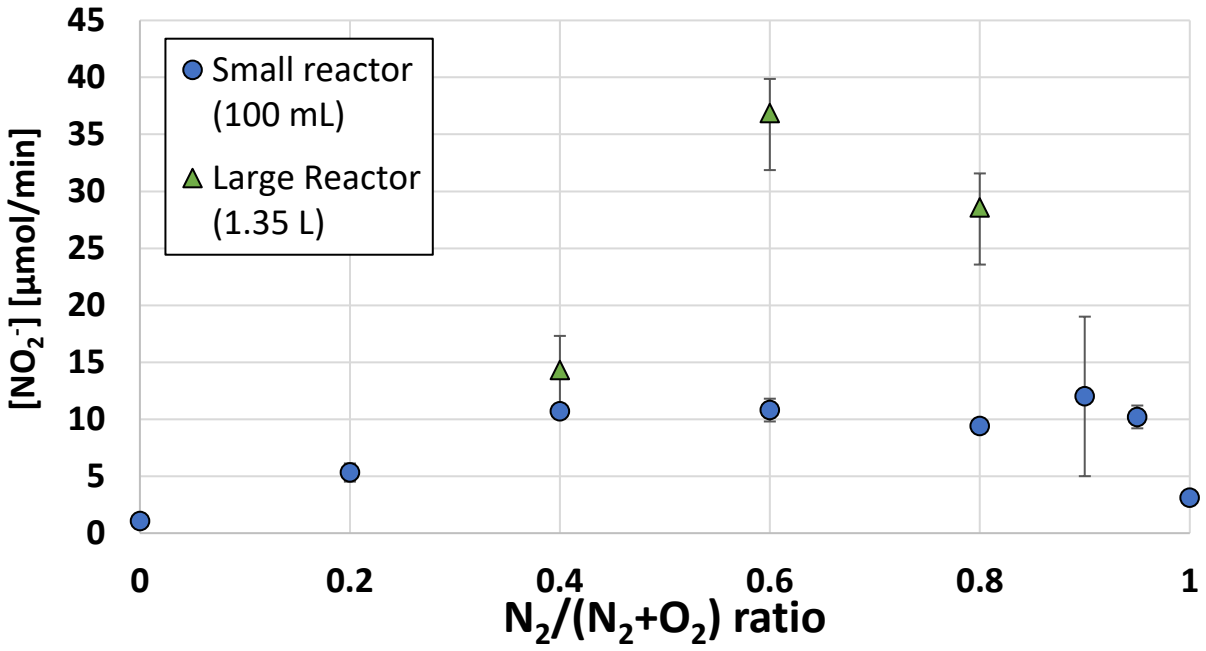

Figure 4.12 Nitrite generation rate comparison between small and larger reactor with bubbling. Note that these values are different than those presented in Chapter 6, for further optimization was achieved in between. Gliding arc discharge over tap water, 60 % voltage (low) and 0.3 A at resonant frequency.

Figure 4.12 shows the results of the nitrite concentration generation of the small reactor design (cf. Figure 4.8) compared to the large reactor design (cf. Figure 4.11). The measurements are done under variation of gas composition in the reactor chamber. Under optimal conditions, the generation rate of nitrite is four times larger for the large reactor chamber with bubble reactor than for the small reactor. The application studies were, nevertheless, performed with the small reactor, due to its higher characterisation at the time where tests with plants were required.

While further optimization of the diffusion can be achieved, using a better diffuser or a venturi, the experiment was nonetheless a success in improving the reaction rate from the initial prototype (cf. 4.10 a)) which produced 3 µmol/min. The improvement was of a factor ca. 10 for in air conditions, and highest production condition (R = 0.6).

4.4 First steps with a microwave system

From literature, both gliding arc and microwave plasma show promise for nitrogen species generation [20] when compared in terms of species generated per energy amount. A microwave source can be designed to generate a plasma under atmospheric [8] or close to atmospheric conditions such as under a venturi vacuum. Microwave sources are known for producing a high amount of reactive species, and scalability of power sources has already been investigated and can be commercially available at high power. The following works are exploratory and preparatory for future work.

Taking advantage of the presence of three microwave sources in the lab, the initial investigation aimed to determine if they could be rendered operational anew, using in-house equipment. These 2.45 GHz microwave power sources are available dating from the 1960's (Varian, USA) the 1980's (Gerling Moore, USA) and 1995 (Muegge, Germany), all capable to deliver over 1 kW of continuous wave power. The first experimental plasma setup using a slow wave applicator, patented in earlier work at Polytechnique [90], is powered with the Muegge power supply and adapted to work at atmospheric pressure. After repair work, including some within the power supply, the equipment has again been rendered operational. Schematic and photographic views of the setup are shown in Figure 4.13.

The first step in operating the microwave generator was to perform the safety check of the different components: a microwave probe calibrated at 2.45 GHz was used in this case to verify that the radiated power (on a low setting first, then at full load) does not exceed 10 mW at any given point other than the slow wave applicator structure. Once the safety test was conducted, the 3 stub-tuner was adjusted to maximize the forward power and reduce the reflected load as much as possible. The first experiment was conducted under atmospheric conditions. In this test, it was so far not possible to ignite a plasma.

In the next steps, a gas cover was designed for injecting gas from above (Ar at 1 slm), and a second cover below to lower the pressure inside the glass tube, down to 20 kPa, roughly 20% of 1 atm. An external Tesla coil was used to attempt to trigger the discharge, however, at the given pressure conditions and with the given plasma source geometry, no plasma ignition was achieved. In a second attempt, the Varian resonant cavity geometry as applicator (also present in the laboratory) was tested unsuccessfully in similar pressure and conditions as the previous test.

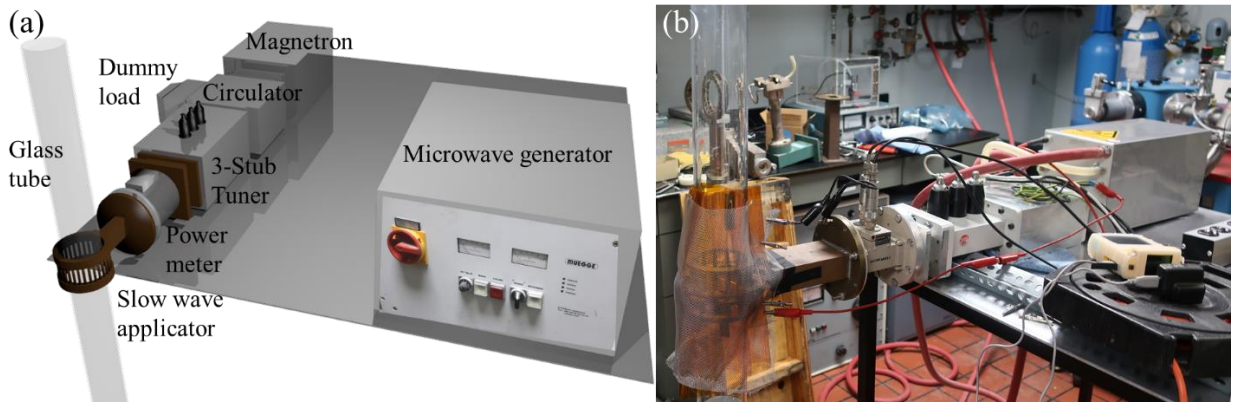

Figure 4.13 Schematic (a) and picture (b) of the first microwave setup.

Having failed to start a plasma with the equipment in the lab, a new applicator was acquired: a Surfaguide® applicator (SAIREM, France), along with a sliding short and relevant quartz tubes. This new setup is presented in Figure 4.14, where i has been installed on a cart for mobility purposes. Similar to the earlier system, the first component of the plasma system consists of the magnetron, which generates the microwave radiation, which is sent through the circulator, a device which prevents reflected power from being transmitted back to the source but instead redirects it to a dummy load. After the circulator, a 3-stub tuner is used to control transmission efficiency into the system. The plasma is then generated inside a vertical quartz tube (absent in this image) inside the applicator, and the excess microwave power is reflected at the sliding short.

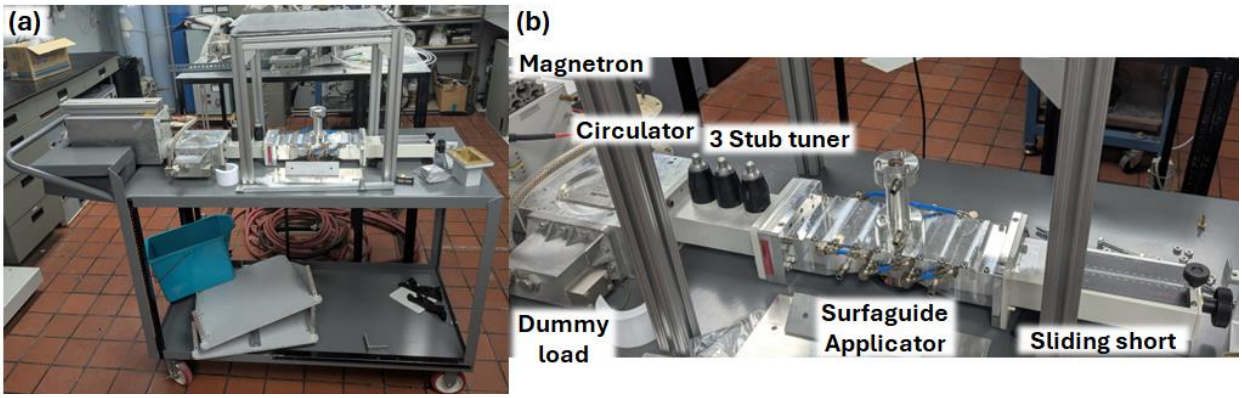

Figure 4.14 Cart assembly of the new microwave system (a), and picture and explanation of the different component of the system.

The system has been set up and designed, ready for deployment in a plasma-liquid system. While this scaling approach was considered, further development of this plasma source is deferred to future works.

CHAPTER 5 ARTICLE 1 : ELECTRIFYING GREENHOUSE AGRICULTURE: COLD ATMOSPHERIC PRESSURE PLASMA TECHNOLOGY FOR PYTHIUM ULTIMUM CONTROL

Sean Watson, Fady Abdelmalek, Élodie Larouche, Mylène Généreux, Julie Monette, Caroline Côté, Emilie Bédard, Jason Robert Tavares, Michael R. Wertheimer, Stephan Reuter

Published in: Environmental Technology & Innovation.

Publication date: April 22nd 2025

5.1 Abstract

Hydroponic growth of food plants in greenhouses is of rapidly increasing importance to assure future autonomy of food supply, especially in harsher climate zones. Greenhouse culture yields are drastically reduced by pathogenic microorganisms that cause root rot in plants. In Canada, the fungus *Pythium ultimum,* which can survive harsh winter conditions, has a particularly large impact on food production. In this work, we present cold physical plasma treatment of liquids with a gliding arc plasma as a novel approach for combating *pythium* growth in liquid media. This study is based on exploring air or other N_2 + O_2 mixtures as a parameter to identify which plasma treatment is best suited for its anti-fungal activity in different media. If sourced from renewable energy and water, the proposed treatment is intrinsically sustainable. 3 media conditions are explored: first distilled water, to identify the production of highly reactive oxygen species (ROS) and reactive nitrogen species (RNS). Second, an inoculated distilled water is used in conjunction with an ELISA assay as a quick response indicator. Third, a Sabouroud 2 % dextrose broth, is used as a culture media in which oomycetes are grown subsequent to plasma treatment, and hyphal mass is compared between untreated and treated samples. Extracting a subset of 80+ chemical reactions from the available literature and databases, a reaction scheme is proposed accounting for liquid-vapor equilibria (through Henry's coefficients) and reaction rate analysis. The most promising plasma treatment condition was found to be using a 95 % N_2: 5 % O_2 gas mixture with a treatment time of 30 min, reducing hyphal mass growth from 1.8 g to 0.4 g over 1 week in Sabouroud broth. The pythium degradation process was observed through scanning electron microscopy (SEM) analysis, showing that Sporangium or oogonia containing structures that terminate the pythium's hyphae have been broken and significantly reduced after plasma treatment.

Keywords: (6-12)

Plasma agriculture; plasma liquid interaction; *pythium ultimum*; fungal inactivation by cold plasma; non-thermal plasma; reactive oxygen and nitrogen species

5.2 Introduction

Rising food insecurity due to climate change and inadequate supply-chain control [91] highlight the need for local and year-round farming technologies such as greenhouse farming. Agriculture in general and indoor farming specifically contribute significantly to greenhouse gases in the atmosphere through the use of carbon intensive nitrogen fertilisers that relies on fossil fuel as cheap source of hydrogen required for its production [4, 92], and through the use of chemically produced pesticides that are also based on fossil fuel educts. As an example, chemically produced fungicides are responsible for between 12 to 30 kg CO_2 emission per kg of produce [93, 94]. Canada's rigorous climate over much of the year strongly favours food production in greenhouses and Canada's agricultural landscape is set to change drastically with the volume of greenhouse crops on track to double by 2025 compared to 2020 [95]. The move towards reliable and climate independent indoor farming, especially in harsher climates such as Canada's, requires decisive steps towards an electrification of greenhouse farming based on renewable sources of energy.

During the humid summer months in Canada, persistent pathogens slow down production in what should be a greenhouse's peak revenue season, resulting in sizable percentages of produce loss. An example of one such destructive pathogen family is the fungus *Pythium ultimum*, which attacks the plants' root system [74, 96]. *Pythium* spp. are plant-damaging, pathogenic oomycetes that are widespread in agricultural soils and water sources. They can inflict significant harm either on their own or in conjunction with other pathogens. *P. ultimum*, in particular, is accountable for various plant ailments such as damping off and wilting in certain crops. While safeguarding against pathogens is essential, relying on chemical fungicides in indoor farming is not sustainable as a long-term solution and may carry potential health risks for agricultural workers and consumers [74, 96].

In this study, we investigate the use of cold atmospheric pressure plasma as means to replace chemical fungicides with the aim to further the electrification of greenhouse farming. Cold atmospheric pressure plasma sterilization has been intensely studied for agricultural and medical applications over the past few decades [97, 98]. Atmospheric pressure plasma can produce

chemically reactive atoms, radicals and molecules, so-called reactive oxygen species (ROS) and reactive nitrogen species (RNS) [7, 98, 99]. Reactive oxygen/nitrogen species (RONS) are important for all living organisms and play major roles not only in plasma-based sterilization, but also in fertilization for the growth of plants [7, 99]. The correlation between plasma-generated RONS and antibacterial/antifungal effects has been widely discussed [98, 100]. Gaseous RONS produced from ambient air by various atmospheric pressure plasma-generating techniques can be transported downstream *via* the gas flow toward a liquid phase target, for example a stationary or flowing reservoir of tap water [101]. The resulting plasma treated water (PTW) can be jointly exploited to combat harmful plant-borne microorganisms, as well as provide nitrogen-containing plant nutrients [100]. Some of the most frequently investigated RONS are singlet oxygen, hydroxyl radicals, peroxynitrites ($HOONO_{(aq)}$/ $ONOO^-_{(aq)}$), peroxynitric acid (PNA, $HOONO_{2(aq)}$), hydroperoxy radicals, ozone ($O_{3(g)}$/$O_{3(aq)}$), and hydrogen peroxide ($H_2O_{2(aq)}$), measured in the gas phase and/or in the liquid phase. The treatment of water by plasma – while requiring initial financial investment in the plasma- and gas-handling infrastructure – is a sustainable technology that is environmentally benign, involving only ambient air, water and electricity.

Contaminated substrates can be treated either directly via the generation of plasma-activated gas (e.g., plasma-processed air, PPA) or indirectly via plasma treated liquids (e.g., plasma-treated water, PTW) [102-105]. Recent studies demonstrated the inactivation of *P. ultimum* mycelia after treatment with PPA [106]. The vegetative state of *P. ultimum* was inactivated and prevention of spore formation was presumed, as no growth of mycelia in any of the plasma treated samples was recorded over a period of 14 days. These PPA experiments highlight the role plasma can play in plant pathogen control. The use of PTW, however, is much more practical and applicable in a greenhouse setting. The technological approach of PTW presented in the present work is based on gliding arc technology [54, 104, 107, 108]. The advantage of gliding arcs is that, due to their transitional nature, they have a high electron density and current comparable to thermal plasmas. However, they operate at a low gas temperature and high electric field, which is more commonly found in non-thermal plasmas. Due to their properties, gliding arc discharges are well-suited for treatment of liquids for pollutant abatement in the scope of sustainable environment [54, 104]. To summarize: in this work, we use cold atmospheric pressure plasma to generate fungicidal agents using only electricity, air, and water means to replace chemical fungicides. Our study demonstrates the capability of plasma treated water to combat the plant pathogen *P. ultimum.*

5.3 Experimental methodologies

5.3.1 Plasma source

Figure (a, b) shows a schematic representation and a photograph of the gliding arc device used in this work. The plasma was sustained from a PVM500 resonant high voltage power supply with a 2500 secondary coil (Information Unlimited Inc., Mont Vernon, NH, USA). The resonance frequency was around 24.5 kHz, the voltage was kept at 60% of the single voltage mode, typically 4-6 kV across the electrodes, and the current measured on the power supply was 0.3-0.4 A, for an average power of 27W. One of the two gliding arc electrodes was connected to the power supply, while the other one was grounded.

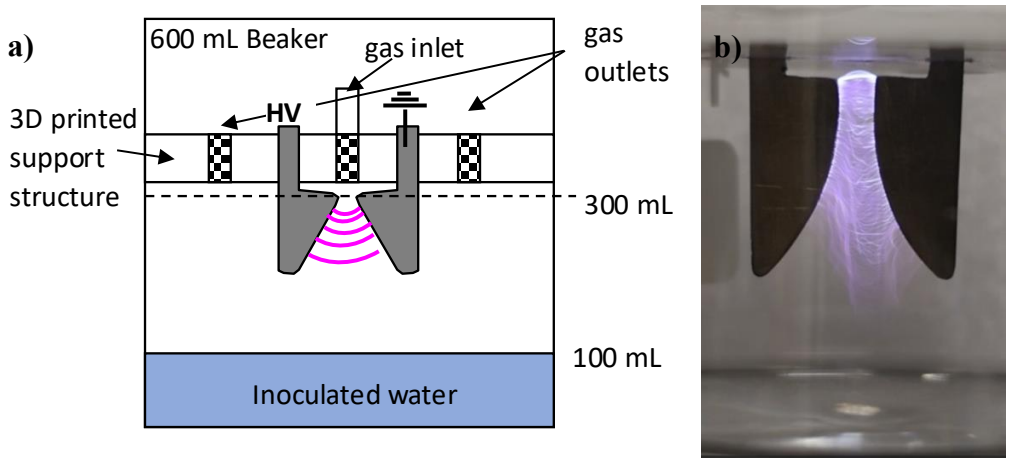

Figure 5.1(a) schematic representation; (b) photograph of the gliding arc device used in this work.

The electrode geometry facilitates the basic properties of a gliding arc: initiated as a thermal arc with gas temperatures around 3000 to 5000K, the moving gas flow and expanding electrode gap distance transforms this initially thermal arc into a non-thermal plasma, cooling the temperature to below 1000K. The electron temperature is about 1 eV and the vibrational temperature remains elevated. About 75% to 80% of the electric energy can be dissipated in the non-thermal plasma region. The hybrid thermal and non-thermal character of a gliding arc make it an ideal plasma source for environmental applications and gas conversion.

In the gas phase, atmospheric pressure cold plasmas in air (or other N_2+O_2 mixtures) contain charged particles (electrons and ions) and reactive species such as ozone (O_3), singlet oxygen ($^1O_2$), and several radicals, mainly superoxide ($O^{\cdot}_2$), hydroxyl ($^{\cdot}OH$), nitric oxide ($^{\cdot}NO$), and nitrogen

dioxide (NO_2). The dissolution of these species in the adjacent water bath (see Figure 5.1(a)) then gives rise to a diversity of short-lived species (µs to second lifetime) and longer-lived species (second to hours/days lifetime) species, cf. to [32]. Of particular importance for biological effects, there are three primary, long-lived species: hydrogen peroxide (H_2O_2), nitrite (NO_2^-) and nitrate (NO_3^-) [63, 104]. Consequently, quantitative detection of these three species will represent the basic criterion for plasma source characterization, and effectiveness with regard to the biological activity associated with PTW. This is described in some detail in section 2.3. A key variable examined in this work was the N_2 / O_2 gas mixture ratio R (equation 5.1):

$$R = [N_2/(N_2 + O_2)] \tag{5.1}$$

R was varied from the subset including (0 0.2 0.4 0.6 0.8 0.9 0.95 1). A second key variable was duration of plasma exposure of the water bath (10 and 20 minutes for ELISA; 15 and 30 minutes for hyphal mass growth, both described in section 5.3.4), the aim being to optimize treatment effectiveness, while maintaining other conditions nominally constant, for example gas flow rate (5 slm total) and applied power.

In order to determine the reaction rates at each gas mixture, tap water underwent plasma treatment to identify the species generation over time (at 0, 0.5, 1, 2, 3 and 4 min) for each of the ratios R identified above, and in technical triplicates. The characteristics of the tap water are recorded for the municipality of Montreal [109].

From these first points, a linear regression is obtained and allows to quantify the reaction rates of the longer-lived species as a function of time. This production is subject to change as a function of pH and temperature; it is only valid if, as in our case, the total concentration of each longer-lived species is below its respective solubility limit. Performing the experiments with dextrose broth directly, instead of with tap water, was prohibited due to the natural optical absorption of dextrose, both in the 407 and 540 nm regions, which interferes with interpretation of the colorimetry results. Measuring the nitrite concentration requires to quantify the absorption spectra at 407 nm, due to the purple azo die, while the titanium oxysulfate is measured at 540 nm.

5.3.2 Design of experiment

In this manuscript, the investigation was first carried out to identify the 3 major reactive species generation (NO_2^-, NO_3^- and H_2O_2) while varying the ratio of nitrogen to oxygen (R). This was done

by sampling 3 x 100 µL (in triplicates for each reactive specie) from 100 mL tap water at intervals of 0, 0.5, 1, 2, 3 and 4 min subsequent to plasma exposure.

In order to identify the efficiency of the plasma treatment with regards to pythium inactivation, the second test was to use the ELISA test for 8 conditions: (Inoculated and distilled water, R=0: 10 and 20 min, R=0.8: 20 min, R=0.95: 10 and 20 min, and R=1: 20 min). The samples were derived from inoculating distilled water with two pythium agar plates in 700 mL: 6 x 100mL were used for the plasma treatment conditions, while the extra 100 mL was used for the inoculated water condition. The samples were filtered and concentrated; 3 technical replicates were collected before following the ELISA procedure.

As a second complementary method to the ELISA, a hyphal mass growth was conducted for 7 conditions: a control sample, R=0: 15 and 30 min, R=0.8: 15 and 30 min and R=0.95: 15 and 30 min. The initial sample consisted of 10 mL of SBD containing a highly concentrated *Pythium ultimum* content inoculated in 90 mL of distilled water. The sample then underwent plasma treatment, from which a subsequent 3 x 10 mL were divided and added to 240 mL of SBD for a 7-day growth cycle.

Finally in order to understand more about the process of *Pythium* inactivation and underlying chemistry, 2 samples (control and R = 0.95, 30 min) were taken for SEM imaging, and the pH and Temperature were investigated for both tap water and SBD conditions.

The conditions are summarized in Table 5.1 below. Further details about each process are presented in the subsequent sections of the methodology.

Table 5.1 Analysis, conditions, and sample size summary

Analysis type	**Conditions**	**Replicas**	**Total samples**
Reactive species	R = [0, 0.2, 0.4, 0.6, 0.8, 0.9, 0.95, 1]: 0, 0.5, 1, 2, 3 and 4 min	Technical : 3	$9 \cdot 6 \cdot 3 \cdot 3 = 486$
ELISA	Negative and positive control Innoculated and distilled water. R=0: 10 and 20 min, R=0.8: 20 min, R=0.95: 10 and 20 min, and R=1: 20 min.	Technical: 3	$10 \cdot 3 = 30$
Hyphal mass growth	Control R=0: 15 and 30 min R=0.8: 15 and 30 min R=0.95: 15 and 30 min	Technical: 3	$7 \cdot 3 = 21$
pH and Temperature	R=0: 30 min, distilled water and SBD R=0.8: 30 min, distilled water and SBD R=0.95: 30 min, distilled water and SBD		6
SEM	Control, R = 0.95 : 30 min		2

5.3.3 Materials and chemicals

N_2 gas and O_2 gas (99.9 + % purity, alphagaz 1) were acquired from Air Liquide Canada, Ltd., Montréal. Sabouroud 2% dextrose broth (SDB), corn meal agar (CMA), phosphoric acid H_3PO_4 (10 % v/v), stabilized reagent grade hydrogen peroxide H_2O_2 (3% w/w), sulfuric acid H_2SO_4 (4.00 $\pm$ 0.04 N, 2M) and 96-well plates (Thermofischer BioLite^{TM} #130188) were obtained from Fisher Scientific (New Hampshire, USA). N-(1-naphthyl) ethylenediamine dihydrochloride (≥98%), titanium(IV) oxysulfate (anhydride); sodium azide NaN_3 (≥99.5%), sodium nitrate $NaNO_3$ (≥ 99.0%), sodium nitrite $NaNO_2$ (≥97%), chloroform $CHCl_3$ (≥ 99.5%), were obtained from Sigma-Aldrich. Nitrate reductase enzyme preparation (#780010), nitrate reductase cofactor preparation (#780012) and nitrate/nitrite assay buffer (#780022) were distributed by Cedarlane Labs for Cayman Chemicals. The *Pythium* spp. ELISA kit was purchased from Creative Diagnostics (New York, USA). Pure *P. ultimum* was provided by the Research and Development Institute for the Agri-environment (IRDA, Québec, Canada).

5.3.4 Detection of generated reactive species in PTW

Deionized (DI) water (MilliQ, 18 MΩ m) was used when dilution was required. Furthermore, the following liquid diagnostics methods were evaluated in a 96-well plate, using a TECAN Infinite M Nano^{+} plate reader in single absorbance mode $\pm$ 4 nm, with 25 flashes, and 2 repetitions.

Determination of nitrite (NO_2^-) concentration

NO_2^- concentration was estimated with an in-house prepared Griess assay and calibration solution, as described in [110], with reagent type A being composed of N-(1-naphthyl)ethylenediamine dihydrochloride in water at 0.0039 mol/L. Reagent B of the standard Griess assay was obtained by combining sulfanilamide (0.0581 mol/L) in phosphoric acid (5% w/w; diluted from 10%). The final Griess reagent was formed by adding reagents A and B together in a 1:1 ratio. 100 µL samples of water are then pipetted (in triplicate) into a 96-well plate and each combined with 100 µL of the Griess reagent, to form a purple azo die after 15 min. These are then measured by absorption at 540 nm with the Tecan plate reader. The detection limits of this method were determined with dilute solutions of $NaNO_2$ stabilised with $CHCl_3$ in the [3-300 µM] range. Higher concentrations (>300 µM) can be measured by dilution in DI water or in nitrate buffer, albeit with less accuracy.

Determination of nitrate (NO_3^-) concentration

NO_3^- concentration was determined with a commercial kit from Cayman Chemicals, prepared according to the supplier's instructions. Briefly, a buffer assay was prepared (100 mL DI water employed for its preparation); 1.2 mL of the buffer was used to reconstitute the enzyme and cofactor, respectively. First, 80 µL of the target liquid is sampled, to which 10 µL of the enzyme preparation was added, as well as 10 µL of the co-factor, yielding a 100 µL sample (repeated in triplicate). The enzyme was left to react for 1 h at room temperature, to reduce the NO_3^- to NO_2^-, before adding the 100 µL of our previously prepared Griess reagent. Second, 100 µL of the target liquid was immediately treated with the Griess reagent, as described in section 2.3.1. The total NO_3^- concentration was found by subtracting the amount of NO_2^- from the initial sample to that of the reduced nitrite after 1 hour. Calibration with $NaNO_3$ dilutions demonstrated that this method is valid for [3-200 µM].

Determination of hydrogen peroxide (H_2O_2) concentration

H_2O_2 concentration measurements serve as a useful indicator of ROS, in general. It was measured here as described in [111], with a few modifications, so as to increase the absorbance and lower the detection limit. Titanium oxysulfate was diluted to 0.1544 mol/L in 2M sulfuric acid, and

briefly heated and agitated to facilitate the dilution, as it is near the solubility limit. A sodium azide solution was prepared by dilution to 60 mM. This second solution's role is to inhibit reaction between H_2O_2 and NO_2^-, and thus needs to be added immediately after sampling. A triplicate sample of 200 µL was pipetted, to which 20µL of NaN_3 solution and 100µL of titanium oxysulfate solution was added to the 96-well plate cell. Calibration with stabilized H_2O_2 solution demonstrated the validity of this measurement over concentrations ranging from 10 to 500 µM.

pH and temperature measurements

Before the chemical characterization of samples, water and SDB samples were tempered for about 20 to 30 minutes to reach room temperature (21 °C) and the pH was determined using an APERA LabSen 214-6 probe. The pH and temperature were also measured after 30 min of plasma treatment using R = 0, 0.8 and 0.95 in correlation to the hyphal biomass experiments.

5.3.5 Quantitative determination of pythium inactivation

Semi-quantitative determination of *Pythium* spp. with an Enzyme Linked Immunosorbent Assay (ELISA) test

Water samples were filtered using a 0.45 µm nitrocellulose membrane following PTW exposure, to recover microorganisms on a small surface area. Within 30 minutes, the entire sample volume was filtered. Membranes were then placed in 1.5 mL tubes containing the kit's conjugate/sample buffer and vortexed for 60 sec to create a solid-liquid extraction sample. A sterile clamp was used to withdraw the membrane from the fluid. *Pythium* spp. concentrations in the extracted samples were determined using an ELISA kit (Creative Diagnostics, New York, USA). The plate was photometrically read at 405 nm, and the findings were compared to the controls. The ELISA kit's negative and positive controls were employed [112].

A concentrated solution containing two agar plates of *Pythium ultimum* was prepared and diluted 1:100. This solution was then used to inoculate four distilled water samples for plasma treatment. The plasma treatment consisted of a discharge in different gas ratios (R = 0, 0.8, 0.95), with exposures lasting 10 and 20 minutes. The analyses were carried out in technical triplicates on 96-well plates, i.e. three wells per sample. The ELISA kit included a negative and positive controls for *Pythium* spp. A blank control (non-inoculated distilled water) as well as a matrix control

(inoculated distilled water) were also added to the ELISA plate to validate the method and compare the results before and after plasma treatment.

Hyphal biomass harvesting

Pythium, are usually characterized by their production of coenocytic hyphae (singular: hypha), long, branching, filamentous structures. In most fungi, hyphae are the main mode of vegetative growth, and are collectively called a mycelium. A hypha consists of one or more cells surrounded by a tubular cell wall [74, 96, 113]. Hyphal mass growth was conducted after the plasma treatment as a *Pythium ultimum* viability indicator.

Pythium ultimum isolated from plants was cultured in corn meal agar (CMA) at 25 °C for 24 h. When the strains were ready for testing, 5.0 mL of 2 % Sabouraud dextrose broth (SDB) was added to each flask and statically incubated at 25°C for 72 h. Following incubation, aliquots of the hyphal mass (10 mL) from each flask was removed and subcultured into 250 mL flasks containing 100 mL SDB [114]. Strains were cultured at 25 °C for two days on a shaker incubator at 160 rpm. A fungal suspension (10 %) was mixed with distilled water, which was then plasma treated. Following this, 10 mL of each treated sample was placed into a 250 mL flask containing 100 mL SDB and incubated for 7 days at 25 °C. By the end of the incubation period, each of the hyphal biomasses were harvested by centrifugation at 5000 rpm for 15 min. The collected hyphae were oven-dried in air at 60 °C for 2 h, then weighed [114].

5.3.6 Scanning electron microscopy (SEM)

To assess the effect of plasma treatment, we conducted SEM analyses. Following a given plasma treatment, the hyphal biomass samples were preserved in Karnovsky's fixative solution (2% v/v para-formaldehyde and 2% v/v glutaraldehyde in 1x PBS) overnight. Samples then underwent post-fixation using 2% osmium tetroxide, followed by dehydration using a series of ethanol solutions of increasing concentration (from 50% to 100%). Finally, ethanol was substituted with hexamethyldisilazane (HMDS), and the samples were coated with a thin layer of carbon (Quorum, Q150T plus, UK) [115]. Analyses were performed on a Hitachi TM3030 plus SEM (Hitachi High-Tech Manufacturing & Service Corp, Japan).

5.3.7 Statistical analysis

To examine the significant changes between trials, a student t-test ($P < 0.05$) was used to compare the inoculated water to that of the plasma treated samples for the ELISA test, while a one-way ANOVA with the Tukey test ($P < 0.05$) was utilized for the hyphal biomass evaluation. The findings of three replicate trials were provided as the mean and standard deviation. For data interpretation, Prism 7 (GraphPad, Inc.) was used.

5.4 Results and discussion

5.4.1 Liquid phase analyses

Figure 5.2 shows a plot of measured NO_2^- and NO_3^- concentrations as a function of R, the plasma gas composition. Peroxide measurements fell below the detection limit (5 µM) for all investigated conditions.

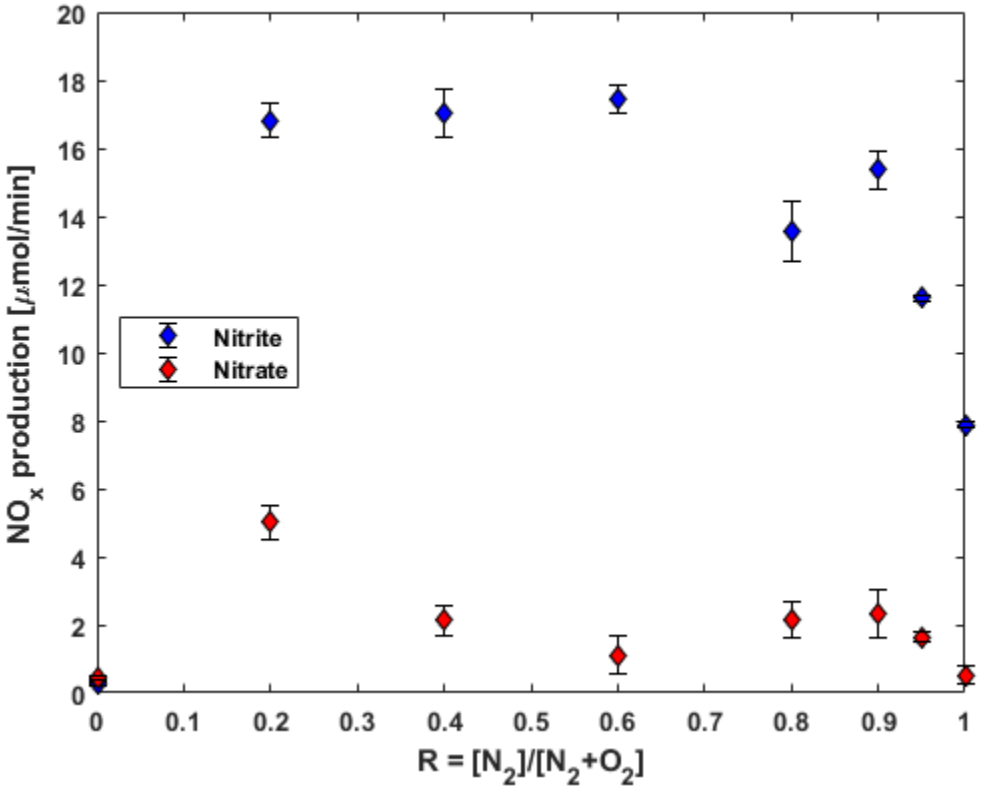

Figure 5.2 Analytical results for production of nitrite NO_2^- and nitrate NO_3^-, as a function of plasma gas composition R. Obtained from a linear regression of n = 6 samples.

The plasma generated NO_x molecules are long lived species and are indicators of the successive phases of chemical interactions. A more detailed explanation of the NO_2^- and NO_3^- production will be given in section 5.4.4, showing the most probable reaction pathways.

The three selected conditions for the successive treatments, namely R = 0, R = 0.8 and R = 0.95, produce distinct amounts of the long-lived species. R = 0 is chosen as the most oxidative composition. R = 0.8 is the closest representative to air. R = 0.95 is known to create highly reactive nitrogen species. The first produces very little NO_2^- or NO_3^-; the second produces 13.6 $\pm$ 0.9 µM/min of NO_2^-, and 2.1 $\pm$ 0.5 µM/min of NO_3^-. The third condition, with the most atomic nitrogen produces 11.6 $\pm$ 0.1 µM/min of NO_2^-, and 1.6 $\pm$ 0.2 µM/min of NO_3^-.

The pH varies differently for tap water and for SDB, due to different buffering capacities. The starting pH value for tap water is around pH 7 and the pH of SDB is normally around pH 5.6 ±0.2. Plasma treatment of tap water for 30 minutes leads to a decrease of pH from neutral to 3.20 for $R = 0.8$ and 3.10 for $R = 0.95$. In the SDB, the same conditions attain a pH of 4.56 and 4.53 respectively. Lowering pH was shown to reduce initial growth of *Pythium* in soil [[116, 117]]. The pH value of 4.5 in SDB does have a mild impact in the initial growth of *Pythium ultimum*, but this is not considered to be the dominant factor for stunted growth. A water pH value of 4 or below would have a bigger impact on *Pythium* growth but would have a detrimental effect on the plants.

The plasma treatment leads to an increase in temperature of the liquid over time. The highest temperature was 37.1°C (after 30 minutes of plasma treatment) from the initial 20 °C, for a 100 mL sample. This temperature increase corresponds to about 4 W thermal power dissipated into heating the liquid phase (out of the ~27W dissipated by the plasma). The measured temperature increase is excluded as a cause for *P. ultimum* inactivation, as described by Döring et al.: *P. ultimum* exhibits the ability to endure temperatures up to 40°C and drought (−50 % of moisture content, w/w) for a period of 4 days (96 h) [118].

5.4.2 Pythium spp. quantification by ELISA and hyphal biomass measurements

Figure 5.3 shows that the inoculated water has a higher absorbance than that of the filtered distilled water, the latter having a similar detection threshold to that of the negative control of the ELISA kit. For the R = 0, 10 min, R = 0.8, 20 min, and R = 1, 20 min treatments, the results are comparable to that of the initial sample, suggesting no decontamination. The only sample that exhibited a

significant difference with the inoculated plasma treated water samples is R = 0.95, 20 min treatment, which identifies it as the optimal condition for *pythium* inactivation by plasma. As most of the inactivation is expected at a low O_2 admixture, only the longer treatment times were considered for $R = 0.8$ and $R = 1$ to verify that the maximal inactivation was indeed at R = 0.95. The tests using the hyphal mass growth therefore aimed at longer treatment times (15 and 30 min).

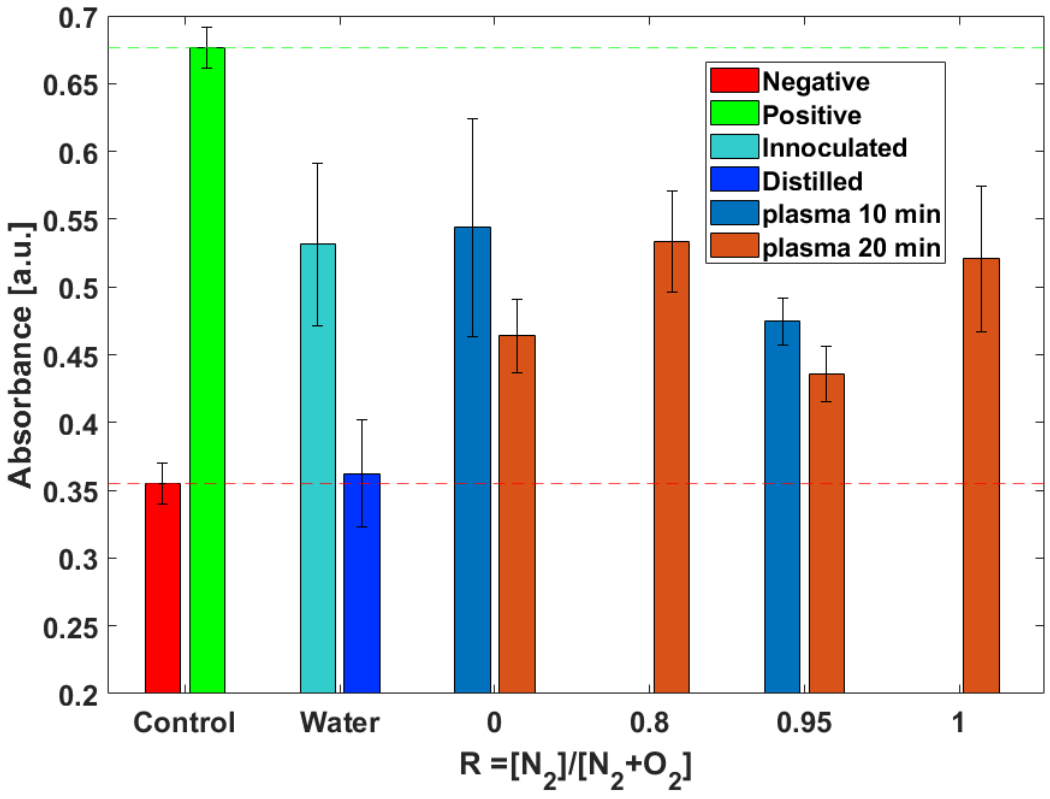

Figure 5.3 ELISA results for various *Pythium* spp. samples. The Pythium-inoculated distilled water is at the same concentration as samples which undergo plasma treatment. The PTW was as follows: R=0: 20 minutes, R=0.8: 20 minutes, R=0.95: 10 and 20 minutes, and R=1: 20 minutes. The error bar corresponds to 1 standard deviation while the bars represent the average of the technical triplicates.

To determine the influence of plasma treatment on hyphal biomass, different hyphal biomass was observed in the growth flasks after 7 days of static incubation (see Figure 5.4 a). The hyphal biomass was collected, dried and weighed to assess the impact of plasma treatment on the hyphal growth. The determined hyphal weights exhibited a significant reduction in case of R = 0.95 plasma treatment for 30 min, with weights of 0.38 ± 0.03 g in comparison with control weight of 1.83 ± 0.04 g. The results of R = 0.95 treatments for 30 and 15 min are compared in Figure 5.4b, where

the former is seen to be much smaller. This is result is expected, as the longer time of treatment increases the production of RONS that can damage the cell membranes, proteins, and DNA of the microorganisms, leading to their inactivation and death [119]. On the contrary, the observation of higher hyphal biomass when $R = 0$ was utilized raises intriguing questions about the potential role of ROS in fostering fungal growth [120]. Fungi, like many microorganisms, rely on oxygen for cellular respiration, a vital process that generates energy for their metabolic activities. High oxygen levels in the growth medium enhance respiration, allowing the fungi to metabolize nutrients more rapidly and efficiently. This results in accelerated fungal growth rates and can often lead to larger, more robust fungal colonies [121].

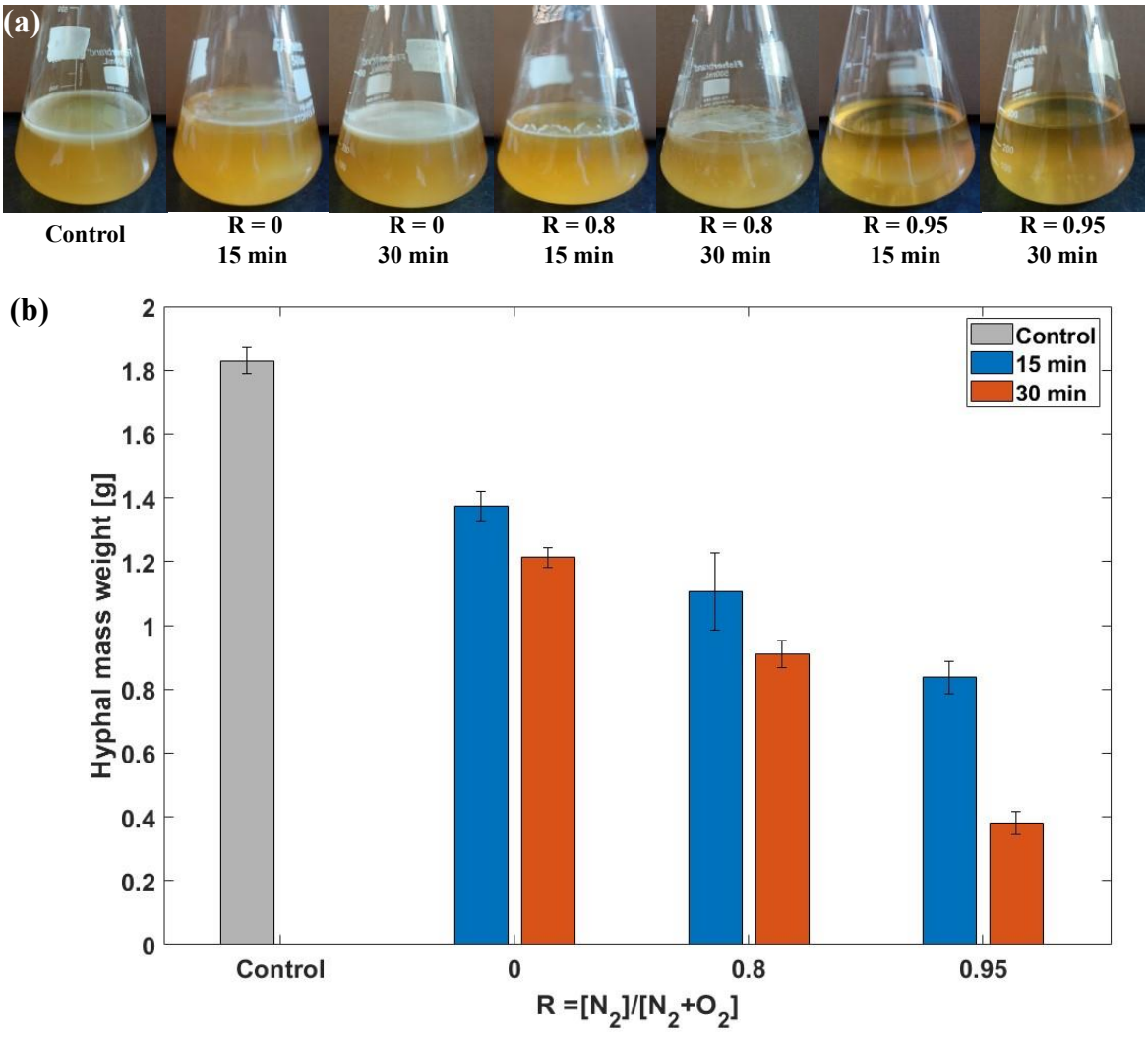

Figure 5.4 Effects of different plasma treatments on the growth of hyphal biomass (a) and the variation of the biomass weight after 7 days of static incubation at 25 °C (b). The error bar corresponds to 1 standard deviation while the bars represent the average of the technical triplicates.

5.4.3 SEM analyses of hyphal biomass

SEM analysis of the control sample group (depicted in Figure 5.5a) revealed a substantial presence of hyphal biomass. The hyphal structures displayed characteristic linear patterns with typical thicknesses in the range of ~10 µm, concurrent with observations by [74]. Additionally, the spores attached to the ends of the hyphae filaments remained intact, with an average size of about 15 µm. In Figure 5.5b, we can observe alterations in hyphal biomass following a 30-minute R = 0.95 plasma treatment. The PTW treatment is seen to have resulted in changes to the mycelial structure, folding of hyphae and a notable reduction in hyphal mass; furthermore, the hyphae filaments appear to have lost some of their characteristic branching. Additionally, the ends of the hyphae filaments showed a significant germination reduction, indicating a suppression of their activity due to the treatment. The SEM images also displayed substantial deformations and collapse in hyphal walls and changes in surface texture. In addition, most of the hyphae became thinner and twisted, with typical size ranging from 6 to 8.5 µm. The treated samples showed broken hyphae, with noticeable collapses and compressions in hyphal structures. These transformations induced by the PTW treatment may likely be attributed to damaged cell envelopes due to etching of macromolecules [122]: PTW exposure thereby likely results in damage to cell walls, rendering them permeable and facilitating the release of intracellular components. Altogether, these combined effects ultimately cause collapse and compression of the *P. ultimum* mycelia, rendering them inactive [123].

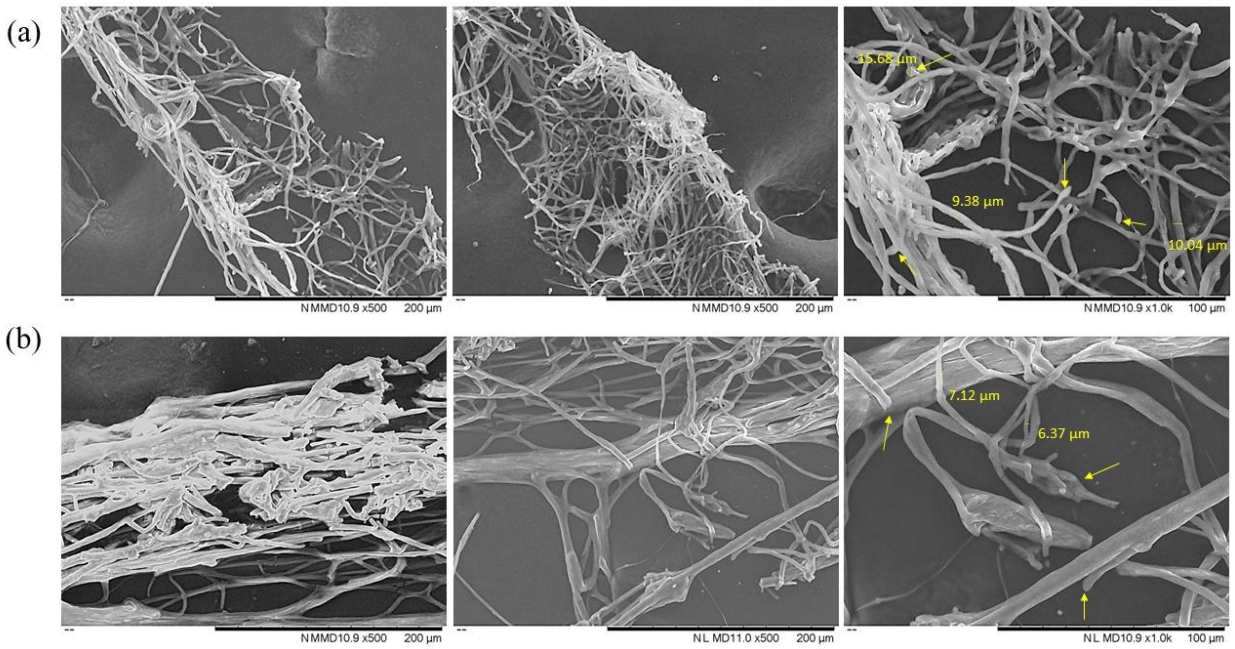

Figure 5.5 Effects of plasma treatment on *P. ultimum* mycelia showing the impact on morphology, spores, and cell integrity for (a) untreated control sample, and (b) $R = 0.95$ (95 % N_2, 5 % O_2) 30 min plasma treatment.

5.4.4 Overall discussion

Because of the N_2 molecule's very high bond strength, 958.4 kJ.mol^{-1} (~10 eV), it is chemically quite inert. Using a combination of both thermal and non-thermal processes, it is possible to convert N_2 into NO and successively to NO_2 and HNO_3 through the Zeldovich process [8]. Using the reactions proposed by [63, 124, 125] and completing with those found on the NIST database, we propose the chemical model presented at Figure 5.6. Starting from the major species produced in the plasma phase, these interact with the species present in the gas phase by collision and diffusion. The species transport to the liquid phase is then controlled by species-specific Henry's law solubility coefficients. Finally, a chemical pathway of the liquid species is proposed in accordance to the species which can be readily measured, such as nitrites, nitrates and H+ ions. In both the gas phase and the liquid phase, the thickness of the arrows indicates the order of magnitude behind the reaction rate enabling for a visualization of the most dominant processes.

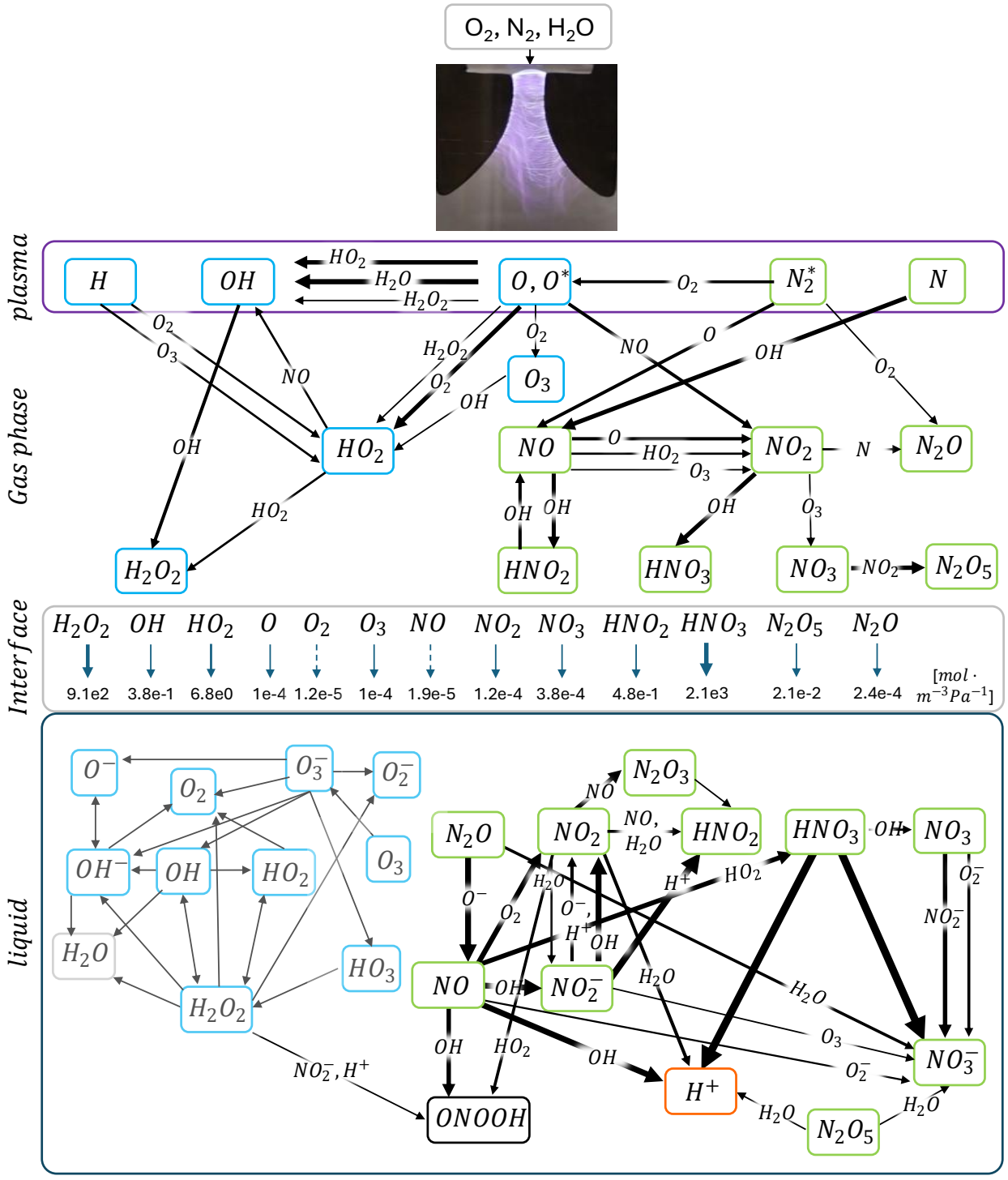

Figure 5.6 Schematic diagram identifying important species generated as a result of predominant air plasma gaseous and aqueous reactions, including their transport from plasma to water driven by species-specific Henry's law solubility coefficients. The arrow thickness are indicators of orders of magnitude of the reaction rates. In the liquid phase, the details of arrow thickness related to reaction rates is kept for the nitrogen species and omitted for the OH derived species for simplification purposes.

The chemical pathways shown in Figure 5.6 help to explain the chemical results in Figure 5.2, which demonstrated the formation of both NO^{-2} and NO^{-3}, as the R ratio increases. Regarding the liquid reactions, Figure 5.6 shows mainly the nitrogen related species in detail rather than the oxygen dominated species, because species that lead to H_2O_2 are not dominantly produced in the glide arc plasma. The liquid phase chemistry is predominantly defined by the initial gas chemistry and resulting gas composition. The following processes are most dominant for each R-value:

- At R = 0 (100% O_2), the production of both NO_2^- and NO_3^- is almost null. The low production is associated to the traces of nitrogen present to be converted into NO_X.
- At R = 0.2, the highest production of NO_3^- is observed. As O_2 is in ample supply, it increases the production of N_2O, O_3 and HO_2. These, in turn, are responsible for creating more NO_2, which react with OH to generate HNO_3. The latter is then transferred quickly through the water phase (high Henry coefficient) and dissociates to form detectable NO_3^-. In this context, OH reacts more readily with NO_2, forming HNO_3 rather than with itself to create H_2O_2.
- Between R = 0.2 to 0.6, a reduction in the NO_3^- content is observed. The oxygen ratio decrease is responsible for a reduction in O, HO_2, and O_3 species: all of which are precursors for converting NO to NO_2. Because the reaction depletes 3 precursors at the same time, the production of HNO_3 drops quicker than that of HNO_2.
- For R = 0.6 to 0.8, the production of HNO_2 species declines because of the decrease of NO concentration, due to the depletion of O.
- Between R= 0.8 to 0.95, NO_2^- is produced with competing mechanisms. In [126], it was observed that the highest creation of N_2O was to be expected around 90% nitrogen content, and is attributed to a rise in excited molecular nitrogen (N_2^*) species. This increase in N_2^* is responsible for the local maximum of O, and therefore as well for a local maximum of NO.
- At $R \leq 0.9$, the depletion of oxygen precursors is responsible for a reduction in the NO formation and thus both NO_2^- and NO_3^- formation.

Both Figure 5.3 and Figure 5.4 are in agreement that the optimal deactivation of *Pythium ultimum* occurs near R = 0.95. The plasma treatment over a duration of 30 min results in a SDB with a pH > 4.5; as explained earlier, although this might reduce somewhat the growth of pythium, it is not expected to be the main contributor. This finding also shows that the growth reduction of pythium is not dominantly attributed to the presence of NO_2^-, which has a toxic effect, since more NO_2^- is present at $R = 0.8$ than at $R = 0.95$. It can thus be presumed that the inactivation effect goes beyond the longer-lived species of NO_2^- and NO_3^-.

The antibacterial effectiveness of oxygen and nitrogen containing plasmas in many cases can be attributed to the generation of peroxynitrous acid (ONOOH) [99]. Gaseous NO and NO_2 dissolve in water, contribute to the formation of NO^{-2} and NO^{-3} and acidic pH, and H_2O_2 and NO^{-2} react in plasma treated water under acidic conditions to form intermediate ONOOH that eventually decays into •OH and •NO_2 radicals responsible for the strong antibacterial effects. It is however typically produced at pH lower than 3 [124], therefore an unlikely pathway at pH 4.5 in the SDB.

In summary, plasma generates reactive species that attack the cell wall and cellular components [108]. This causes severe damage that can lead to cell death. Oxidative stress caused by the plasma generated RONS can damage the cell membrane integrity, causing structural and functional damage to the cells and fungal hyphae [106]. Disruption and morphological changes thus occur, in addition to the damage and leakage of the proteins and genetic components (DNA and RNA), leading to microbial inactivation. Although these arguments have been proposed primarily in connection with bacteria, this is likely to apply generally to most living cells, including fungi [39] and *Pythium ultimum.* Indeed, the SEM microscopic examinations confirm these mechanisms of cell wall erosion (etching), mass loss, hyphal breakage, all resulting in *Pythium ultimum* inactivation.

5.5 Conclusions

The research we report here constitutes an innovative laboratory-scale feasibility demonstration of cold plasma treatments using atmospheric pressure gliding arc discharges in N_2 + O_2 mixtures of differing ratios. Such treatments of *Pythium ultimum*-inoculated water clearly demonstrate that the PTW, particularly that corresponding to R = 0.95, is capable of oomycete inactivation. Plasma treatment can thus contribute significantly to increase greenhouse agriculture production efficiency, where annual yield losses due to *Pythium* infections are substantial.

A second beneficial effect of cold atmospheric pressure plasmas applied to various *R* mixtures is that resulting RONS, by their very definition, include stable chemical compounds of atomic nitrogen, in other words fixated nitrogen, that can act as fertilizer for greenhouse-cultured crops. Thus, cold atmospheric pressure plasma technology is a potentially very powerful new tool for greenhouse culture in both respects, inactivation of pathogenic microorganisms, and fertilization. The advantages lie in the intrinsic sustainable properties of plasma technology, as it is based on locally available, abundant, and low-cost resources, namely air, electric power and water. Its carbon footprint and cost are mostly defined by the source of electricity and its infrastructure's impact. Plasma can potentially replace established conventional chemical insecticides and fertilizers, which are both expensive, and in cases of disruption of logistic chains, are of limited global accessibility, and are heavily polluting. In our work, we successfully showed that cold plasma treatment can be tuned to achieve the desired effect in *Pythium ultimum* inactivation for future use in greenhouse farming.

5.6 Acknowledgments

The authors are grateful to Jules Bourdages-Desjardins from Serres Lefort, as well as Mylène Généreux, Thomas Jeanne and Richard Hogue from IRDA for their project collaboration. The authors also acknowledge the financial support from the Natural Sciences and Engineering Research Council of Canada, the TransMedTech Institute through its main financial partner, the Apogee Canada First Research Excellence Fund, as well as funding through the Ministère de l'Agriculture, des Pêcheries et de l'Alimentation of Québec.

Author Contributions:

SW performed plasma device design, plasma chemical characterisation and the pythium inactivation procedures. FA together with SW performed the hyphal mass measurements. FA performed the SEM measurements and analysis. First draft writing was done by SW and FA. Elisa Tests were conducted by EL. The paper strategy, writing and corrections were done by all authors.

Conflicts of Interest: The authors declare no conflict of interest.

CHAPTER 6 ARTICLE 2: USING GLIDING ARC PLASMA TO PROVIDE NITROGEN AND CONTROL FUNGAL PLANT PATHOGENS IN HYDROPONIC GROWTH MEDIA: IMPACT ON GREENHOUSE BOSTON LETTUCE GROWTH.

Sean Watson, Élodie Larouche, Thomas Jeanne, Julie Monette, Richard Hogue, Caroline Côté, Jason Robert Tavares, Stephan Reuter

Published in : Plasma Processes and Polymers

Submission date: October 31st, 2025

6.1 Abstract

In the context of sustainable hydroponics, a gliding arc plasma is proposed as a solution. This works attempts to validate plasma treatment of hydroponic solution as an alternative source to implement nitrogen fertilisers and pesticides, in the context of Boston lettuce growth. Plants parameters serve as growth and phytotoxicity indicators, in combination with pictures of the lettuce after a 2-week growth period. The main findings are that plasma activated hydroponic solution can improve the growth of plants when compared to a lack of nitrogen, but the substitution of nitrates needs to be further improved. By testing a plasma treatment aimed at reducing pathogens in conditions where proliferation is limited, plasma treatment has been found not conducive to any phytotoxicity.

6.2 Introduction

Increasing food insecurity, climate change and inadequate supply-chain control are burdening modern agriculture. One of the solutions to address these changes is hydroponic greenhouse growth. However current hydroponics are far from being intrinsically sustainable, as they rely on commercially produced nitrogen fertilizer, typically generated using the Haber-Bosch process which relies on heavy consumption of fossil fuels [92] in large manufacturing processes. Added to this negative environmental impact of the Haber-Bosch process is the impact of transporting synthetic fertilizer on site. Conversely, when combined with sustainable electricity generation, nitrogen fixation by non-equilibrium discharges – so called cold plasma – can be used to substitute these fertilizers *in situ*, via a turnkey process, with readily available resources: air, water and electricity, without requiring the high temperature and pressure of its Haber-Bosch counterpart.

Research involving nitrogen fixation from cold plasma is currently divided into two branches:

1. Catalytic reactions: reducing NO_X to NH_3[51], or using catalysts in combination with plasma for NH_3 synthesis from N_2 and H_2 [30].
2. Direct nitrite and nitrate generation in gaseous discharges or gas-liquid hybrids.

While both can provide a nitrogen source, the second path can also be repurposed for pathogen inactivation [63]. This provides the opportunity to ideally enable nitrogen nutrient supply and pathogen inactivation at the same time, or in a two-step process.

The present work involves directing a gliding arc plasma on the surface of a water volume, enabling the creation of reactive oxygen and nitrogen species (RONS) in the gas phase, transferable to the aqueous phase. RONS synthesis can be tailored for both nitrogen fixation and pathogen inactivation. A gliding arc combines both thermal and non-equilibrium processes [54], enabling for a high throughput of nitric oxide due to the Zeldovich mechanism in the thermal phase [126], which then combines with the oxygen in the non-equilibrium process to form NO_X, and directly incorporates part of the required plant nutrients in the plasma treated water (PTW).

This work has 2 concurrent aims:

1) Substitute nitrogen-based plants nutrients solely by plasma, in the context of Boston lettuce (*Lactuca sativa var. Capitata*) production, investigating possible phytotoxic effects.
2) Investigate the effect of plasma treatment using contaminated growth media, under conditions previously optimized for oomycete and pathogen inactivation [83], on plant health.

A study by Hoque et al.[127] has demonstrated that from the NO_X species, nitrates (NO_3^-) improve plant growth, while nitrite (NO_2^-) and ammonia (NH_3) can cause toxicity in iceberg and romaine lettuce, stunting growth output and producing a crown discoloration (brownish color) as well as root system damage. Nitrite concentrations as low as 16.4 mg NO_2/L were reported to cause significant harm. As a gliding arc plasma incorporates both nitrites and nitrates, this presents a unique opportunity to compare effects.

While incorporating nitrogen in water can be achieved by plasma, it is important to do so in a controlled output [128]. Nitrates are essential compounds to promote the growth of plants. However, excess nitrates have been shown to cause plants to grow deficient in other minerals,

especially in the case of calcium. Two organizations have set out regulations with regards to nitrate content in plants:

- The World Health Organization (WHO) has established a maximum daily dose for the presence of NO_x in food and water : 3.7 mg NO_3/kg/day and 0.06 mg NO_2/kg/day [129]. This dose was established from a 100x safety factor based on a chronic toxicity study on rats, and assuming that a portion of the nitrate will be converted into nitrites. The maximum dose for pregnant women and babies below 3 months of age is lower, as they are more susceptible to convert nitrates into a larger concentration of nitrites, possibly inducing methemoglobinemia [130].
- The European Commission has also provided a maximum level of nitrates in different foods [131], namely between 2 and 5 g NO_3/kg of lettuce, depending on the season, while no such regulations are found in North America, beyond the regulated use of nitrites and nitrates as food additives in the meat cuts sector.

In north American drinking water [81, 132], the recommended threshold is typically of 45 mg/L of NO_3 and 3 mg/L of NO_2. A study on the potential health effects of leafy vegetables nitrite and nitrate content [80] has measured nitrates content in lettuce in the order of 1000 mg NO_3 /kg, and nitrite contents in the order of 30 mg NO_2 /kg, but both with quite high variance from sample to sample; in fact, several samples were found to exceed the WHO's recommended daily dose with only 100 g of produce. While nitrite has the potential to be more harmful, there are no specific regulations targeting its content beyond the WHO recommendations.

In the field of plasma agriculture, PTW using a gliding arc was also involved in oak lettuce growth [133] comparing tap water to PTW. A similar approach to this paper but using a different growth media for Boston lettuce [134] and without pathogen inactivation considerations, has also been considered for pilot scaling. PTW was also used to disinfect lettuce after its growth cycle by Schnabel et al. [43], and shown to improve the maturity rate of seeds[68].

Herein, we demonstrate that, while a high concentration of nitrites is present in plasma-treated water, Boston lettuce crops do not exhibit significant signs of phytotoxicity in terms of plant growth.

6.3 Methodology

6.3.1 Plasma source

The plasma was sustained from a PVM500 resonant high voltage power supply with a 2500 secondary coil transformer (Information Unlimited Inc., Mont Vernon, NH, USA). The resonance frequency was around 24.5 kHz, the voltage was kept at 60% of the single voltage mode. Gas was supplied to the plasma feed using a combination of nitrogen and oxygen (Air Liquide Canada, Aphagaz 1 $\geq$ 99.99% purity), with a total flow of 5 slm. For more details on the plasma source and analysis of the resulting plasma interaction with water, the reader is referred to [83]. Modifications to the plasma setup are presented in Figure 6.1, namely the inclusion of a peristaltic pumping system between the plant-containing basin and the plasma reactor.

Using the data from [83], 3 nitrogen-to-oxygen ratio plasma treatments were considered. Nitrogen-rich plasma was composed of 20% O_2; 80% N_2, for its similarity to air. The oxygen-rich plasma, at 80% O_2; 20% N_2 was the condition producing the highest selectivity for nitrates. Finally, a third condition at 5% O_2; 95 % N_2 was retained for its pathogen inactivation properties. Treatment times are based on the following:

- For the oxygen-rich and nitrogen-rich conditions, treatment time is calculated such as to replace the amount of nitrates normally present in a hydroponic solution (see Table 6.1). As such, the oxygen-rich treatment is 3h20 min, while the nitrogen-rich plasma is 4h26 min.
- For the pathogen inactivation treatment, treatment time is based on [83], which identified 30 min per 100 mL, or 5 h for 1 L.

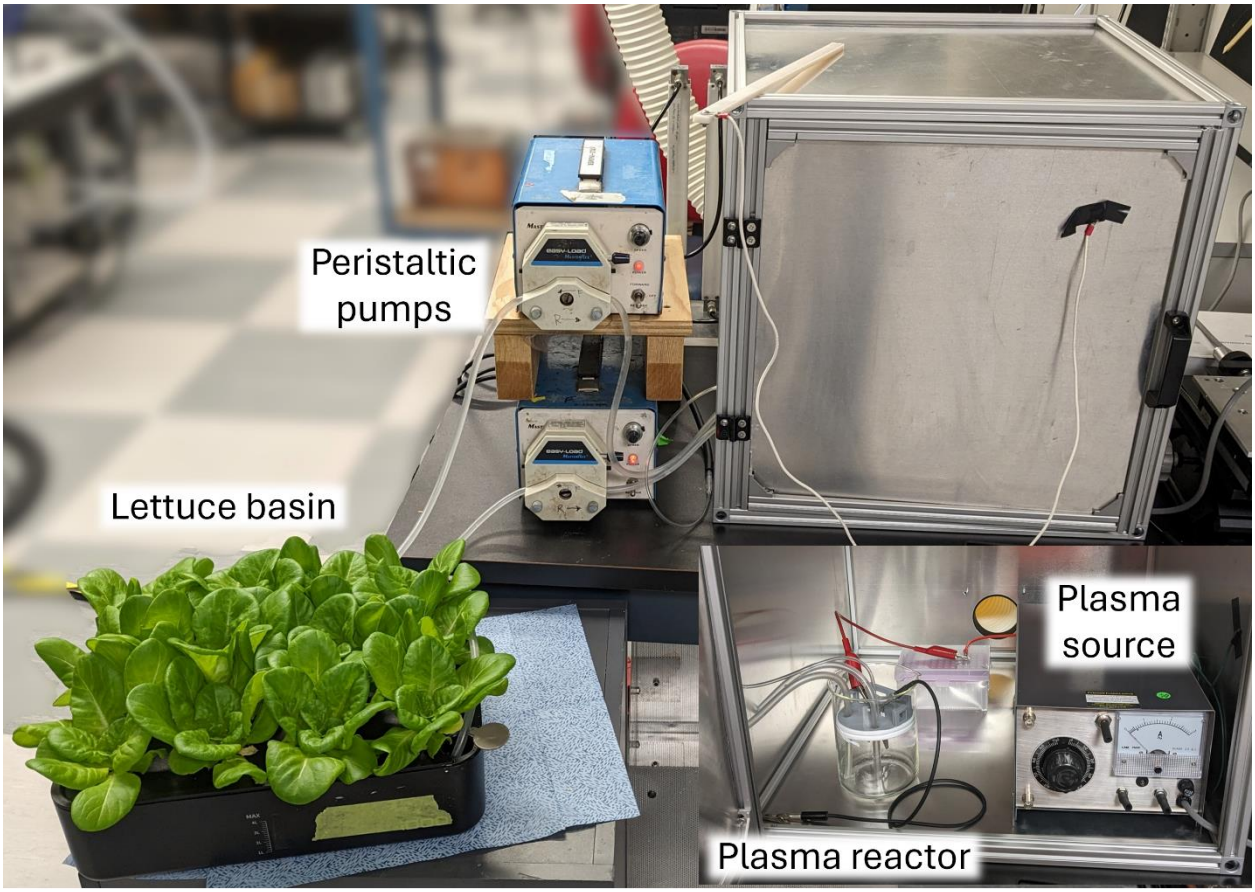

Figure 6.1 Photograph of the plasma reactor and hydroponics recirculation system used for PTW generation.

6.3.2 Preparation of the hydroponic solution

A hydroponic solution tailored to lettuce growth, sourced from GenV, was prepared from distilled water, with the ingredients listed in Table 6.1. All ingredients listed in table 1, with the exception of chelated iron, were sourced from Sigma Aldrich. Chelated iron was sourced from Gecko Grow, Alberta Canada. This hydroponic solution was used as the control for the samples in set 1 and 2, as well as for the nutrient solution in set 3.

Table 6.1 Chemical reagents and concentrations added to distilled water to form the positive control hydroponic solution.

Chemical Reagent	**Concentration [g/L]**
calcium nitrate tetrahydrate	0.842
potassium nitrate	0.070
monopotassium phosphate	0.175
potassium sulfate	0.099
chelated iron DTPA 11%	0.03182
manganese(II) sulfate monohydrate	0.00075
zinc sulfate monohydrate	0.00086
copper sulfate	0.00014
borax 15%	0.00253
sodium molybdate	0.00009
potassium bicarbonate	0.1
magnesium sulfate	0.36

In the first part of this study (Growth sets 1 and 2), we aim to replace the nitrogen content in the hydroponic solution by plasma generated nitrogen:

- In Set 1, both nitrate sources (calcium nitrate and potassium nitrate) are substituted with corresponding molar amounts of calcium sulfate (also from Sigma Aldrich) and potassium sulfate, to maintain calcium and potassium levels, while enabling plasma to provide for the nitrate substitution. This substituted composition is used to provide the negative control and corresponding plasma treated solutions for set 1.
- In Set 2, both nitrate sources (calcium nitrate and potassium nitrate) are substituted with calcium phosphate dibasic (also from Sigma Aldritch) and potassium bicarbonate, to constitute the negative control and plasma treated solutions. It is important to note that the solubility of calcium phosphate dibasic in water solubility (0.2 g/L) is lower than its concentration (0.7 g/L) in the control hydroponic solution. Thus, a white solid undissolved fraction is observed in the water basins.

For the second phase of the study (Set 3), experiments were conducted to simulate the growth of plants in contaminated water conditions, sourced from an experimental basin of water at GenV. During the summer of 2024, hydroponic lettuce cultures grown with this basin water were severely affected by *Phytophthora* spp. and *Pythium* spp., which justifies its use for plasma treatment trials

targeting oomycete inactivation, using plasma conditions known to inactivate *Pythium* spp. growth [83]. 4 conditions are compared:

1) Using GenV sourced water alone.
2) Using 1L of GenV water subsequently treated with disinfecting plasma conditions and 1 L of the control solution (Table 1).
3) Using GenV sourced water inoculated with additional *Pythium dissotocum* (approximately 1 gelose of *P. dissotocum* per 6 L, the exact initial concentration was measured by qPCR, cf. figure 7.).
4) Using 1L of water GenV sourced water inoculated with additional *P. dissotocum*, treated with disinfecting plasma conditions combined with 1L of the control solution (Table 6.1).

For conditions 2 and 4, plasma treatment was applied to the contaminated hydroponic solution (1L) to which fresh uncontaminated hydroponic solution (1L) based on Table 6.1's recipe was added. In all experiments sets, the water solution is replaced at the beginning of each week within a time frame of $\pm$ 2 hours.

6.3.3 Hydroponics system

Seedlings were provided from GenV greenhouses, after having undergone a 2-week germination period. The seedlings, and the growing medium in which they were grown, were then directly transplanted into their respective hydroponic systems for growth observation, or watered with control solution for a day before being transplanted.

Two hydroponics systems were used. For sets 1 and 2, 6 12-pod IDOO® Home Garden kits were used. The light source provided from the hydroponic systems was set at the vegetable setting, which adds additional red and blue LEDs to the white light source, along with a day/night cycle of 16/8 hours. Temperature and humidity were controlled through constant air circulation using the fans included in the hydroponic systems. The hydroponic kits were maintained in a plastic wrapped enclosure to avoid environmental contamination.

For set 3, tests were conducted in a class 1 biological confinement room, using 12 5-pod IDOO® Home Garden kits, connected to a small aquarium water pump (model 4547 Adafruit industries) to simulate water circulation in hydroponics systems. The hydroponic kits were housed inside a

Conviron Gen 1000 environmental chamber, which allowed for precise settings of temperature (25 °C), humidity (70%) and lighting of 12 $\text{moles}/\text{m}^2 \cdot \text{day}$.

6.3.4 Design of experiment

A summary of the different hydroponic solutions and plasma conditions is presented in Table 2.1, as well as the number of biological replicas and total samples.

Table 6.2 Group, water and plasma conditions as well as sample distribution for lettuce growth.

Group	Sample label	Hydroponic solution	Plasma conditions	Plant Replicas	Total samples
Set 1	Positive Control	Table 6.1 recipe	N/A	12	72
	Negative Control	Replaced Ca(NO3)2 and KNO3 with CaSO4 and K2SO4		12	
	O2 rich plasma		80% O2: 20 % N2; 3h20	24	
	N2 rich plasma		20% O2: 80 % N2; 4h26	24	
Set 2	Positive Control	Table 6.1 recipe	N/A	12	72
	Negative Control	Replaced Ca(NO3)2 and KNO3 with Ca3(PO4)2 and KHCO3		12	
	O2 rich plasma		80% O2: 20 % N2; 3h20	24	
	N2 rich plasma		20% O2: 80 % N2; 4h26	24	
Set 3	GenV water	GenV water	N/A	12	36
	GenV water + plasma		5% O2: 95 % N2; 5h	3	
	Inoculated GenV water	GenV water + P. dissotocum inoculum	N/A	12	
	Inoculated GenV water + plasma		5% O2: 95 % N2; 5h	9	

For all of the identified conditions in Table 6.2, measurement of plant growth was conducted using the following indicators after 2 weeks of lettuce growth:

- Root mass (humid), and aerial mass (humid) were weighted with a balance with $\pm$ 0.5 g precision;
- The number of leaves was counted from the plants, excluding the cotyledons;

- The plant leaf spread was measured as the distance, viewed from above, from the end of one leaf to another in the longest direction;
- Root length was measured using a forensic ruler.

Plants used for measurement purposes were not returned to the growth basin.

6.3.5 Real-time PCR detection and metagenomics

DNA from the samples was extracted within 72 hours or stored frozen until extraction using the FastDNA SPIN Kit for Soil™ in combination with the FastPrep® system (MP Biomedicals). Oomycete DNA was quantified by qPCR using QuantiTect SYBR Green PCR reagents (Qiagen) and primers from Grojean & Mugnier (1995). The qPCR protocol consisted of an initial denaturation at 95 °C for 15 minutes, followed by 39 cycles of 20 seconds at 95 °C, 30 seconds at 50 °C, and 30 seconds at 72 °C. Melting curve analysis was also performed to confirm the specificity of the qPCR method for oomycetes, primarily targeting *Phytophthora* spp. and *Pythium* spp.

Metagenomic analyses were performed to assess the diversity of fungal and oomycete communities. Amplification of the ITS11 region was carried out using primer sequences targeting specific regions previously described [135, 136] and applying a two-step PCR (dual-indexed PCR approach) specifically designed for high-throughput sequencing on the Illumina MiSeq platform. Bioinformatic processing of the sequences was conducted on the IRDA bioinformatics platform and involved different processing strategies (Qiime2 [137] and R [138], including quality validation steps, filtering using the DADA2 strategy [139, 140], and taxonomic identification with the UNITE9 [141] and EUKARYOME [140] reference databases. Microbial richness indices and diversity comparison measures were also determined. An additional identification step for oomycetes was performed using the ASVmaker tool [142] with the full set of publicly available oomycete sequences.

6.3.6 Color processing of images

The images presented in the next sections for plant growth were color corrected, to allow better comparison, using the forensic ruler (Forensigraph®) as a reference basis in each picture, using a MATLAB based code. It makes use of the least mean square deviation of the respective RGB values of each square on the ruler, as well as the white, black and neutral gray correction. The user

is prompted to define the black, white and grey region, before determining the edges of the color rectangle, from red [143 0 0], to teal [1 83 83] in a clockwise order. From there, the 14 color subsections are calculated, and the user is prompted if any corrections are required before compiling the measured RGB values of the region of interest (ROI). The measured RGB values are compared to the reference RGB values of the forensic ruler, using a least square regression, according to a linear RGB dependent model, in the form of $\text{reference Red}_1 = \alpha_0 + \alpha_1 R_1 + \alpha_2 G_1 + \alpha_3 B_1$, where R_1, B_1 and G_1 correspond to the 1st measured value for that reference square. The original images are presented in the supplementary material section.

6.4 Results and discussion

6.4.1 Comparison of plants after 2 weeks growth

Figure 6.2, Figure 6.3 and Figure 6.4 show pictures of the plants after 2 weeks of growth, according to their respective water and plasma treatment conditions, presenting both a view of the plants as well as the state of their roots. A forensic ruler is provided in each picture for color and size reference.

From the comparison between Figure 6.2 and Figure 6.3, the first observation is that depriving the plants of nitrates drastically affects their growth: the positive control has grown significantly over 2 weeks, while the negative control has barely grown from its seedling state. Plasma treatment of water, regardless of the selected conditions, effectively appears to provide part of the NO_X content needed for the plants, hence improving lettuce growth. However, the specificity of the plasma treatment towards generating nitrates needs further tuning to obtain comparable results to the positive control.

In the growth set conditions 1, in Figure 6.2, there are more yellow-colored leaves, which can be attributed to excess sulfates in the replacement of Ca and P nutrients [143]. Burnt browning on the edges of the leaves, present in all 3 conditions without calcium nitrate also implies that both sets 1 and 2 are not providing sufficient Ca [144] to the plants, due to limited Ca solubility or availability. Replacing $Ca(NO_3)_2$ with other calcium sources in hydroponic media can be difficult due to toxicity and solubility issues.

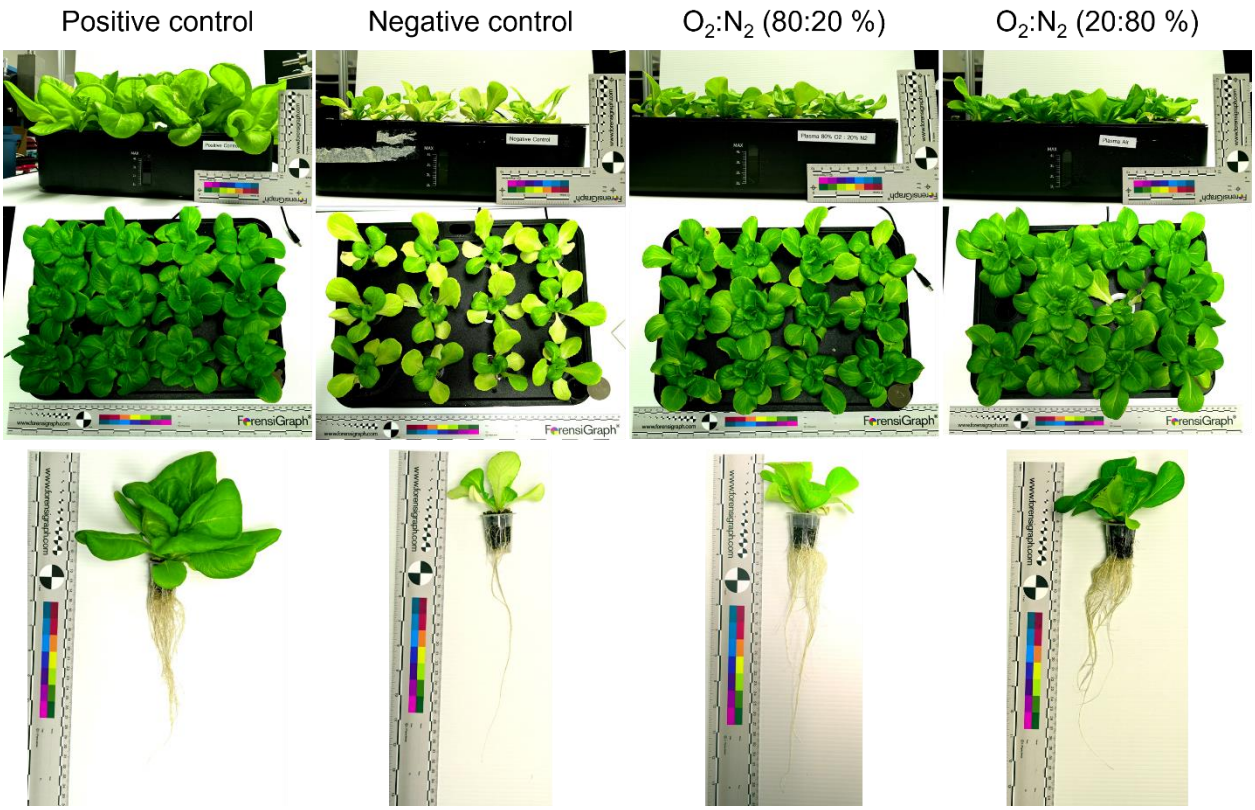

Figure 6.2 Color corrected pictures of lettuce growth after two weeks under growth set conditions 1 for nitrogen incorporation by plasma (Positive control from GenV recipe, negative control with substituted calcium sulfate and potassium sulfate, two plasma conditions using negative control hydroponic solution). The first row consists of a side view, the second of a top-down view, while the third row of pictures highlights the plant and root lengths.

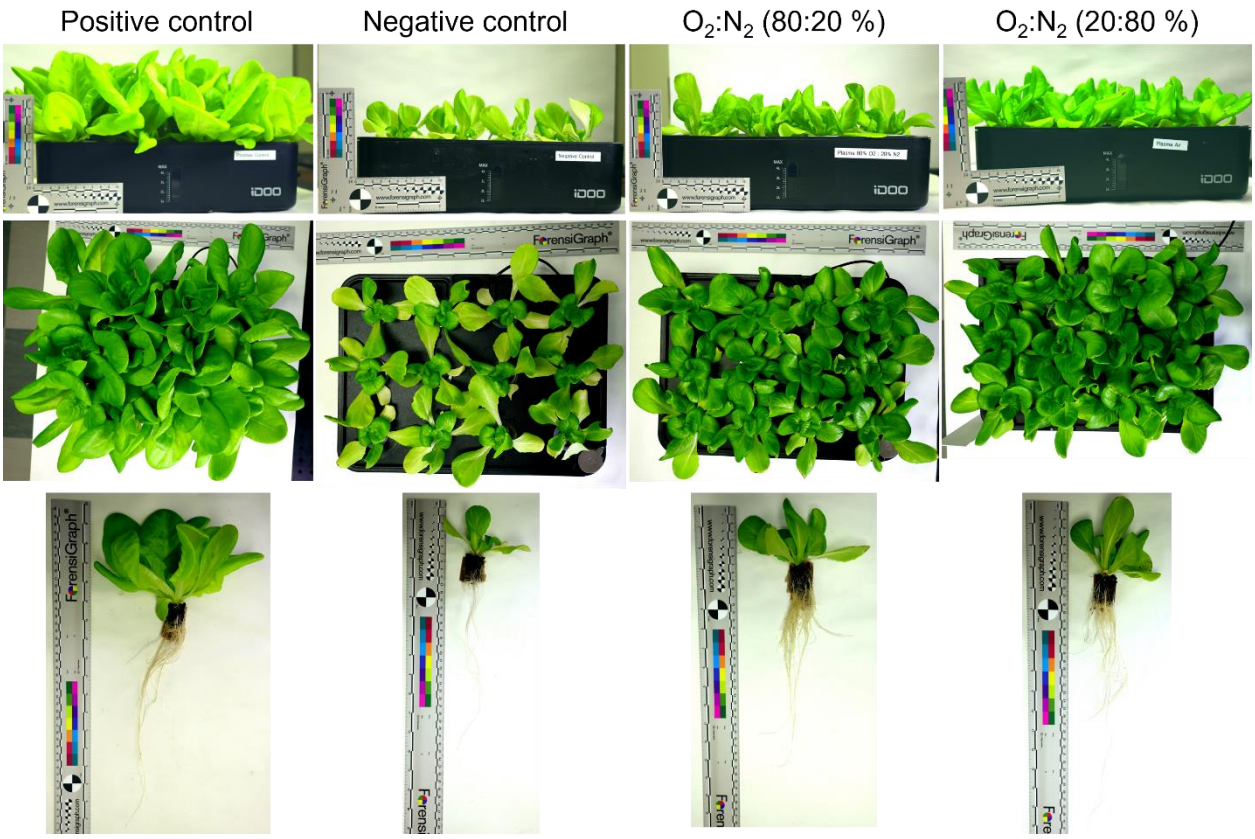

Figure 6.3 Color corrected pictures of lettuce growth after two weeks under growth set conditions 2 for nitrogen incorporation by plasma (Positive control from GenV recipe, negative control with substituted calcium phosphate and potassium bicarbonate, two plasma conditions using negative control solution). The first row consists of a side view, the second of a top-down view, while the third row of pictures highlights the plant and root lengths.

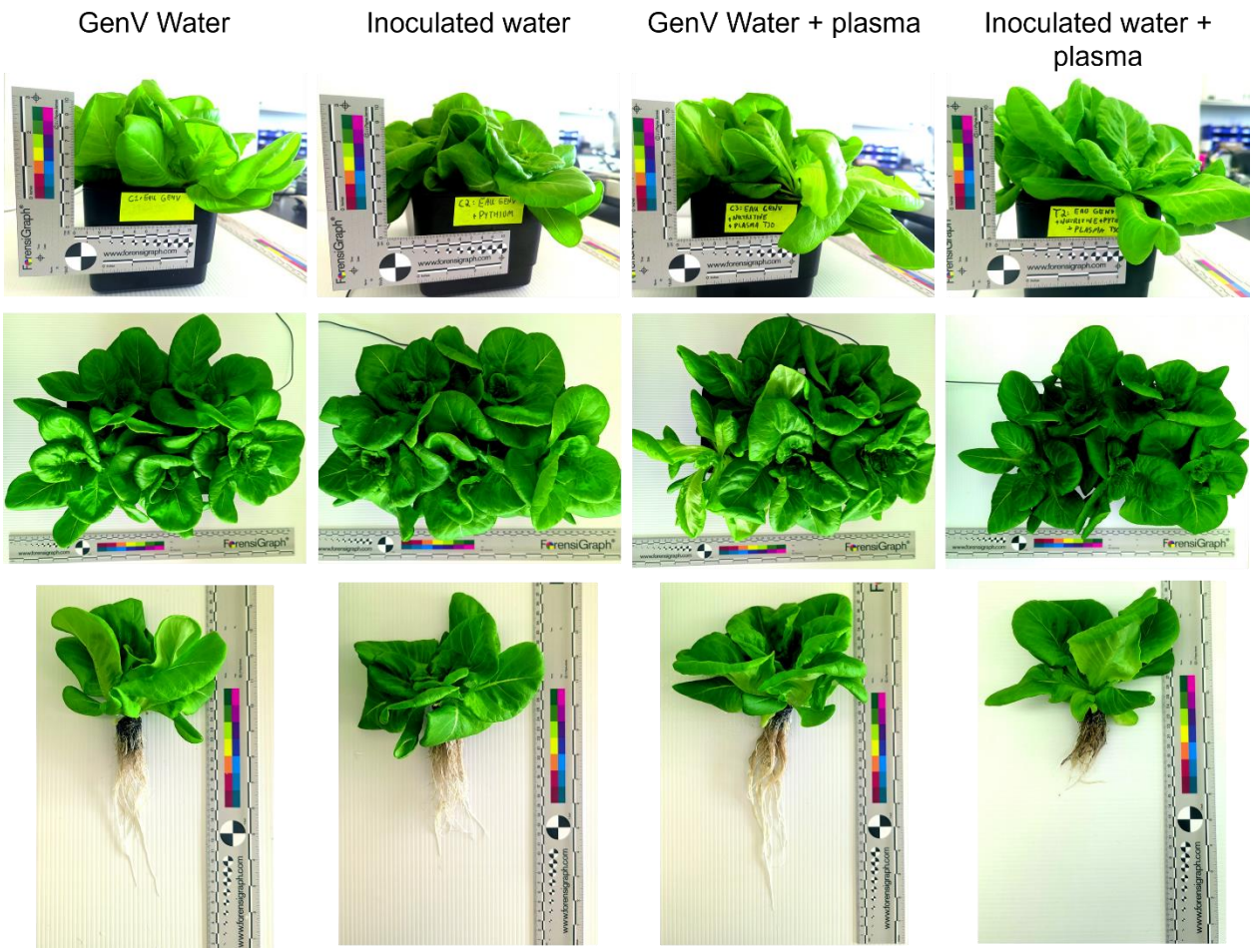

Figure 6.4 Color corrected pictures of lettuce growth after 2 weeks under growth set conditions 3 for *P. dissotocum* inhibition by plasma.

Figure 6.4 illustrates comparable growth to that of the positive controls for both sets 1 and 2, throughout all tested conditions. Further discussion will be provided after considering metrics from plant growth, presented in Figure 6.6.

Plant parameters

To quantify growth impact, the plant parameters root weight, aerial weight, number of leaves, plant leaf spread, and root length were measured as growth indicators. These are presented in Figure 6.5 for sets 1 and 2, as well as in Figure 6.6 for the *P. dissotocum* inhibition plasma treatment.

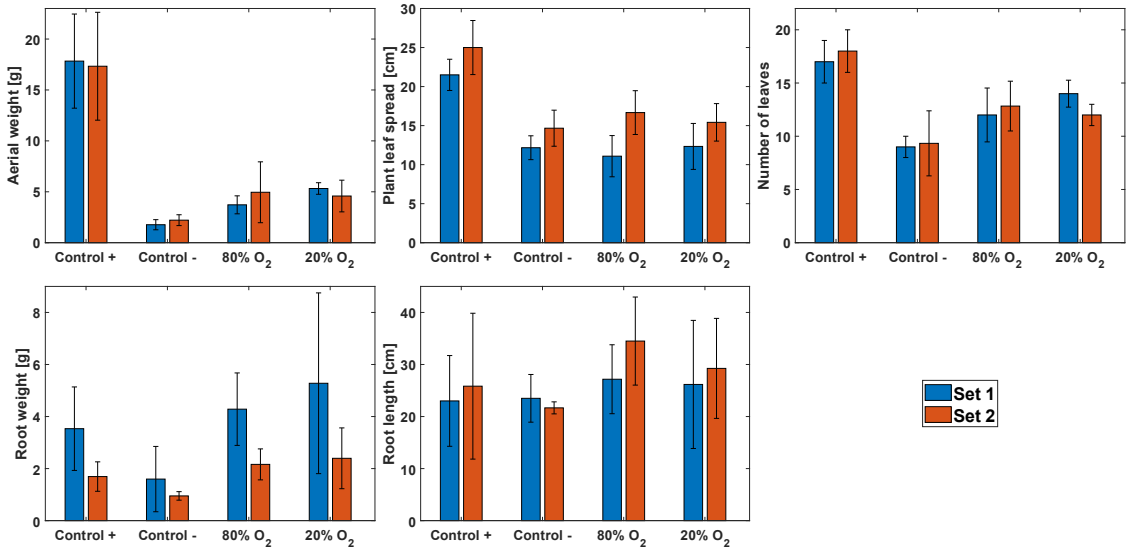

Figure 6.5 Plant measurements after 2 weeks growth for Set 1 (Blue) and Set 2 (Orange). The error bar corresponds to the 95% confidence interval.

Figure 6.5 shows that the positive control plants grow the most with the highest number of leaves, leaf spread, root weight, and aerial weight. The plants' root lengths are all within the error margins of one another, so this parameter does not reveal significant changes. It is difficult to identify which plasma condition has the better impact on lettuce growth due to the variation between samples, but both results show that plasma treatment seems to be increasing the growth of plants in terms of weight and leaves number compared to the negative control. If we compare growth set conditions 1 and 2, with the metrics provided in Figure 6.5, there does not seem to be any major impact beyond higher root weight for set 1, and slightly reduced leaf spread.

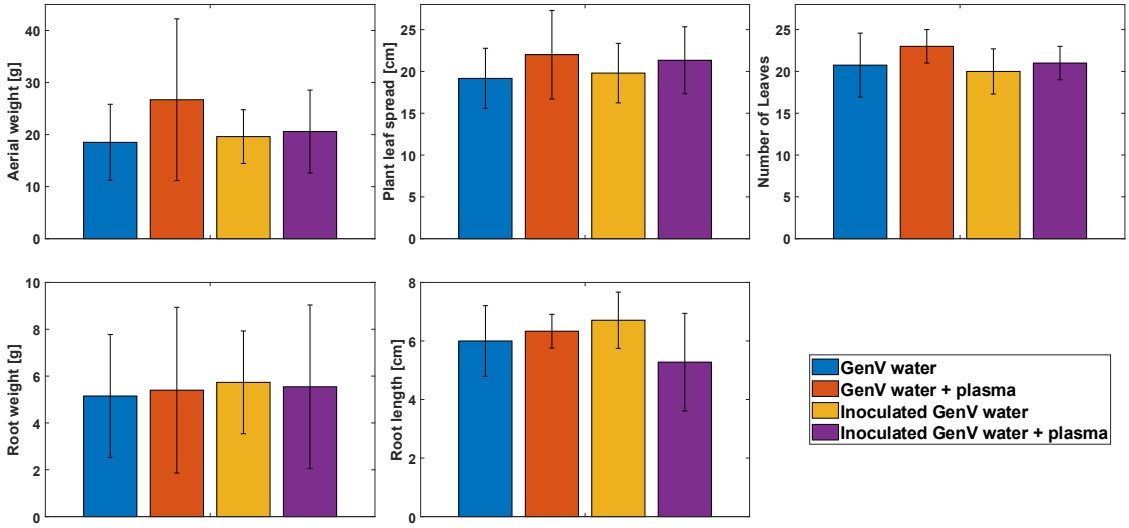

Figure 6.6 Plant measurements after 2 weeks growth for Set 3. The error bar corresponds to the 95% confidence interval. Sample size : GenV water, n=12; GenV water + plasma, n=3; Inoculated GenV water, n=12; Inoculated GenV water + plasma, n=9.

The results presented in Figure 6.6 are comparable to that of the positive controls for root weight, aerial weight, number of leaves, and leaf spread. For each parameter, the results are comparable between water types and plasma treatment. The metagenomics results (see supplementary material) confirmed that water samples contaminated with *P. dissotocum* have higher relative proportions for this genus. Water from the GenV greenhouses also consistently showed detections of *Pythium* spp. After the treatment phase (end of the cultivation week), the detection of *Pythium* spp. varied across experimental blocks. To more precisely assess the effects of the treatments on *Pythium* spp. abundance, diversity data and qPCR results were combined to estimate the number of ITS ribosomal gene copies of the genus *Pythium* in the water samples (Figure 6.7). These results confirm that contaminated water contained a significantly higher amount of *P. dissotocum* compared to non-contaminated water ($p = 0.000032$). In addition, treatment of water from the experimental greenhouse basins with cold plasma significantly reduced the concentration of the oomycete ($p = 0.0094$). Finally, a decrease in *P. dissotocum* concentration was also observed when comparing contaminated greenhouse water with contaminated water treated with cold plasma ($p = 0.016$).

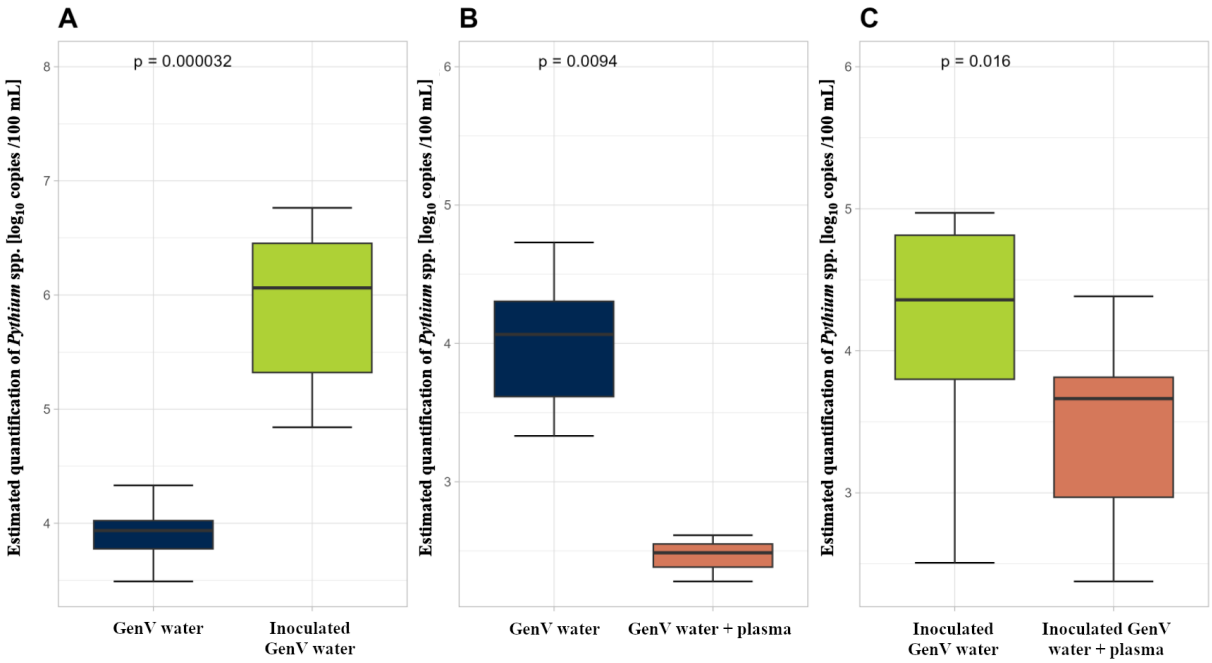

Figure 6.7 Estimated quantification of *Pythium* spp. (log_{10} copies/100 mL) in different treatments at the beginning (A) and at the end of the week (B and C). The boxplots show the distribution of values for each treatment across all blocks and the three weeks of cultivation. The Kruskal–Wallis test was used to compare the groups. Calculations were performed from the relative proportion of *Pythium* spp. identified in the water samples.

From these results and those of Figure 6.4, we can conclude that the operating conditions employed do not lead to *P. dissotocum* proliferation or plant growth hindrance. The focus of our study was to analyze if plasma treatment at conditions that inhibit *P. dissotocum* growth [83] negatively impacts the plants. For this, the plant growth conditions were set to conditions where *P. dissotocum* does not proliferate, i.e. at a fixed temperature of 25°C. While the study can thus not be conclusive as to the impact of the plasma treatment in inhibiting *P. dissotocum* growth (already proven separately[83]), the following valuable insights can be derived:

1) The control conditions for lighting and humidity were improved using an environmental growth chamber, thus more likely to reflect realistic conditions.
2) plasma generated species, in disinfection conditions, do neither seem to affect lettuce growth negatively nor cause significant phytotoxicity.

The selected plasma conditions for all 3 sets do generate a significant amount of nitrites, ca. 100 mg/L, much higher than the 5 mg/L threshold identified as toxic to romaine and iceberg lettuce in other studies[127]. This implies that Boston lettuce is either more resistant to nitrites than its

counterparts, or lettuce can thrive in nitrite-rich water. As a limitation of the experiments presented in this paper, the impact of nitrite and nitrate content in the resulting lettuce post plasma treatment has not been measured for consumer impact.

6.4.2 Conclusion

A gliding arc plasma system was used to treat water for lettuce growth in water conditions as close as possible to hydroponic solutions used in commercial greenhouses. In the first section of this paper, it was shown how lettuce reacts to receiving nitrogen through a plasma treatment of water. While not at the level of the control samples, implying that further optimization of the nitrate production from PTW is required, the exhibited growth of lettuce demonstrated that PTW is still better than its negative control counterpart, devoid of nitrogen.

In the second series of lettuce growth experiments, plasma was used at parameters previously demonstrated to inactivate oomycetes. This experiment was successful in improving the control parameters and imitation of real-life parameters of lettuce growth compared to the first two sets, and has proven that the specific plasma treatment conditions does not create phytotoxicity or adverse effects on lettuce growth.

Combined with green sourced electricity, air and water availability, plasma has the potential to replace established conventional chemical insecticides and fertilizers, with the added benefits of on demand and direct on-site production, and as demonstrated in this work, without harming lettuce growth.

Acknowledgements

The authors are grateful to Ariane Duval and Mylène Généreux from IRDA for their project collaboration. A sincere thank you to Michael Wertheimer for the supporting discussions. The authors acknowledge financial support from the Natural Sciences and Engineering Research Council of Canada (ALLRP 588479 - 23), as well as funding through the Ministère de l'Agriculture, des Pêcheries et de l'Alimentation of Québec. (IA120619)

CHAPTER 7 ADAPTING THE PROTOTYPES TO REAL OPERATING CONDITIONS

At the onset of the project, the main oomycete species identified in the water of the contaminated test basins of the industrial partner during summer of 2021 were *Pythium* spp. (60-80%) and *Phytophthora* spp. (ca 15 %) [145], motivating the work described in Chapter 5 targeting Pythium for inactivation. While the treatment worked for 2 simple media, such as SDB or tap water, one of the objectives of moving the plasma system to the partner's greenhouses was to test out a more complex actual growth media used in agriculture under real world conditions. This would allow to verify whether the plasma treatment is effective despite a change in solubility, pH, and the presence of organic material and being done in a non-controlled environment. For these studies, a first prototype of the plasma source would need to be adapted for an agricultural environment.

To deploy a plasma source in a greenhouse environment, it is important to take into account safety measures, described in section 7.1. The second section of this chapter will cover electrical interference shielding and present ways to improve on the current system. The results of the plasma tests which were conducted during the summer of 2024 are presented in the third section.

7.1 Plasma source safety considerations

The power supply used for this project is a PVM500 from Information Unlimited, United States of America. It makes use of a flyback transformer generating high voltage (kV range) at resonance, at frequencies of 20-40 kHz, depending on the flyback number of coils and gap spacing. More specifically, in this project, the PVM500 operates in a resonant mode at 24.5 kHz. Figure 7.1 (a,b,c) below presents the waveform data at early resonance as measured using a CT4028 voltage probe (Cal test, United States of America) and a 2877 current probe (Pearson, United States of America) and an SDS1104X-U oscilloscope (Siglent, United States of America), To remain in the operational range of the measurement equipment ($40kV_{rms}$), the PVM500 was used at 10% power instead of 60% and in single voltage mode. Single voltage mode is the default operational mode of the PVM500, otherwise the voltage can be doubled initially. The resonant frequency during the measurement of the voltage is reduced 23.5 kHz due to the change of the total impedance of the system caused by the addition of the voltage and current probes in the circuit. Figure 7.1 a) presents the overall waveform of the high voltage, Figure 7.1 b), shows a higher resolution of the voltage and the observed current peak, Figure 7.1c) shows a higher resolution of the current peak.

Measuring the voltage at values between 4kV and 6 kV using a Tektronix P6015a probe (Tektronix, United States of America) results in perfectly sinusoidal signals of the PVM500. This probe, however, affects the total impedance of the circuit so much that it prevents observation of resonance within the range of frequencies of the 2500 turns coil of the PVM500 (23 to 32 kHz).

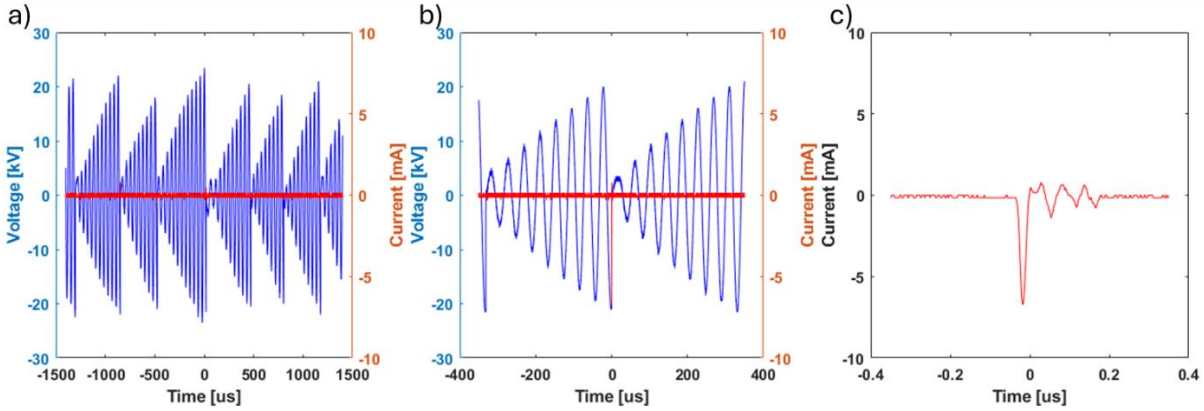

Figure 7.1 Current-Voltage waveforms at early resonance for the PVM500; a) Overview of the high voltage variations during resonance; b) Higher resolution of the voltage oscillations with observable current peak; c) Higher resolution of the current peaks.

In Chapter 5, the power was calculated using the amplitude of the current meter imbedded within the circuit of the PVM500, knowing that the transformer starts with 110 V which is then multiplied from 0 to 100% (in single voltage mode) before heading into the later stages of the circuit. This allows an approximation of the total power used by the PVM500. However, this approach does not represent the total power dissipated in the plasma. Because of these studies, the development of a new in-house plasma source was initiated, which allows the control of frequency and amplitude of the high voltage including a power monitoring in future studies. The high voltages above one kV required for plasma operation carry risks: under contact to the human body, high voltages can lead to possible involuntary muscle contractions, tetanization with the risk of not being able to release from the voltage source, deep burns or even cardiac arrest, if directly exposed to the high voltage output. While frequency at 20 kHz transfers power less efficiently to the body than at 60 Hz, most of the shielding of high voltage rated wires (rated typically only at 60 Hz) are less efficient at 20 kHz, and thus it is more likely to create undesired arcing or shock. Plasma discharges also act as antennae and can generate multiple higher frequency signals from resonance, which can perturb nearby electrical apparatus.

To mitigate the risk of electrical hazards, the following measures- among others – were taken to adapt the source for greenhouse use. As a first measure, the plasma source and discharge were installed inside a Faraday cage, made of aluminum sheets. The Faraday cage provides nearby sources of ground to the plasma discharge, as well as attenuation of electromagnetic interference, which protects most other nearby equipment. A safety key button was installed to ensure that only allowed and trained personnel can operate the plasma. Along with the safety, an emergency kill switch was installed to allow for a quick termination of any dangerous process. The power plug outlet in the back connected to the safety mechanism was also chosen to be splash proof (IPX4 rating [146]) to prevent dangers from nearby water. Additionally, large notification signs, highlighting the danger types, were added in three languages: French, English and Spanish. Spanish was added, because the majority of agricultural workers of GenV are Spanish native speakers. The Faraday enclosure and plasma equipment is presented in Figure 7.2a) and b), while Figure 7.2 c) and d) show its deployment in two different environments, namely at the greenhouses of Gen-V and at IRDA.

In addition to electrical hazards, gliding arc plasma generates a variety of reactive oxygen and nitrogen species, of which some can be hazardous, such as NO, NO_2 and ozone, and with thresholds as little as 0.1 ppm of long-term exposure. To prevent accumulation of the species, a fan was added to the exhaust system (cf. Figure 7.2 b), which can also be connected to a fume hood or evacuation vent (cf. Figure 7.2 d)). The fan used was calculated to dilute with ambient air the reactive species to below the safety threshold, provided that the exhaust is in an open space or connected to a fume hood exhaust. This was done with the worst-case assumption that all of the species generated from the gliding arc would remain in gas phase (not be absorbed in the plasma-water interaction) before the dilution.

To fireproof the gliding arc discharge, Tygon® flexible tubes, used for water transport, were replaced by glass pipes of about 10 cm in length that were added to convey water in the periphery of the gliding arc discharge, thus enabling for the flexible tubes to be distanced enough from any ignition source.

Figure 7.2 a) Safety box for the plasma source; b) Interior of the safety box; c) GenV installation setup; d) Safety box setup at IRDA and fume hood connection

7.2 Electromagnetic interference shielding and design improvements

Electromagnetic interference (EMI) shielding is based on two mechanisms: reflection and absorption of electromagnetic radiation. Reflection usually occurs at lower frequencies (< 1MHz) before absorption becomes the dominant mechanism. EMI usually originates from 3 types of sources: electrical plane waves, electrical fields and magnetic fields.

While material considerations are important in high end and very strong EMI applications, it remains that a good conductor is usually all that is required for most situations, provided that the integrity of the shielding material is maintained. Using a Faraday cage made of copper or iron should normally cover attenuations of the order of at least 60 dB for plane waves and E-field across

the board, see Figure 7.3. According to reference [147] Aluminum, as used in our current Faraday cage would have a similar profile to 7.3 a), but with 60% efficiency, due to the difference in conductivity. The attenuation figures specific to aluminum were not provided in the reference. More conductive materials such as copper are better at reflection, but fare less well with magnetic fields. Ferromagnetic materials such as iron offer more absorption of such fields, but the absorption component is only relevant at around 1 MHz.

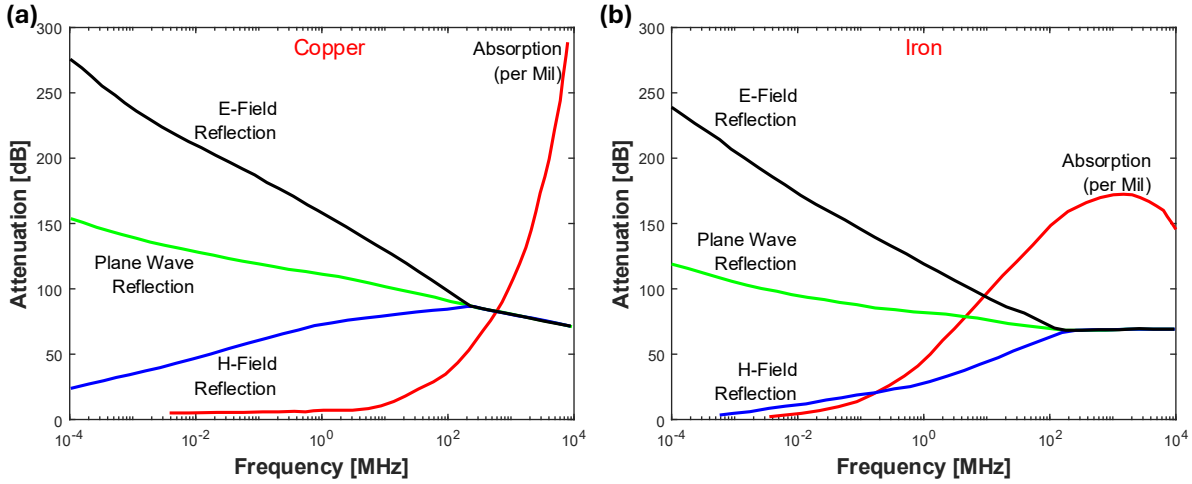

Figure 7.3 Shielding effectiveness for (a) copper and (b) iron.

EMI shielding failures are usually due to breaches in the shield for openings or where wires can carry current through the shield. The determining factor for the impact of an opening on the shielding efficiency is the longest dimension of the opening. In other words, a narrow hole of 1 mm by 25 cm has the shielding equivalent of a 25 cm circular hole. To improve on the current state, it is recommended to add conductive gaskets to the seams of the Faraday cage as well as to improve the conductivity between the plates and support structure. The largest opening, which currently is for the ventilation, can also be remedied using a honeycomb structure with smaller openings. Note however, that it currently only poses a risk for EMI leaks at frequencies above 10 MHz, and not for lower frequencies. For the wires, any wire over 1/20 of a wavelength must be considered as an antenna. Wavelength of the electromagnetic waves at 20kHz are in the order of 15km, so 1/20 is 750 m. Below 30 MHz, the most likely path for transmission is through conduction, above 30MHz, cable radiation is dominant. While designing shielding, one can expect at most 60 dB across all but especially for lower frequencies for a single shield layer. If higher attenuation is required, multiple shields must be used.

For further future improvements, it is recommended to add measures that remove the resonant noise created by the power supply in the plug relay. This noise can come from multiple sources, from a conducted emission, common impedance coupling or ground loops, or finally from inductive coupling. The alternative is to use two wall power outlets: one for the water pumps and the other for the power supply. During the experiments, the USB 5V plug included in the outlet was damaged after multiple uses of the high voltage source due to these interferences. To remedy such noise propagation, the first step is to analyse the noise's signal frequency and amplitude. Then, an appropriate shielding of the wires going through the cage can be designed. Finally, some passive attenuation of the outgoing signal of the PVM can be achieved using passive band pass filters from capacitors and resistors, so that it may be compliant to the CSA norms.

7.3 Green house conditions

The following describes the growth cycle conditions under regular and problematic environmental conditions in the greenhouses. They are summarized from the discussions about the experimental conditions required for the present studies. The conditions described are not considered complete or absolute, but they are presented as a general guide to the process.

The growth of lettuce on the site of St-Clotilde is divided into 3 stages. The first stage consists of planting lettuce seeds in a peat moss matrix mixed with growth media, watering them over a period of 2 weeks. Once the seedlings from step 1 are ready (cf. Figure 7.4 a), they are transferred by hand, with the growth media attached, directly to floating barges of Styrofoam (0.9 x 1.8 m), and inserted into holes of the same diameter, roughly 4-5 cm. During this stage, each lettuce is separated by ca.12 cm (center to center) as shown in Figure 7.4 c), for a total of 72 lettuce per barge. The lettuce is grown in a slow flowing water basin; 1 pool pump for an area of ca. 26 m^2, 4 x 4 barges, in the experimental basins, with ca. 20 cm water depth, which amounts to about 5 m^3 of water. The larger basins for industrial production have similar conditions but on a significantly larger scale. After a two-week growth period, lettuce heads attain a 3rd growth stage. At this stage, they are transferred into similar foam barges as used for stage 2, but with a larger spacing (ca. 17 cm between each lettuce (cf. Figure 7.4 b)), 36 lettuce per barge, where growth will be conducted until maturity one week later. During this period, the growth of lettuce conducted at IRDA exhibited larger needs for nutrient water intake, 0.5 to 0.6 L of water for 1 week, for 3 lettuces, compared to the average 0.2 to 0.3 L during weeks 3 and 4 of stage 2, for 5 lettuces.

The growth cycle during most of the year occurs without issues. However, during the summer months, with the increased temperature in the greenhouse, the immune system of the plants lowers, and the environmental conditions favor proliferation of oomycete species. Due to these conditions, the plants are no longer able to defend themselves from oomycete attacks and eventually have their root network get invaded resulting in their withering and dying. The exact threshold for both water and air temperatures at which this occurs still needs to be verified. The conditions during the IRDA test were set at constant 25°C, as an average for ambient air during day and night cycles. While this temperature is suitable for pythium development [74], it seems that the oomycetes are not yet affecting the plants, or that the water sample at a different date had a different pathogen composition. *P. dissocotum*, injected during this period as a *P. ultimum* substitute, also seems not to thrive as much under these conditions. The growth spurt of oomycetes, origin and what exact conditions trigger it is to date unknown and part of future studies. Due to the variability of the weather during the summer, the investigation under greenhouse conditions can be difficult; multiple continuous hot days are required for the lettuce to be affected, and multiple trials with different conditions are required to sample appropriately the plant's response to a treatment. To mitigate impact of pathogen load, between each growth cycle, the barges are cleaned with a steam process, before new plants are added.

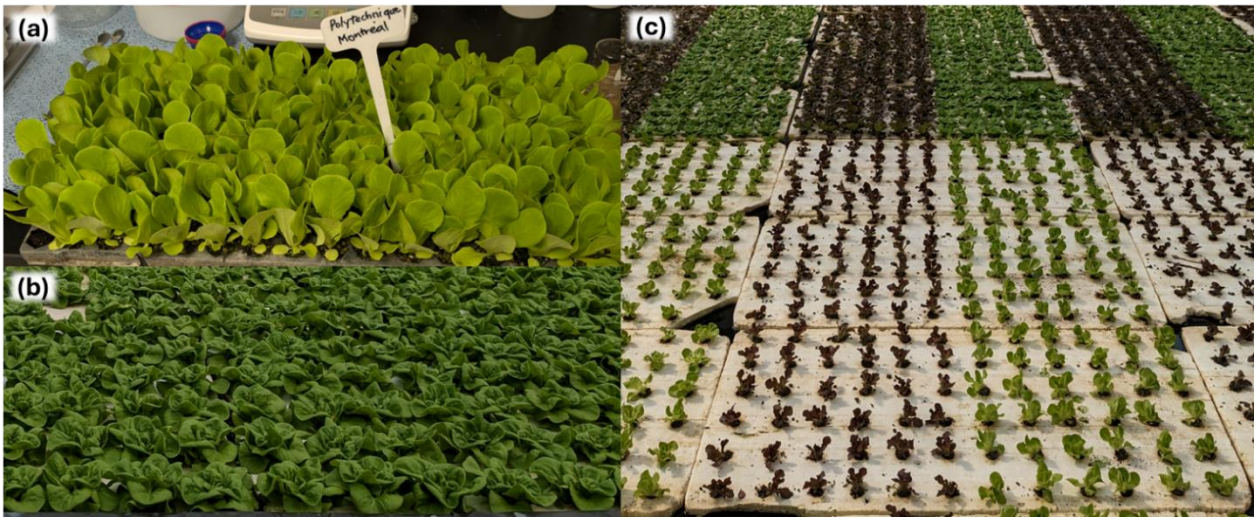

Figure 7.4 a) Saplings after 2 weeks growth, as received from GenV. b) lettuce during the 3rd cycle, c) lettuce at the beginning of the 2nd cycle (below) as well as in the second week of cycle 2 (above).

7.4 Results from greenhouse experiments

7.4.1 Experimental setup

The plasma source used for this experiment was described in detail in 7.1 and will be used under the same conditions as described in the first article (cf. CHAPTER 5) to have been efficient at reducing pythium growth, namely under 95% N_2 and 5% O_2, 60% max voltage output. The setup was installed at the GenV facility, in their experimental basin section, near where the oxygen bottles were previously stored (cf. Figure 7.2c). The oxygen line was connected to the oxygen tanks on site (supplier Praxair, Canada), while a nitrogen bottle (Alpha gaz 1, Air Liquide, Canada <99.999%) was ordered from Polytechnique and installed on-site.

A portable fridge was used to store water samples on site and during transport to prevent any changes on the bio activity. The samples were then transported to IRDA every 2 experiment days.

7.4.2 Methodology

The initial plan was to treat 1L water samples from the same basin (B, as labeled from IRDA) in a continuous treatment with circulating water flow, for an equivalent residence time of the 100 mL sample of 20 min and 30 min. Increasing the volume results in a factor 10 increase in treatment times. This results in two treatment times of 3h20 min and 5 h. For reproducibility purposes three replicates were done of each sample, with the water composition changing slightly in between the experiments due to the greenhouse conditions in which they were stored. The initial samples were taken the 29th of July 2024, while the later were taken the 20-21st of August due to complications in supply and access to the site. Half-way through the process however, due to a pump failure, caused by the humid environment, the circulation process was halted, and samples had to be done in batch of 100 mL and then recombined to 1L.

For each condition, 3 samples were taken: an initial water sample stored directly in the fridge, a second water sample, the control sample, stored at ambient conditions during the plasma exposure time and then in the fridge along with the 3rd sample, which has undergone plasma treatment. Care was taken to sample the water in the middle of the depth of the basin, as instructed by IRDA to avoid surface algae, as well as away from the edges of the basin itself. This control sample aimed to highlight any possible growth or changes due to ambient conditions which may occur during the

3-5 h treatment of the water by plasma. Temperatures and pH were recorded of the water samples before and after treatment.

Samples sent to IRDA then underwent *E. coli* analysis and quantitative polymerase chain reaction analysis on-site. *E*. *coli* was added as a reference measurement to further assess the capability of plasma as a tool for sanitation purposes. The first analysis type was done to have an idea of the sanitation of the process, while the latter is used to quantify oomycete populations and metagenomic analysis at Québec IRDA facility to investigate which species have been reduced by the plasma process. For a detailed description of the methodology the reader is referred to CHAPTER 6, section 6.3.

7.4.3 Results and discussion

Figure 7.5 presents pH and temperature variations as a function of sampling date and repetition. While large fluctuations from one sample to another are observed, the following conclusions can be drawn; plasma treatment reduces the pH from a neutral point towards acidic values, depending on the initial pH of the water. In both cases of pH starting at 6.9 (samples 3, 20 and 30 min residence time), the reduction is less compared to the other samples treatment. As shown in the lower part of Figure 7.4, plasma treatment increases water temperature. The temperature did not increase to values above 40 °C. Similar to the explanation presented in Chapter 5, it can be concluded that temperature increase is not significant for reducing pythium growth.

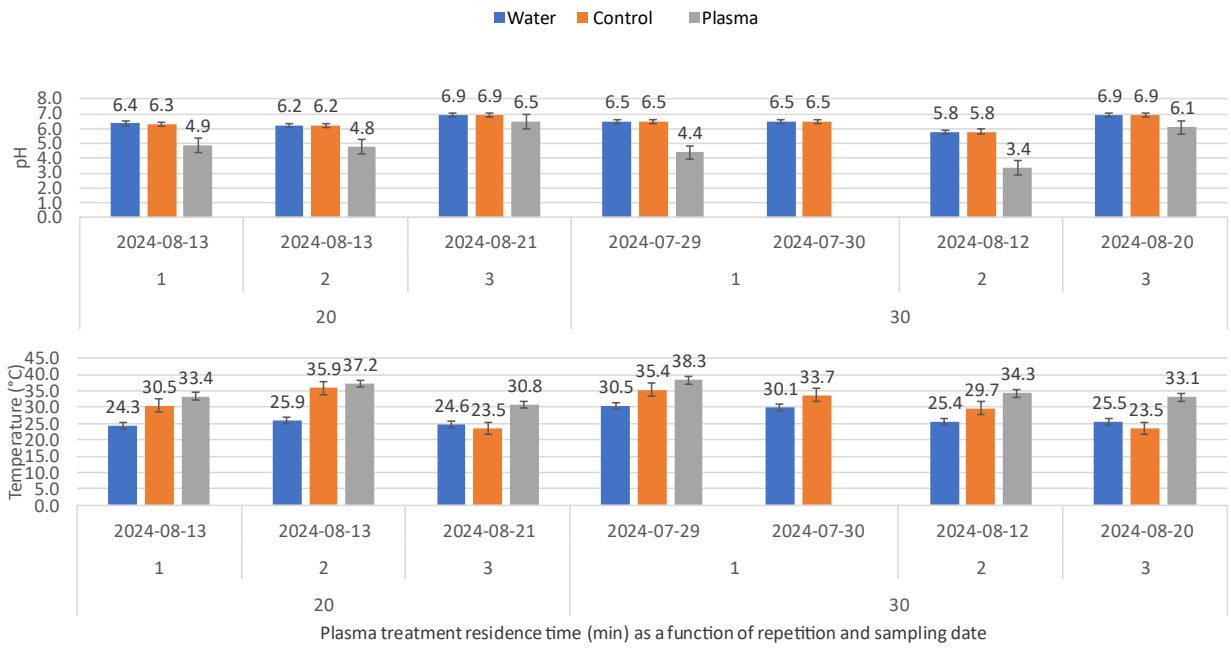

Figure 7.5 pH and temperature measurements of the GenV water, control sample at ambient temperature and plasma treated sample, taken at water sampling, and after plasma treatment respectively.

During the trials of water treatment in GenV greenhouses in 2024, the water of the experimental basin was compared to the control and plasma treated sample. The *E. coli* test revealed no detection within the water samples. Sampling the water under different days and condition also highlighted that green house conditions and temperature can cause a variation in the oomycete populations. The quantity of oomycete DNA increased 4 times due to ambient storage conditions compared to the first water sample (cf. Figure 7.6). The 20-min. residence time (time equivalent for the interaction of the plasma and liquid for a batch 100 mL reactor), equivalent was successful for the first 2 replicas, but the 30-min. residence time is clearly more effective in reducing oomycete populations (1.5 to 2 log reduction). This condition will therefore be retained for further testing.

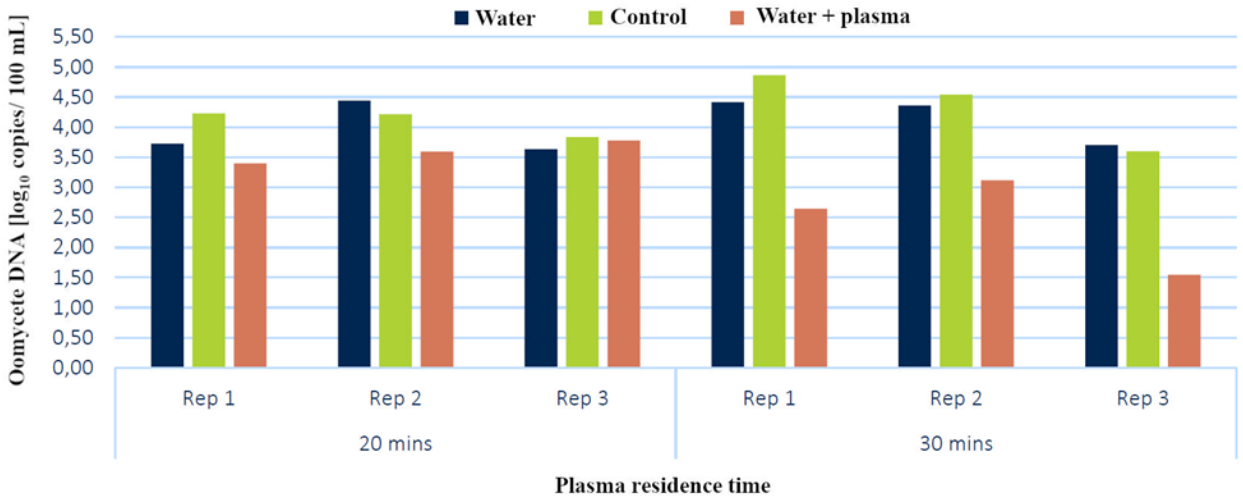

Figure 7.6 Oomycete DNA concentration in greenhouse water from GenV as function of water replica and plasma treatment residence time. 3 samples were analysed per replica: the culture basin water, the culture basin water exposed to greenhouse environment and the treated water. Replicas are presented individually as they correspond to different water sampling time and conditions. Gas composition for the plasma treatment was 95% N_2 and 5% O_2.

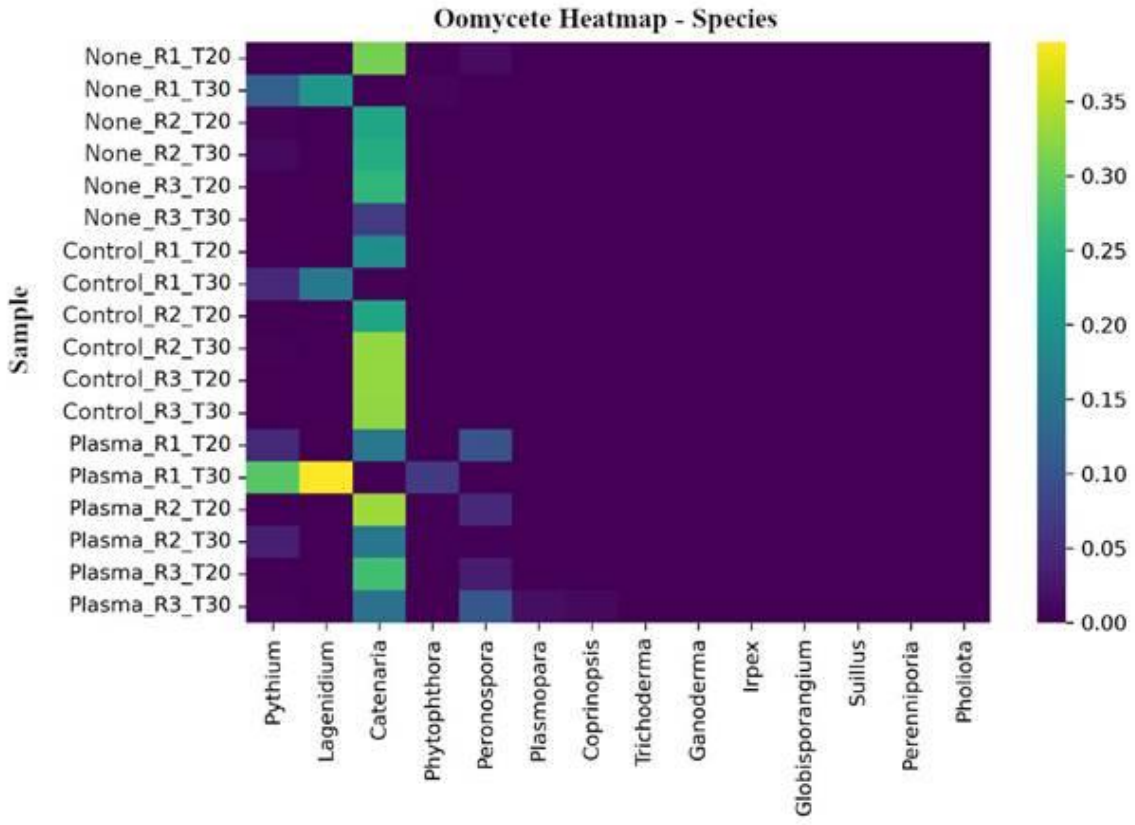

Figure 7.7 Relative oomycete proportions heatmap detected in the water samples. The color gradient from purple (low) to yellow (high) illustrates the distribution across samples.

The relative proportions of oomycete population in water samples from summer 2024 are presented in Figure 7.7. While Pythium and Phytophthora are present on July 29th's sample (R1_T_30), there is a strong presence of *Catenaria* and weak presence of *Peronospora* oomycetes. A confirmation of the species present by q-PCR such as this allows to map the threats more appropriately.

7.4.4 Conclusion

The tests conducted in the greenhouses of GenV have highlighted that cold plasma treatment can be used to reduce oomycetes beyond Saboroud growth media, distilled or tap water, but also with the complexity of actual greenhouse water. While the oomycete diversity was different than its 2021 counterpart, in the sense that pythium and phytophtora spp. where not prevalent during our sampling events in 2024, the 30 min residence time equivalent treatment was successful in reducing oomycete populations through inactivation by plasma.

Conceiving the Faraday cage for risk mitigation was successful, with two further suggestions to improve on the design. Electrical risk and how to handle it was discussed in section 7.1. The greenhouse environment did impact the rate at which wires and electrodes would degrade, which needs to be considered in future designs.

CHAPTER 8 CONCLUSION

8.1 Closing remarks

The entirety of this thesis was motivated by a specific problem, which conventional means could not solve: the combined stressors of growing oomycetes and excessive heat periods lead to significant crop failure in greenhouse environments. Approaching this issue from the perspective of plasma treatment, the first step of the thesis was to see if oomycetes, organisms with a thick cellular membrane, could be inactivated by a plasma treatment in water. For this objective, *Pythium ultimum*, a species of oomycetes considered the most likely problematic oomycete at the preliminary investigations, was chosen as a target for inactivation. To further expand our capability for exploratory work, original diagnostic tools were added to our repertoire, namely adapting an ELISA test to liquid analyses and comparing hyphal mass growth after plasma treatment.

One of the success criteria for the industrial partner was to develop the means to inactivate the pathogens without harming the plants. As such the growth tests demonstrated in the second article have shown that even in the same inactivation conditions, the plants remain unaffected or exhibit no significant signs of phytotoxicity. Further testing still remains to replicate the problematic conditions and see if plasma treatment of the growth media can obtain a favorable response, but the second specific objective has been completed.

One of the side effects of using a plasma treatment in air, is the generation of nitrogen species in the water. While this is undesired in drinkable water, nitrogen incorporation can benefit plants in the appropriate form. In the second article, we have shown that nitrates in the form of calcium and potassium nitrates, typically used in a conventional growth media, can be substituted with other sources of Ca and K, so that it is possible to observe directly the impact of the nitrogen incorporation. Most examples of plant growth in the literature would only present tap water vs treated water, without looking into the complexity of a growth media, and show an improvement in growth due to added nitrogen. Despite that the current state of the gliding arc generates more nitrites than nitrates, resulting in a lower growth than the positive control sample, the lettuce still would grow better than its negative control counterpart, without nitrates. The optimization of both the plasma treatment specificity to target nitrates and the substitution recipe for Ca and K sources containing nitrates, tailored for Boston lettuce, remains for further study.

In an attempt to test the plasma treatment with actual contaminated media, the reactor was deployed at the industrial partner's site. The test was successful in replicating the same plasma conditions for *P. ultimum* inactivation, from Chapter 5, with the added complexity of actual liquid media: floating particulates, natural pathogens and growth agents. The reactor was adapted, considering electrical and chemical safety, to the reality of the workplace. This field study highlighted the variation of water samples in time, as well as the oomycete diversity following a qPCR metagenomic analysis.

The last specific objective, to evaluate the up-scaling potential of the selected reactor design, was achieved partially during reactor development, to consider the scaling potential of a chosen reactor design.

Our initial prototype started with a batch process at 100 mL, which was then extended to 2L and 4L recirculating hydroponic systems. This design produces a constant species generation rate, provided they are not close to the solubility limits when compared to the earlier jet prototypes. Some mechanisms were proposed to improve the mass transfer efficiency, by choosing an appropriate reactor geometry favoring the production of NO_X, or by forcing diffusion of the effluent gas to improve the transfer to the liquid phase. While these were only initial investigations, the overall improvement demonstrated an increase by a factor 10 in terms of efficiency compared to the initial prototype, going from 2 μmol/min to 37 μmol/min. Relying on these results, the next prototype, of 60 L planned in the collaborative research project, PLANET, now becomes feasible. PLANET is an interdisciplinary project combining four research institutions and 10 research groups, which pursues the topic of the use of plasma in greenhouse farming. The improvements on the prototype will combine the mass transfer efficiency and further parallelization of plasma sources will enable the project to go towards higher treatment volumes, and eventually reach the 100 kL/day required by the industrial partner. Furthermore, a microwave system was built to be ready for larger scale studies, which will enable to start producing species with 50 times more power from the start.

Scaling attempts in the plasma community should address chemical specificity in terms of energy costs, i.e. MJ/mol, this limited study looked into the productivity of nitrite as a target nitrogen species diagnostic. Due to the nature of the resonant plasma source, only an estimate of power can be given; it cannot be directly measured. As such, the best candidate amounts to 43 MJ/mol of NO_2^-

(37 μmol/L, at 26.4 W, for 1 min), comparable to other reactors of the type in the literature. While the reported efficiency is below the best reactors in the literature, three factors explain this discrepancy: the first is that the reported production is currently in the liquid phase, while the comparison established by Rouwenhorst et al [60], reports the efficiency in the gas phase. The second is that the power of the plasma reported here was the power of the plasma source, and not the measured plasma energy, since it could not be measured directly. The third, is that this reactor can be further refined to improve on its efficiency.

This thesis has presented that cold atmospheric pressure plasma can be used in the context of greenhouse agriculture for both inactivation of pathogens and well as fertilization. Acquiring all the knowledge required to understand this multidisciplinary topic, involving physics, chemistry, electrical, civil and bio engineering in the context of application for plants was certainly a challenge. However, considering the green potential of the technology in substituting chemistry from basic resources such as water, air and electricity, the path forward is paved to lead to a commercially viable prototype, as well as into the developments in pulsed power sources and the rest of the PLANET project which will continue on from this research.

8.2 Limitations and recommendations

The results presented in the context of this thesis are mostly based on investigative work towards reaching an ideal solution and therefore are limited in scope. By identifying project limitations, it will become easier to propose improvements and formulate further research topics for the continuation of the mandate.

As a start, of the O_2:N_2 parameter space explored, only three candidates were chosen for bio testing due to test availability with our IRDA partnership. It could be possible that other conditions are more optimal for either pathogen inactivation or fertilizer incorporation which tested two conditions. While the project development was using a mixture of nitrogen and oxygen, ideally, it would be preferable from a cost perspective to source the gas directly from air. From a biological perspective, more repetitions are required to properly see impacts of plasma treatment, not only from multiple plants, but also in repeating the treatment batch a few times. The development of rapid diagnostic tools for identifying if pythium can be inactivated should help in that regard.

Continuing with plasma chemistry limitations, this research has not considered possible creation of nanoparticles from direct exposure of the electrodes to the plasma and related toxicity effects.

The industrial partner would ideally like a chemical specificity only in creating inactivating species and nitrates, as such resulting changes in nitrite/nitrate content in the lettuce have not been investigated. Further work in the project will involve scaling the treatment to larger volumes of water in the order of kL or m^3; as such the destruction of the NO_X/O_3 species before release in the atmosphere at safe levels will become an important safety aspect of the project.

From an electrical perspective, the shielding of the source, especially at higher power will become important. Further work in scaling will need to evaluate plasma treatment as function of energy costs for efficiency comparison with literature. Ideally this would entail measuring from three sources for better comparison; from the wall, the plasma source and the actual energy taken by the plasma, since the first two could also be optimized at some point. Noise cancelling of higher resonant modes is also required for adapting a device to CSA norms for commercial development.

In terms of biology, the current forms of oomycete issues are well documented for soil farming, but not very well known when it comes to hydroponics. The exact conditions behind the abnormal growth of oomycete and plant failure are also unknown and difficult to recreate on site. As such, the *in vivo* growth cabinet at IRDA will most likely be very useful, once problematic growth conditions can be replicated. For future works, IRDA is establishing a microbiological safety level 2 greenhouse.

A further difficulty of the project originated with plants at the Polytechnique laboratories: even in the absence of bio contaminants, project approval took 6 months. Plant contaminants in this research were all class 1, namely involving any pathogenic organisms for plants, but not for humans. However, bio contaminants, even of class 1, result in strict procedure establishment. For example, *P. dissocotum* was used in Chapter 6 instead of *P. ultimum* due to safety concerns.

Most of the work initially considered *P. ultimum* as the target species for inactivation. The qPCR test conducted in summer of 2024 identified other oomycetes which seem to react differently to the plasma treatment, and the industrial partner was also worried about *Phytophtora* species. The tests have shown inactivation of the pathogens following immediate treatment. However, oomycete resistance to the treatment over the long term was not considered. Oomycetes are well known in the literature for their ability to develop a resistance to fungicidal treatments within a short timeframe.

The scope of the project did not investigate the impacts of any water heating effects plasma might have due to the scale of the project. What conditions are more problematic for lettuce, water heat increase or air temperature increase?

From the literature, the presence of nitrite in the growth media should hinder the growth of lettuce plants. Questions that remain to be answered, are whether Boston lettuce is more resistant to nitrite, or is nitrite availability in conjunction with nitrate availability linked, due to long term degradation of nitrite into nitrate? This topic and the influence of both species would need to be better explored. As a hypothesis from observed tests, it could be proposed that, so long as lettuce has enough nitrates in the water, it seems to be growing well and does not look to compensate for nitrogen availability. It could also be due to nitrifying bacteria; how do these respond to plasma treatment? Monitoring both nitrite and nitrate content in the water along with nitrifying bacteria populations and other plant stress factors would help investigate such questions.

Answering these research questions and many more only places this thesis project in a forefront position out of a continued plasma agriculture project. More solutions will be developed as the product develops towards an industrial prototype and green electrification of chemistry.

REFERENCES

[1] I. FAO, UNICEF, WFP and WHO, "The State of Food Security and Nutrition in the World 2023.." Rome, Italy : FAO ; IFAD ; UNICEF ; WFP ; WHO ;, 2023, p. 316.

[2] F. Bilea *et al.*, "Non-Thermal Plasma as Environmentally-Friendly Technology for Agriculture: A Review and Roadmap," *Critical Reviews in Plant Sciences,* vol. 43, nº 6, p. 428-486, 2024, 428.

[3] H. Cheng *et al.*, "Numerical analysis of nitrogen fixation by nanosecond pulse plasma," *Journal of Physics D: Applied Physics,* vol. 54, nº 18, 2021, 184003.

[4] S. Ghavam *et al.*, "Sustainable Ammonia Production Processes", *Frontiers in Energy Research,* vol. 9, 2021-March-29 2021. [En ligne]. Disponible : https://www.frontiersin.org/articles/10.3389/fenrg.2021.580808

[5] E. Massicotte *et al.*, "Profil sectoriel de l'industrie bioalimentaire au Québec," 2019e éd. Bibliothèque et Archives nationales du Québec : Gouvernement du Québec, 2019. [En ligne]. Disponible : http://www.stat.gouv.qc.ca/statistiques/agriculture/index.html

[6] P. Ranieri *et al.*, "Plasma agriculture: Review from the perspective of the plant and its ecosystem," *Plasma Processes and Polymers,* vol. 18, nº 1, 2020.

[7] N. N. Misra, O. Schlüter et P. J. Cullen, "Plasma in Food and Agriculture," dans *Cold Plasma in Food and Agriculture*, N. N. Misra, O. Schlüter et P. J. Cullen, édit. San Diego: Academic Press, 2016, p. 1-16.

[8] A. Fridman, *Plasma Chemistry*. New York, USA : Cambridge University Press, 2008.

[9] A. Schmidt-Bleker *et al.*, "How to produce an NOx- instead of Ox-based chemistry with a cold atmospheric plasma jet," *Plasma Processes and Polymers,* vol. 13, nº 11, p. 1120-1127, 2016, 1120.

[10] Y. Cao *et al.*, "Review on reactive species in water treatment using electrical discharge plasma: formation, measurement, mechanisms and mass transfer," *Plasma Science and Technology,* vol. 20, nº 10, 2018, 103001.

[11] M. Hijosa-Valsero *et al.*, "Decontamination of waterborne chemical pollutants by using atmospheric pressure nonthermal plasma: a review," *Environmental Technology Reviews,* vol. 3, nº 1, p. 71-91, 2014, 71.

[12] B. Jiang *et al.*, "Review on electrical discharge plasma technology for wastewater remediation," *Chemical Engineering Journal,* vol. 236, p. 348-368, 2014, 348.

[13] T. Sugai *et al.*, "The Effect of Scale-Up of Pulsed Corona Discharge for Treatment of Pollution Water Sprayed in Discharge Gap," *IEEE Transactions on Plasma Science,* vol. 44, nº 10, p. 2204-2210, 2016, 2204.

[14] D. Ziuzina *et al.*, "Investigation of a large gap cold plasma reactor for continuous in-package decontamination of fresh strawberries and spinach," *Innovative Food Science & Emerging Technologies,* vol. 59, 2020, 102229.

[15] A. Mizuno et S. M. Thagard, "Special issue on environmental applications of thermal and non-thermal plasmas," *Journal of Physics D: Applied Physics,* vol. 52, nº 2, 2019, 020301.

[16] R. Brandenburg *et al.*, "White paper on the future of plasma science in environment, for gas conversion and agriculture," *Plasma Processes and Polymers,* vol. 16, nº 1, 2018, 1700238.

[17] NSERC. (2018) Technology readiness levels. Government of Canada. [En ligne]. Disponible: https://www.ic.gc.ca/eic/site/080.nsf/eng/00002.html

[18] M. A. Malik, "Water Purification by Plasmas: Which Reactors are Most Energy Efficient?," *Plasma Chemistry and Plasma Processing,* vol. 30, nº 1, p. 21-31, 2009, 21.

[19] R. I. Asisov *et al.*, *High Energy Chem. (Khimia Vysokikh Energii),* vol. 14, 1980, 366.

[20] R. Snoeckx et A. Bogaerts, "Plasma technology - a novel solution for CO2 conversion?," *Chemical Society Reviews,* vol. 46, nº 19, p. 5805-5863, Oct 2 2017. [En ligne]. Disponible : https://www.ncbi.nlm.nih.gov/pubmed/28825736

[21] P. Vanraes, A. Y. Nikiforov et C. Leys, "Electrical Discharge in Water Treatment Technology for Micropollutant Decomposition," dans *Plasma Science and Technology - Progress in Physical States and Chemical Reactions*, Tetsu Mieno: Testu Mieno, 2016.

[22] B. R. Locke *et al.*, "Electrohydraulic Discharge and Nonthermal Plasma for Water Treatment," *Industrial & Engineering Chemistry Research,* nº 45, p. 882-905, 2006, 882.

[23] K. Yasuoka, K. Sasaki et R. Hayashi, "An energy-efficient process for decomposing perfluorooctanoic and perfluorooctane sulfonic acids using dc plasmas generated within gas bubbles," *Plasma Sources Science and Technology,* vol. 20, nº 3, 2011, 034009.

[24] S. K. Sharma et A. Shyam, "Design and testing of 45 kV, 50 kHz pulse power supply for dielectric barrier discharges," *Review of Scientific Instruments,* vol. 87, nº 10, p. 105115, Oct 2016. [En ligne]. Disponible : https://www.ncbi.nlm.nih.gov/pubmed/27802699

[25] R. P. Gott *et al.*, "Plasma activated water: a study of gas type, electrode material, and power supply selection and the impact on the final frontier," *Physical Chemistry Chemical Physics,* vol. 25, nº 6, p. 5130-5145, Feb 8 2023. [En ligne]. Disponible : https://www.ncbi.nlm.nih.gov/pubmed/36722991

[26] V. Rathore et S. K. Nema, "Effects of electrodes surface texture, electrodes materials and dielectric material on properties of plasma activated water," *Physics Letters A,* vol. 524, 2024, 129831.

[27] W. Ye *et al.*, "Advancements in Metallic Electrode Materials for Plasma Discharges Applications: Corrosion and Erosion Mechanisms in Liquid Phase Discharges," *Plasma Chemistry and Plasma Processing,* vol. 45, nº 4, p. 1313-1336, 2025, 1313.

[28] R. Brandenburg, "Dielectric Barrier Discharge," dans *Encyclopedia of Plasma Technology - Two Volume Set*, : CRC Press, 2016, p. 12.

[29] J. Reece Roth, *Industrial Plasma Engineering* vol. 2. Bristol and Philadelphia : Institute of Physics Publishing, 2001.

[30] B. S. Patil *et al.*, "Deciphering the synergy between plasma and catalyst support for ammonia synthesis in a packed dielectric barrier discharge reactor," *Journal of Physics D: Applied Physics,* vol. 53, nº 14, 2020, 144003.

[31] F. M. Fajar *et al.*, "Influence of the high-voltage of non-thermal plasma on the pH of aqueous solution for bacteria inactivation," communication présentée à, 2019.

[32] F. Tampieri, Y. Gorbanev et E. Sardella, "Plasma-treated liquids in medicine: Let's get chemical," *Plasma Processes and Polymers,* vol. 20, nº 9, 2023.

[33] B. R. Locke et P. Lukeš, "Special issue: Plasma and Liquids," *Plasma Processes and Polymers,* vol. 15, nº 6, 2018, 1815062.

[34] S. M. Thagard *et al.*, "An Experimental Investigation of the Liquid Flow Induced by a Pulsed Electrical Discharge Plasma," *Plasma Chemistry and Plasma Processing,* vol. 38, nº 4, p. 719-741, 2018, 719.

[35] J. Lang et I. Moussallem, "Fertilizing with Wind," *Elements - the Evonik innovation magazine,* nº 55, p. 14-16, 2016.

[36] "Microwave, Ultrasonic and Plasma assisted Syntheses (MAPSYN)," CORDIS EU research results, 2016. [En ligne]. Disponible : https://cordis.europa.eu/project/id/309376

[37] C. McCullough. (2019) Nitrogen-fixing plasma reactor trialed. [En ligne]. Disponible: https://agriview.photoshelter.com/gallery/CHRIS-Plasma-reactor/G00003yQGH4sKTEs/C0000H8QyMhSStOk

[38] (2021) Why Plasmaleap Power Sources? [En ligne]. Disponible: https://www.plasmaleap.com/products

[39] C. Sarangapani *et al.*, "Dissipation of Pesticide Residues on Grapes and Strawberries Using Plasma-Activated Water," *Food and Bioprocess Technology,* vol. 13, nº 10, p. 1728-1741, 2020, 1728.

[40] R. K. Singh *et al.*, "Breakdown Products from Perfluorinated Alkyl Substances (PFAS) Degradation in a Plasma-Based Water Treatment Process," *Environ Sci Technol,* vol. 53, nº 5, p. 2731-2738, Mar 5 2019. [En ligne]. Disponible : https://www.ncbi.nlm.nih.gov/pubmed/30768259

[41] R. K. Singh *et al.*, "Rapid Removal of Poly- and Perfluorinated Compounds from Investigation-Derived Waste (IDW) in a Pilot-Scale Plasma Reactor," *Environmental Science & Technology,* vol. 53, nº 19, p. 11375-11382, Oct 1 2019. [En ligne]. Disponible : https://www.ncbi.nlm.nih.gov/pubmed/31479249

[42] U. Schnabel *et al.*, "Sanitation of fresh-cut endive lettuce by plasma processed tap water (PPtW) – Up-scaling to industrial level," *Innovative Food Science & Emerging Technologies,* vol. 53, p. 45-55, 2019, 45.

[43] U. Schnabel *et al.*, "Plasma-Functionalized Water: from Bench to Prototype for Fresh-Cut Lettuce," *Food Engineering Reviews,* vol. 13, nº 1, p. 115-135, 2020, 115.

[44] F. Holzer et B. R. Locke, "Multistage Gas-Liquid Electrical Discharge Column Reactor For advanced Oxidation Processes," *Industrial and Engineering Chemistry Research,* nº 47, p. 2203-2212, 2008.

[45] J. Golda *et al.*, "Concepts and characteristics of the 'COST Reference Microplasma Jet'," *Journal of Physics D: Applied Physics,* vol. 49, nº 8, 2016, 084003.

[46] R. Niquet *et al.*, "Characterising the impact of post-treatment storage on chemistry and antimicrobial properties of plasma treated water derived from microwave and DBD sources," *Plasma Processes and Polymers,* vol. 15, nº 3, 2018, 1700127.

[47] J. E. Foster, "Plasma-based water purification: Challenges and prospects for the future," *Physics of Plasmas,* vol. 24, nº 5, 2017, 055501.

[48] B. R. Locke et K.-Y. Shih, "Review of the methods to form hydrogen peroxide in electrical discharge plasma with liquid water," *Plasma Sources Science and Technology,* vol. 20, nº 3, 2011, 034006.

[49] D. B. Miklos *et al.*, "Evaluation of advanced oxidation processes for water and wastewater treatment - A critical review," *Water Research,* vol. 139, p. 118-131, Aug 1 2018. [En ligne]. Disponible : https://www.ncbi.nlm.nih.gov/pubmed/29631187

[50] S. Mededovic Thagard *et al.*, "Plasma-based water treatment: development of a general mechanistic model to estimate the treatability of different types of contaminants," *Journal of Physics D: Applied Physics,* vol. 50, nº 1, 2017, 014003.

[51] J. Sun *et al.*, "A hybrid plasma electrocatalytic process for sustainable ammonia production," *Energy & Environmental Science,* vol. 14, nº 2, p. 865-872, 2021, 865.

[52] C. Nau-Hix *et al.*, "Field Demonstration of a Pilot-Scale Plasma Reactor for the Rapid Removal of Poly- and Perfluoroalkyl Substances in Groundwater," *ACS ES&T Water,* vol. 1, nº 3, p. 680-687, 2021, 680.

[53] W. Wang *et al.*, "Nitrogen Fixation by Gliding Arc Plasma: Better Insight by Chemical Kinetics Modelling," *ChemSusChem,* vol. 10, nº 10, p. 2145-2157, May 22 2017. [En ligne]. Disponible : https://www.ncbi.nlm.nih.gov/pubmed/28272779

[54] A. Fridman, *Physics and applications of the Gliding Arc discharge*, 2004.

[55] E. Carbone *et al.*, "Analysis of the C_2 (d^3 Π_g-a^3 Π_u) Swan bands as a thermometric probe in CO2 microwave plasmas," *Plasma Sources Science and Technology,* vol. 29, nº 5, 2020, 055003.

[56] A. Schmidt - Bleker *et al.*, "Disinfection method using a publication classification disinfection agent formed in situ by reaction of H2O2 and NO2," US 2021/0069361 A1, 2021.

[57] K. Doclo et U. Rothlisberger, "Conformational Equilibria of Peroxynitrous Acid in Water: A First-Principles Molecular Dynamics Study," *The Journal of Physical Chemistry A,* vol. 104, nº 27, p. 6464-6469, 2000, 6464.

[58] P. Bourke *et al.*, "The Potential of Cold Plasma for Safe and Sustainable Food Production," *Trends in Biotechnology,* vol. 36, nº 6, p. 615-626, Jun 2018. [En ligne]. Disponible : https://www.ncbi.nlm.nih.gov/pubmed/29329724

[59] *Cold Plasma in Food and Agriculture - Fundamentals and Applications*. London, U.K. : Academic Press, 2016.

[60] K. H. R. Rouwenhorst *et al.*, "From the Birkeland-Eyde process towards energy-efficient plasma-based NO (X) synthesis: a techno-economic analysis," *Energy Environ Sci,* vol. 14, nº 5, p. 2520-2534, Mar 31 2021. [En ligne]. Disponible : https://www.ncbi.nlm.nih.gov/pubmed/34046082

[61] A. Anastasopoulou *et al.*, "Eco-efficiency analysis of plasma-assisted nitrogen fixation," *Journal of Physics D: Applied Physics,* vol. 53, nº 23, 2020, 234001.

[62] N. C. Roy *et al.*, "NOx synthesis by atmospheric-pressure N2 /O2 filamentary DBD plasma over water: Physicochemical mechanisms of plasma–liquid interactions," *Plasma Processes and Polymers,* vol. 18, nº 3, 2020, 2000087.

[63] Z. Machala *et al.*, "Chemical and antibacterial effects of plasma activated water: correlation with gaseous and aqueous reactive oxygen and nitrogen species, plasma sources and air flow conditions," *Journal of Physics D: Applied Physics,* vol. 52, nº 3, 2019, 034002.

[64] A. A. Abdelaziz et H.-H. Kim, "Temperature-dependent behavior of nitrogen fixation in nanopulsed dielectric barrier discharge operated at different humidity levels and oxygen contents," *Journal of Physics D: Applied Physics,* vol. 53, nº 11, 2020, 114001.

[65] M. Moisan *et al.*, "Low-temperature sterilization using gas plasmas: a review of the experiments and an analysis of the inactivation mechanisms," *International Journal of Pharmaceutics,* vol. 226, p. 1-21, 2001.

[66] S. Lerouge, M. R.Wertheimer et L. H. Yahia, "Plasma Sterilization: A Review of Parameters, Mechanisms, and Limitations," *Plasma and Polymers,* vol. 6, nº 3, p. 175-188, 2001.

[67] C. Bradu *et al.*, "Reactive nitrogen species in plasma-activated water: generation, chemistry and application in agriculture," *Journal of Physics D: Applied Physics,* vol. 53, nº 22, 2020, 223001.

[68] M. H. Kang *et al.*, "Differential Inactivation of Fungal Spores in Water and on Seeds by Ozone and Arc Discharge Plasma," *PLoS One,* vol. 10, nº 9, p. e0139263, 2015. [En ligne]. Disponible : https://www.ncbi.nlm.nih.gov/pubmed/26406468

[69] K. Takahashi *et al.*, "Development of automatically controlled corona plasma system for inactivation of pathogen in hydroponic cultivation medium of tomato," *Journal of Electrostatics,* vol. 91, p. 61-69, 2018, 61.

[70] M. Laroussi, "Low Temperature Plasma-Based Sterilization: Overview and State-of-the-Art," *Plasma Processes and Polymers,* vol. 2, nº 5, p. 391-400, 2005, 391.

[71] S. Ikawa, K. Kitano et S. Hamaguchi, "Effects of pH on Bacterial Inactivation in Aqueous Solutions due to Low-Temperature Atmospheric Pressure Plasma Application," *Plasma Processes and Polymers,* vol. 7, nº 1, p. 33-42, 2010, 33.

[72] L. Tesoriero *et al.*, "Effective management of root diseases in hydroponic lettuce," Elizabeth Macarthur Agricultural Institute, Menangle, 179 Elizabeth Street Sydney NSW 2000, HAL Project VG04012, 2008. [En ligne]. Disponible : https://ausveg.com.au/app/data/technical-insights/docs/VG04012_complete.p

[73] F. R. BAPTISTA *et al.*, "The genus Pythium Pringsheim from Brazilian cerrado areas, in the state of São Paulo, Brazil," *Revista Brasil Botanica,* vol. 27, nº 2, p. 281-290, 2004.

[74] A. J. Van der Plaats-Niterink, "Monograph of the genus Pythium," *Studies in mycology,* nº 21, 1981.

[75] C. McGehee, R. E. Raudales et W. H. Elmer, "First Report of Pythium dissotocum Causing Pythium Root Rot on Hydroponically Grown Lettuce in Connecticut," *Plant Disease,* vol. 102, nº 10, 2018, 2043.

[76] G. Rodriguez-Alvarado *et al.*, "Root Rot of Hydroponically Grown Lettuce Caused by Phytophthora drechsleri in Mexico," *Plant Disease,* vol. 93, nº 10, p. 1077, Oct 2009. [En ligne]. Disponible : https://www.ncbi.nlm.nih.gov/pubmed/30754351

[77] S. B. Fan *et al.*, "Rise and Fall of Phytophthora infestans Resistance to Non-Specific Fungicide in Experimental Populations," *J Fungi (Basel),* vol. 11, nº 9, Aug 30 2025. [En ligne]. Disponible : https://www.ncbi.nlm.nih.gov/pubmed/41003189

[78] N. Puač et N. Škoro, "Plasma–Liquid Interaction for Agriculture—A Focused Review," *Plasma Processes and Polymers,* vol. 22, nº 1, 2024.

[79] P. Kumar *et al.*, "Insights into nitrogen metabolism in the wild and cultivated lettuce as revealed by transcriptome and weighted gene co-expression network analysis," *Sci Rep,* vol. 12, nº 1, p. 9852, Jun 14 2022. [En ligne]. Disponible : https://www.ncbi.nlm.nih.gov/pubmed/35701518

[80] S. Luetic *et al.*, "Leafy Vegetable Nitrite and Nitrate Content: Potential Health Effects," *Foods,* vol. 12, nº 8, Apr 15 2023. [En ligne]. Disponible : https://www.ncbi.nlm.nih.gov/pubmed/37107450

[81] "Page 2: Guidelines for Canadian Drinking Water Quality: Guideline Technical Document - Nitrate and Nitrite." Government of Canada, 2014. [En ligne]. Disponible : https://www.canada.ca/en/health-canada/services/publications/healthy-living/guidelines-canadian-drinking-water-quality-guideline-technical-document-nitrate-nitrite/page-2-guidelines-canadian-drinking-water-quality-guideline-technical-document-nitrate-nitrite.html

[82] A. Martínez-Moreno *et al.*, "Reducing nitrate accumulation through the management of nutrient solution in a floating system lettuce (Lactuca sativa, L.)," *Scientia Horticulturae,* vol. 336, 2024, 113377.

[83] S. Watson *et al.*, "Electrifying greenhouse agriculture: Cold atmospheric pressure plasma technology for Pythium ultimum control," *Environmental Technology & Innovation,* vol. 39, 2025, 104222.

[84] Y. Liu, D. Bluck et F. Brana-Mulero, "Static and dynamic simulation of NOx absorption tower based on a hybrid kinetic-equilibrium reaction model," dans *Computer Aided Chemical Engineering*, vol. 34, 2014, p. 363-368.

[85] B. Nisol *et al.*, "Cold plasma oxidation of harmful algae and associated metabolite BMAA toxin in aqueous suspension," *Plasma Processes and Polymers,* vol. 16, nº 2, Feb 2019. [En ligne]. Disponible : <Go to ISI>://WOS:000457831600004

[86] A. Fridman *et al.*, "Gliding arc gas discharge," *Progress in Energy and Combustion Science,* vol. 25, nº 2, p. 211-231, 1999, 211.

[87] S. Kolev et A. Bogaerts, "A 2D model for a gliding arc discharge," *Plasma Sources Science and Technology,* vol. 24, nº 1, 2014, 015025.

[88] D. Iya-Sou *et al.*, "Specific Role of Reactor Configurations on the Mass Transfer and Energy Yield: Case of “Batch” and "Circulating” Gliding arc Liquid–Gas Reactors—Part 1: Experimental Study," *Plasma Chemistry and Plasma Processing*, 2021.

[89] Y. B. Zel'dovich, "The Oxidation of Nitrogen in Combustion Explosions," *Acta Physicochimica,* vol. 21, p. 577–628, 1946.

[90] C. F. Weissfloch, M. R. Wertheimer et R. G. Bosisio, "Apparatus and Method for Plasma Generation and Material Treatment with Electromagnetic Radiation," 3,814,983, 1974.

[91] S. Aday et M. S. Aday, "Impact of COVID-19 on the food supply chain," *Food Quality and Safety,* vol. 4, nº 4, p. 167-180, 2020, 167. [En ligne]. Disponible : https://doi.org/10.1093/fqsafe/fyaa024

[92] E. Walling et C. Vaneeckhaute, "Greenhouse gas emissions from inorganic and organic fertilizer production and use: A review of emission factors and their variability", *Journal of Environmental Management,* vol. 276, p. 111211, Dec 15 2020. [En ligne]. Disponible : https://www.ncbi.nlm.nih.gov/pubmed/32987233

[93] E. Audsley *et al.*, "Estimation of the greenhouse gas emissions from agricultural pesticide manufacture and use," Crop Protection Association, Cranfield University, 2009.

[94] Pesticide Action Network North America, "Pesticides and Climate Change: A Vicious Cycle," *PAN Report,* vol. https://www.panna.org/wp-content/uploads/2023/02/202308ClimateChangeEng.pdf, 2023.

[95] G. LaPlante *et al.*, "Canadian Greenhouse Operations and Their Potential to Enhance Domestic Food Security," *Agronomy,* vol. 11, nº 6, p. 1229, 2021, 1229. [En ligne]. Disponible : https://www.mdpi.com/2073-4395/11/6/1229

[96] W. R. Jarvis, *Managing diseases in greenhouse crops*: Amer Phytopathological Society, 1992.

[97] M. Domonkos *et al.*, "Applications of Cold Atmospheric Pressure Plasma Technology in Medicine, Agriculture and Food Industry," *Applied Sciences,* vol. 11, nº 11, p. 4809, 2021, 4809. [En ligne]. Disponible : https://www.mdpi.com/2076-3417/11/11/4809

[98] G. Divya Deepak, "Review on recent advances in cold plasma technology," *The European Physical Journal Applied Physics,* vol. 97, p. 39, 2022, 39.

[99] Z. Machala, K. Hensel et Y. Akishev, *Plasma for Bio-Decontamination, Medicine and Food Security*: Springer Science & Business Media, 2012.

[100] Y. Todorova *et al.*, "Non-Thermal Atmospheric Plasma for Microbial Decontamination and Removal of Hazardous Chemicals: An Overview in the Circular Economy Context with Data for Test Applications of Microwave Plasma Torch," *Processes,* vol. 10, nº 3, p. 554, 2022, 554. [En ligne]. Disponible : https://www.mdpi.com/2227-9717/10/3/554

[101] X. Lu *et al.*, "Reactive species in non-equilibrium atmospheric-pressure plasmas: Generation, transport, and biological effects," *Physics Reports,* vol. 630, p. 1-84, 2016/05/04/ 2016, 1. [En ligne]. Disponible : https://www.sciencedirect.com/science/article/pii/S0370157316300187

[102] V. Rathore *et al.*, "Investigation of Physicochemical Properties of Plasma Activated Water and its Bactericidal Efficacy," *Plasma Chemistry and Plasma Processing,* vol. 41, nº 3, p.

871-902, 2021/05/01 2021, 871. [En ligne]. Disponible : https://doi.org/10.1007/s11090-021-10161-y

[103] A. Khlyustova *et al.*, "Important parameters in plasma jets for the production of RONS in liquids for plasma medicine: A brief review," *Frontiers of Chemical Science and Engineering,* vol. 13, nº 2, p. 238-252, 2019/06/01 2019, 238. [En ligne]. Disponible : https://doi.org/10.1007/s11705-019-1801-8

[104] J.-L. Brisset *et al.*, "Chemical Reactivity of Discharges and Temporal Post-Discharges in Plasma Treatment of Aqueous Media: Examples of Gliding Discharge Treated Solutions," *Industrial & Engineering Chemistry Research,* vol. 47, nº 16, p. 5761-5781, 2008/08/01 2008, 5761. [En ligne]. Disponible : https://doi.org/10.1021/ie701759y

[105] P. Lu *et al.*, "Achieving reactive species specificity within plasma-activated water through selective generation using air spark and glow discharges," *Plasma Processes and Polymers,* vol. 14, nº 8, p. 1600207, 2017. [En ligne]. Disponible : https://onlinelibrary.wiley.com/doi/abs/10.1002/ppap.201600207

[106] N. Wannicke et H. Brust, "Inactivation of the Plant Pathogen Pythium ultimum by Plasma-Processed Air (PPA)," *Applied Sciences,* vol. 13, nº 7, p. 4511, 2023, 4511. [En ligne]. Disponible : https://www.mdpi.com/2076-3417/13/7/4511

[107] L. Lie *et al.*, "Characteristics of Gliding Arc Discharge Plasma," *Plasma Science and Technology,* vol. 8, nº 6, p. 653-655, 2006, 653.

[108] A. D. G. Sampaio *et al.*, "Effect of the pH on the Antibacterial Potential and Cytotoxicity of Different Plasma-Activated Liquids," *Int J Mol Sci,* vol. 23, nº 22, p. 13893, Nov 11 2022. [En ligne]. Disponible : https://www.ncbi.nlm.nih.gov/pubmed/36430372

[109] M. Rémillard, M. Joseph et L. Laroche, "Municipal drinking water produced by atwater and charles-j. Des baillets drinking water treatment plants and distributed to montréal (x0008084),montreal-west (x0008899) and royalmount (x0008092) water distribution networks," 2023.

[110] L. S. Clesceri, A. E. Greenberg et A. D. Eaton, "4500-NO2– B. Colorimetric Method," dans *Standard Methods for the Examination of Water and Wastewater*, 20the éd., : American Public Health Association, American Water Works Association, 1999.

[111] B. Tarabová *et al.*, "Specificity of detection methods of nitrites and ozone in aqueous solutions activated by air plasma," *Plasma Processes and Polymers,* vol. 15, nº 6, 2018.

[112] K. L. Schroeder *et al.*, "Molecular Detection and Quantification of Pythium Species: Evolving Taxonomy, New Tools, and Challenges," *Plant Disease,* vol. 97, nº 1, p. 4-20, Jan 2013. [En ligne]. Disponible : https://www.ncbi.nlm.nih.gov/pubmed/30722255

[113] J. C. Sutton *et al.*, "Etiology and epidemiology of Pythium root rot in hydroponic crops: current knowledge and perspectives," *Summa Phytopathologica,* vol. 32, nº 4, p. 307-321, 2006, 307.

[114] R. Vilela, P. Viswanathan et L. A. Mendoza, "A biochemical screening approach to putatively differentiate mammalian pathogenic Oomycota species in the clinical laboratory," *Journal of Medical Microbiology,* vol. 64, nº 8, p. 862-868, Aug 2015. [En ligne]. Disponible : https://www.ncbi.nlm.nih.gov/pubmed/26293112

[115] J. Guo *et al.*, "Inactivation effects of plasma-activated water on Fusarium graminearum," *Food Control,* vol. 134, p. 108683, 2022/04/01/ 2022, 108683. [En ligne]. Disponible : https://www.sciencedirect.com/science/article/pii/S0956713521008215

[116] A. T. Bolton, "Effects of temperature and pH of soilless media on root rot of poinsettia caused byPythium aphanidermatum," *Canadian Journal of Plant Pathology,* vol. 2, nº 2, p. 83-85, 2009, 83.

[117] K. M. Alhussa, "Effect of Soil Acidity on Diseases Caused by Pythium ultimum and Fusarium oxysporum on Tomato Plants," *Journal of Biological Sciences,* vol. 12, nº 7, p. 416-420, 2012, 416.

[118] T. F. Döring *et al.*, "Disease suppressive soils vary in resilience to stress," *Applied Soil Ecology,* vol. 149, p. 103482, 2020/05/01/ 2020, 103482. [En ligne]. Disponible : https://www.sciencedirect.com/science/article/pii/S0929139319306067

[119] H. Xu *et al.*, "Subcellular mechanism of microbial inactivation during water disinfection by cold atmospheric-pressure plasma," *Water Research,* vol. 188, p. 116513, Jan 1 2021. [En ligne]. Disponible : https://www.ncbi.nlm.nih.gov/pubmed/33091801

[120] Y. Zhou *et al.*, "Appropriate dissolved oxygen concentration and application stage of micro-nano bubble water oxygation in greenhouse crop plantation," *Agricultural Water Management,* vol. 223, p. 105713, 2019/08/20/ 2019, 105713. [En ligne]. Disponible : https://www.sciencedirect.com/science/article/pii/S037837741930188X

[121] O. Braissant *et al.*, "A Review of Methods to Determine Viability, Vitality, and Metabolic Rates in Microbiology," *Front Microbiol,* vol. 11, p. 547458, 2020-November-17 2020. [En ligne]. Disponible : https://www.ncbi.nlm.nih.gov/pubmed/33281753

[122] N. Recek *et al.*, "Improved fermentation efficiency of S. cerevisiae by changing glycolytic metabolic pathways with plasma agitation," *Sci Rep,* vol. 8, nº 1, p. 8252, May 29 2018. [En ligne]. Disponible : https://www.ncbi.nlm.nih.gov/pubmed/29844402

[123] N. N. Misra *et al.*, "Cold Plasma for Effective Fungal and Mycotoxin Control in Foods: Mechanisms, Inactivation Effects, and Applications," *Compr Rev Food Sci Food Saf,* vol. 18, nº 1, p. 106-120, Jan 2019. [En ligne]. Disponible : https://www.ncbi.nlm.nih.gov/pubmed/33337013

[124] P. Lukes *et al.*, "Aqueous-phase chemistry and bactericidal effects from an air discharge plasma in contact with water: evidence for the formation of peroxynitrite through a pseudo-second-order post-discharge reaction of H2O2and HNO2," *Plasma Sources Science and Technology,* vol. 23, nº 1, 2014, 015019.

[125] C. A. J. van Gils *et al.*, "Mechanisms of bacterial inactivation in the liquid phase induced by a remote RF cold atmospheric pressure plasma jet," *Journal of Physics D: Applied Physics,* vol. 46, nº 17, 2013, 175203.

[126] A. Schmidt-Bleker *et al.*, "On the plasma chemistry of a cold atmospheric argon plasma jet with shielding gas device," *Plasma Sources Science and Technology,* vol. 25, nº 1, 2016, 015005.

[127] M. M. Hoque, H. A. Ajwa et R. Smith, "Nitrite and Ammonium Toxicity on Lettuce Grown under Hydroponics," *Communications in Soil Science and Plant Analysis,* vol. 39, nº 1-2, p. 207-216, 2007, 207.

[128] B. Lei *et al.*, "The positive function of selenium supplementation on reducing nitrate accumulation in hydroponic lettuce (Lactuca sativa L.)," *Journal of Integrative Agriculture,* vol. 17, nº 4, p. 837-846, 2018, 837.

[129] N. a. F. S. N. Joint FAO/WHO Expert Committee on Food Additives (JECFA), Standards & Scientific Advice on Food Nutrition (SSA), *Evaluation of certain food additives and contaminants : forty-fourth report of the Joint FAO/WHO Expert Committee on Food Additives*.

[130] M. D. Croitoru *et al.*, "Growing patterns to produce 'nitrate-free' lettuce (Lactuca sativa)," *Food Addit Contam Part A Chem Anal Control Expo Risk Assess,* vol. 32, nº 1, p. 80-6, 2015. [En ligne]. Disponible : https://www.ncbi.nlm.nih.gov/pubmed/25345876

[131] *On maximum levels for certain contaminants in food and repealing Regulation (EC) No 1881/2006,* T. E. COMMISSION 2023/915, 2023.

[132] "Archived Consumer Factsheet on Nitrates/Nitrites." United States Environmental Protection Agency, 2009, p. 5. [En ligne]. Disponible : https://archive.epa.gov/water/archive/web/pdf/archived-consumer-fact-sheet-on-nitrates-and-or-nitrites.pdf

[133] K. Matra *et al.*, "Enhancement of Lettuce Growth by PAW Spray Gliding Arc Plasma Generator," *IEEE Transactions on Plasma Science,* vol. 50, nº 6, p. 1430-1439, 2022, 1430.

[134] Z. 泽. Han 韩 *et al.*, "Plasma nitrogen fixation system with dual-loop enhancement for improved energy efficiency and its efficacy for lettuce cultivation," *Plasma Science and Technology,* vol. 26, nº 1, 2024, 015505.

[135] J. Mugnier et M. C. Grosjean, "PCR catalogue in plant pathology: Pythium.," Rhône–Poulenc Agro, Lyon, France, 1995.

[136] N. A. Bokulich et D. A. Mills, "Facility-specific "house" microbiome drives microbial landscapes of artisan cheesemaking plants," *Appl Environ Microbiol,* vol. 79, nº 17, p. 5214-23, Sep 2013. [En ligne]. Disponible : https://www.ncbi.nlm.nih.gov/pubmed/23793641

[137] E. Bolyen *et al.*, "Reproducible, interactive, scalable and extensible microbiome data science using QIIME 2," *Nature Biotechnology,* vol. 37, nº 8, p. 852-857, Aug 2019. [En ligne]. Disponible : https://www.ncbi.nlm.nih.gov/pubmed/31341288

[138] (2014) R: A language and environment for statistical computing. Vienna, Austria: R Foundation for Statistical Computing. [En ligne]. Disponible : http://www.R-project.org/

[139] B. J. Callahan *et al.*, "DADA2: High-resolution sample inference from Illumina amplicon data," *Nature Methods,* vol. 13, nº 7, p. 581-3, Jul 2016. [En ligne]. Disponible : https://www.ncbi.nlm.nih.gov/pubmed/27214047

[140] L. Tedersoo *et al.*, "EUKARYOME: the rRNA gene reference database for identification of all eukaryotes," *Database (Oxford),* vol. 2024, Jun 12 2024. [En ligne]. Disponible : https://www.ncbi.nlm.nih.gov/pubmed/38865431

[141] K. Abarenkov *et al.*, "The UNITE database for molecular identification and taxonomic communication of fungi and other eukaryotes: sequences, taxa and classifications reconsidered," *Nucleic Acids Research,* vol. 52, nº D1, p. D791-D797, Jan 5 2024. [En ligne]. Disponible : https://www.ncbi.nlm.nih.gov/pubmed/37953409

[142] C. Plessis *et al.*, "ASVmaker: A New Tool to Improve Taxonomic Identifications for Amplicon Sequencing Data," *Plants (Basel),* vol. 12, nº 21, Oct 25 2023. [En ligne]. Disponible : https://www.ncbi.nlm.nih.gov/pubmed/37960035

[143] Z. Bie, T. Ito et Y. Shinohara, "Effects of sodium sulfate and sodium bicarbonate on the growth, gas exchange and mineral composition of lettuce," *Scientia Horticulturae,* vol. 99, nº 3-4, p. 215-224, 2004, 215.

[144] D. Story *et al.*, "Lettuce calcium deficiency detection with machine vision computed plant features in controlled environments," *Computers and Electronics in Agriculture,* vol. 74, nº 2, p. 238-243, 2010.

[145] C. Côté, "Évaluation du potentiel des plasmas froids pour le traitement de l'eau en production serricole," IRDA, 2025.

[146] *IEC 60529 Consolidated version*, 2013.

[147] W. D. Kimmel et D. D. Gerke, "Shielding and Shielding Materials," dans *Electromagnetic Compatibility in Medical Equipment*, : CRC Press, 1995, p. 21.

[148] R. Dorai et M. J. Kushner, "A model for plasma modification of polypropylene using atmospheric pressure discharges," *Journal of Physics D: Applied Physics,* vol. 36, nº 6, p. 666-685, 2003, 666.

[149] K. Ikuse et S. Hamaguchi, "Roles of the reaction boundary layer and long diffusion of stable reactive nitrogen species (RNS) in plasma-irradiated water as an oxidizing media — numerical simulation study," *Japanese Journal of Applied Physics,* vol. 61, nº 7, 2022, 076002.

APPENDIX A CHEMICAL EQUATIONS IN GAS AND LIQUID PHASE FOR FIGURES 4.1 AND 5.6

Table A.1 Gas phase reactions for the reaction scheme

Eq #	Reaction formula	Rate constant	Reference
G1	$O + O_2 + M \rightarrow O_3 + M$	$6.0 \cdot 10^{-34}$	[126]
G2	$O_2^* + O_3 \rightarrow O + 2O_2$	$2.4 \cdot 10^{-27}$	[126]
G3	$H + O_2 + M \rightarrow HO_2 + M$	$5.4 \cdot 10^{-32}$	[126]
G4	$O + HO_2 \rightarrow OH + O_2$	$5.8 \cdot 10^{-11}$	[126]
G5	$O + OH \rightarrow H + O_2$	$3.5 \cdot 10^{-11}$	[126]
G6	$N_2^* + O \rightarrow NO + N$	$1 \cdot 10^{-12}$	[126]
G7	$NO + O + M \rightarrow NO_2 + M$	$1.0 \cdot 10^{-31}$	[126]
G8	$O + HO_2 \rightarrow O_2 + OH$	$5.5 \cdot 10^{-11}$	[126]
G9	$NO + O_3 \rightarrow NO_2 + O_2$	$2.4 \cdot 10^{-14}$	[126]
G10	$NO_2 + O_3 \rightarrow NO_3 + O_2$	$6.4 \cdot 10^{-17}$	[126]
G11	$NO_2 + NO_3 + M \rightarrow N_2O_5 + M$	$3.7 \cdot 10^{-30}$	[126]
G12	$N_2^* + O_2 \rightarrow N_2O + O$	$7.8 \cdot 10^{-14}$	[126]
G13	$NO_2 + N \rightarrow N_2O + O$	$1.4 \cdot 10^{-12}$	[126]
G14	$NO + OH + M \rightarrow HNO_2 + M$	$7.5 \cdot 10^{-31}$	[126]
G15	$NO_2 + OH + M \rightarrow HNO_3 + M$	$3.3 \cdot 10^{-30}$	[126]
G16	$2OH + M \rightarrow H_2O_2 + M$	$5.9 \cdot 10^{-31}$	[126]
G17	$OH + H_2O \rightarrow O_2 + H_2O$	$3.8 \cdot 10^{-11}$	[126]
G18	$2HO_2 + M \rightarrow H_2O_2 + O_2 + M$	$5.0 \cdot 10^{-32}$	[126]
G19	$N_2^* + O_2 \rightarrow 2O + N_2$	$1.5 \cdot 10^{-12}$	[148]

Table A.2 Liquid phase reactions for the reaction scheme

Eq #	Reaction formula	Rate constant	Reference
L1	$OH + NO \rightarrow NO_2^- + H^+$	$1 \cdot 10^{10}$	[125]
L2	$OH + NO_2^- \rightarrow OH^- + NO_2$	$1 \cdot 10^{10}$	[125]
L3	$O_3 + NO_2^- \rightarrow O_2 + NO_3^-$	$2.5 \cdot 10^{5}$	[125]
L4	$OH + OH \rightarrow H_2O_2$	$5 \cdot 10^{9}$	[125, 149]
L5	$OH + O_3 \rightarrow O_2 + HO_2$	$1 \cdot 10^{8}$	[125]
L6	$OH + HO_2 \rightarrow O_2 + H_2O$	$7.5 \cdot 10^{9}$	[125]
L7	$HO_2 + HO_2 \rightarrow O_2 + H_2O_2$	$1 \cdot 10^{6}$	[125]
L8	$HO_2 + NO \rightarrow HO_2NO$	$3.2 \cdot 10^{9}$	[125]
L9	$OH + OH^- \rightarrow H_2O + O^-$	$1.3 \cdot 10^{10}$	[125]
L10	$H^+ + NO_2^- + O^- \rightarrow OH^- + NO_2$	$3 \cdot 10^{8}$	[125]
L11	$NO_2 + NO \rightarrow N_2O_3$	$1.1 \cdot 10^{9}$	[125]
L12	$NO + NO + O_2 \rightarrow NO_2 + NO_2$	$2.3 \cdot 10^{6a}$	[125]
L13	$H_2O + NO_2 + NO \rightarrow HNO_2 + HNO_2$	$2 \cdot 10^{8}$	[125]
L14	$H_2O + NO_2 + NO_2 \rightarrow NO_2^- + NO_3^- + H^+ + H^+$	$0.5 \cdot 10^{8}$	[125]
L15	$H_2O + NO_2 + NO_2 \rightarrow HNO_2 + NO_3^- + H^+$	$1.5 \cdot 10^{8}$	[125]
L16	$H_2O_2 + OH \rightarrow H_2O + O_2^- + H^+$	$2.7 \cdot 10^{7}$	[125]
L17	$O_2^- + NO \rightarrow ONO_2^-$	$5 \cdot 10^{9}$	[125]
L18	$O_2^- + O_3 \rightarrow O_2 + O_3^-$	$1.6 \cdot 10^{9}$	[125]
L19	$O_3^- + H^+ \rightarrow HO_3$	$5.2 \cdot 10^{10}$	[125]
L20	$O_3^- + H^+ \rightarrow O_2 + OH$	$9 \cdot 10^{10}$	[125]
L21	$O_3^- + OH \rightarrow HO_2 + O_2^-$	$8.5 \cdot 10^{9}$	[125]

L22	$O_3^- \rightarrow O_2 + O^-$	$5 \cdot 10^{3b}$	[125]
L23	$O^- + O_3^- \rightarrow O_2^- + O_2^-$	$7 \cdot 10^8$	[125]
L24	$H_2O + HO_2 + O_2^- \rightarrow O_2 + H_2O_2 + OH^-$	$9.7 \cdot 10^7$	[125]
L25	$OH^- + H^+ \rightarrow H_2O$	$1.4 \cdot 10^{11}$	[149]
L26	$O^- + H^+ \rightarrow OH$	$1.0 \cdot 10^{11}$	[149]
L27	$O^- + H_2O \rightarrow OH + OH^-$	$1.0 \cdot 10^8$	[149]
L28	$OH + OH^- \rightarrow O^- + H_2O$	$1.3 \cdot 10^{10}$	[149]
L29	$2O^- \rightarrow HO_2^- + OH^-$	$1.0 \cdot 10^9$	[149]
L30	$O^- + OH \rightarrow HO_2^-$	$2.5 \cdot 10^{10}$	[149]
L31	$O^- + O_2^- \rightarrow O_2 + 2OH^-$	$6.0 \cdot 10^8$	[149]
L32	$O^- + HO_2 \rightarrow O_2 + OH^-$	$6.0 \cdot 10^9$	[149]
L33	$O^- + HO_2^- \rightarrow O_2^- + OH^-$	$4.0 \cdot 10^8$	[149]
L34	$O^- + H_2O_2 \rightarrow O_2 + H_2O$	$5.0 \cdot 10^8$	[149]
L35	$OH + O_2^- \rightarrow O_2 + OH^-$	$8.2 \cdot 10^9$	[149]
L36	$OH + HO_2 \rightarrow O2 + H_2O$	$6.0 \cdot 10^9$	[149]
L37	$OH + HO_2^- \rightarrow O_2^- + H_2O$	$7.5 \cdot 10^9$	[149]
L38	$OH + H_2O_2 \rightarrow HO_2 + H_2O$	$2.7 \cdot 10^7$	[149]
L39	$H_2O^+ \rightarrow OH + H^+$	$3.3 \cdot 10^5$	[149]
L40	$O_2^- + H^+ \rightarrow HO_2$	$2 \cdot 10^{10}$	[149]
L41	$HO_2 + OH^- \rightarrow O_2^- + H_2O$	$5.0 \cdot 10^{10}$	[149]
L42	$2O_2^- (+ 2H_2O) \rightarrow O_2 + H_2O_2 + 2OH^-$	$1.0 \cdot 10^2$	[149]
L43	$O_2^- + HO_2 \rightarrow O_2 + HO_2^-$	$8.0 \cdot 10^7$	[149]
L44	$O_2^- + HO_2^- \rightarrow O_2 + O^- + OH^-$	$1.3 \cdot 10^{-1}$	[149]
L45	$O_2^- + H_2O_2 \rightarrow O_2 + OH + OH^-$	$1.3 \cdot 10^{-1}$	[149]
L46	$2HO_2 \rightarrow O_2 + H_2O_2$	$7.0 \cdot 10^5$	[149]
L47	$HO_2 + HO_2^- \rightarrow O_2 + OH + OH^-$	$5 \cdot 10^{-1}$	[149]
L48	$HO_2 + H_2O_2 \rightarrow O_2 + OH + H_2O$	$5 \cdot 10^{-1}$	[149]
L49	$HO_2^- + H^+ \rightarrow H_2O_2$	$2.0 \cdot 10^{10}$	[149]
L50	$HO_2^- + H_2O \rightarrow H_2O_2 + OH^-$	$5.8 \cdot 10^7$	[149]
L51	$H_2O_2 + OH^- \rightarrow HO_2^- + H_2O$	$1.3 \cdot 10^{10}$	[149]
L52	$O + O_2 \rightarrow O_3$	$4.0 \cdot 10^9$	[149]
L53	$O^- + O_2 \rightarrow O_3^-$	$3.6 \cdot 10^9$	[149]
L54	$O_3^- + O^- \rightarrow O_2 + O_2^-$	$5.0 \cdot 10^9$	[149]
L55	$O_3 + OH^- \rightarrow HO_2 + O_2^-$	$1.6 \cdot 10^9$	[149]
L56	$O_3 + O_2^- \rightarrow O_2 + O_3^-$	$2.8 \cdot 10^6$	[149]
L57	$O_3^- + H^+ \rightarrow HO_3$	$5.2 \cdot 10^{10}$	[149]
L58	$O_3 + O^- \rightarrow 2O_2^-$	$7.0 \cdot 10^8$	[149]
L59	$O_3^- + OH \rightarrow O_3 + OH^-$	$2.6 \cdot 10^9$	[149]
L60	$O_3^- + OH \rightarrow 2O_2 + H^+$	$6.0 \cdot 10^9$	[149]
L61	$HO_3 \rightarrow O_2 + OH$	$1.1 \cdot 10^5$	[149]
L62	$2HO_3 \rightarrow 2O_2 + H_2O_2$	$5.0 \cdot 10^9$	[149]
L63	$HO_3 + OH \rightarrow O_2 + H_2O_2$	$5.0 \cdot 10^9$	[149]
L64	$HO_3 + O_2^- \rightarrow 2O_2 + OH^-$	$1.0 \cdot 10^{10}$	[149]
L65	$NO + OH \rightarrow HNO_2$	$1.0 \cdot 10^{10}$	[149]
L66	$NO + HO_2 \rightarrow ONOOH$	$3.2 \cdot 10^9$	[149]
L67	$HNO + O_3 \rightarrow O_2 + HNO_2$	$5.8 \cdot 10^6$	[149]
L68	$HNO + OH \rightarrow NO + H_2O$	$4.8 \cdot 10^{10}$	[149]
L69	$NO_2 + OH \rightarrow NO_3^- + H^+$	$1.2 \cdot 10^{10}$	[149]
L70	$NO_2^- + H^+ \rightarrow HNO_2$	$5.0 \cdot 10^{10}$	[124, 149]
L71	$HNO_2 \rightarrow NO_2^- + H^+$	$2.7 \cdot 10^7$	[149]
L72	$NO_2^- + O_3 \rightarrow O_2 + NO_3^-$	$3.7 \cdot 10^5$	[149]
L73	$NO_2^- + O^- \rightarrow NO_2 + 2OH^-$	$2.5 \cdot 10^8$	[149]

L74	$NO_2^- + OH \rightarrow NO_2 + OH^-$	$4.5 \cdot 10^9$	[149]
L75	$NO_2^- + H_2O_2 + H^+ \rightarrow ONOOH + H_2O$	$1.1 \cdot 10^3$	[149]
L76	$HNO_2 + OH \rightarrow NO_2 + H_2O$	$3.0 \cdot 10^9$	[149]
L77	$HNO_3 + OH \rightarrow NO_3 + H_2O$	$8.6 \cdot 10^7$	[149]
L78	$NO_3 + OH^- \rightarrow OH + NO_3^-$	$9.4 \cdot 10^7$	[149]
L79	$NO_3 + O_2^- \rightarrow O_2 + NO_3^-$	$3.0 \cdot 10^9$	[149]
L80	$NO_3 + HO_2 \rightarrow O_2 + NO_3^- + H^+$	$3.0 \cdot 10^9$	[149]
L81	$NO_3 + H_2O_2 \rightarrow HO_2 + NO_3^- + H^+$	$7.1 \cdot 10^6$	[149]
L82	$NO_3 + NO_2^- \rightarrow NO_2 + NO_3^-$	$1.4 \cdot 10^9$	[149]
L83	$NO_3 + HNO_2 \rightarrow NO_2 + NO_3^- + H^+$	$8.0 \cdot 10^6$	[149]
L84	$NO_3 + H^+ \rightarrow HNO_3$	$5.0 \cdot 10^{10}$	[149]
L85	$HNO_3 \rightarrow NO_3 + H^+$	$1.1 \cdot 10^{12}$	[149]
L86	$HNO_3^- \rightarrow NO_2 + OH^-$	$2.0 \cdot 10^5$	[149]
L87	$ONOO^- + H^+ \rightarrow ONOOH$	$5.0 \cdot 10^{10}$	[149]
L88	$O_2^- + NO \rightarrow ONOO^-$	$6.7 \cdot 10^9$	[149]
L89	$OH + NO_2 \rightarrow ONOOH$	$4.5 \cdot 10^9$	[149]
L90	$ONOO^- + OH \rightarrow NO + O_2 + OH^-$	$4.8 \cdot 10^9$	[149]
L91	$N_2O + O \rightarrow 2NO$	$4.0 \cdot 10^{10}$	[149]
L92	$NO + NO_2 \rightarrow N_2O_3$	$1.1 \cdot 10^9$	[149]
L93	$NO_2 + NO_3 \rightarrow N_2O_5$	$1.7 \cdot 10^9$	[149]